NASA CR-111970

INVESTIGATION OF PULSED QUASI-STEADY MPD ARC JET

by

A. C. Ducati and R. G. Jahn

prepared for

NATIONAL AERONAUTICS AND SPACE ADMINISTRATION

Contract NAS 1-10140

Plasmadyne
a division of GEOTEL, INC.
Santa Ana, California

NASA CR-111970

Report FR-061-10140

INVESTIGATION OF PULSED QUASI-STEADY MPD ARC JETS

by

A. C. Ducati and R. G. Jahn

prepared for

NATIONAL AERONAUTICS AND SPACE ADMINISTRATION
Langley Research Center
Hampton, Virginia 23365

Contract NAS 1-10140

June 1971

Plasmadyne
a division of GEOTEL, INC.
Santa Ana, California

FOREWORD

This is the report on work carried out during the period of 26 June 1970 to 26 June 1971 by Plasmadyne, a division of Geotel, Inc., on "Investigation of Pulsed Quasi-Steady MPD Arc Jets," Contract NAS 1-10140, originating in the Plasma Physics Division, Langley Research Center, Hampton, Virginia, under the direction of James M. Hoell.

Adriano C. Ducati was the Principal Investigator in charge of the work. Robert G. Jahn collaborated as a consultant, René Bregozzo participated actively in the conduction of the experiments, and Willis Stoner contributed to the preparation of the report. F. A. Block, A. O. Jones, S. E. Killops and W. A. Stanfill provided invaluable help in the shop and laboratory.

ABSTRACT

This report succeeds Reference 1 and describes the work performed for continued evaluation of MPD arc thrusters operating in the quasi-steady mode and using electrode vapor as the propellant. A primary goal of the program is to determine the performance potential of this type of engine by measurement of the main performance parameters including the direct measurement of total impulse. Most of the effort has been directed toward the development of a propulsion system and a test facility that will permit efficient testing with the desired environmental conditions, and most of this report deals with this effort. However, some preliminary performance data have been obtained, and are reported and discussed toward the close of this report.

In order to resolve questions regarding the effect of ambient gas on performance, a high priority has been placed on testing at pressures low enough that the flow surrounding the plume is in the free molecular regime. This is accomplished by using propellants that condense readily on the walls of the test chamber and vacuum system without the need for cryogenic cooling and by developing equipment and methods of testing that permit vacuum in the chamber to be maintained while the thruster is removed and replaced. Repeated lengthy outgassing periods are thereby avoided. It is now possible rapidly to conduct tests with varying conditions and thruster geometries while maintaining an ambient pressure that is less than 10^{-6} torr.

A major part of the effort concerns the development of a propulsion system that is suitable for the test work. Precise measurement of total impulse requires that the complete capacitor bank be mounted on the torsional pendulum so that heavy conductors leading to the pendulum are not needed. A compact capacitor bank using electrolytic capacitors and an innovative pulse generating circuit arrangement has been developed for storing energies up to 5 kilojoules on the pendulum. Electromagnetic interactions with the environment are minimized by the use of a vacuum chamber made of insulating material. To avoid excessive interference with the measurement of arc current and voltage during a discharge, a low voltage contact type arc triggering system has been developed and coaxial leads with a coaxial shunt have been installed.

Extensive operation of thrusters using carbon gas as the propellant shows no evidence of instabilities even though the thrusters are normally operated at high values of current and low mass flow. This suggests that the introduction of propellant directly into the arc by vaporization of material at the arc attachment point may have a beneficial effect on arc stability, permitting smooth operation at high specific impulse even with storable propellants of relatively high molecular weight. These studies have made clear the overriding need for care and good technique in determining the electrode mass consumed in each discharge. In the absence of extensive precautions, hygroscopic effects distort, if not

completely obscure the true mass determination, and all related performance estimates become equally invalid.

The preliminary data indicate that these carbon arcs have impedances of a very few milliohms, independent of the current over a range of 11 to 25 kiloamps. Their match with the capacitor line is such that some 70 percent of the initially stored energy is delivered to the electrodes. The mass consumed per pulse is quite low, and roughly proportional to the square of the current over the range tested, leading to a nearly constant specific impulse. The overall thrust efficiency is quite low, as was expected from the high internal resistance of the carbon electrodes in this first thruster design, and their relatively ineffective geometry for electromagnetic thrust optimization.

The steps for direct improvement of both testing technique and thruster performance are clearly defined by the studies completed to date.

TABLE OF CONTENTS

LIST OF ILLUSTRATIONS

LIST OF ILLUSTRATIONS (continued)

LIST OF ILLUSTRATIONS (continued)

1.0 INTRODUCTION

This report describes the work performed under Contract NAS 1-10140 for continued evaluation of arc thrusters operating in the quasi-steady mode and using electrode vapor as the propellant. The body of the report is organized into four main sections, each of which deals with one of the basic tools needed for the evaluation of quasi-steady thruster performance potential. These are the vacuum environment, the power supply, the plasma head, and the thrusting system. Each of these sections is written to give a fairly complete story of its subject without reference to the other sections. Some repetition is therefore introduced for the convenience of the reader who is concentrating on one aspect of the discussion. The following pages summarize the findings that are presented in the report.

Results of recent experiments make it evident that for conclusive tests of a thruster destined to operate in space, the actual ambient pressure should be closely simulated. Because of the erratic measurements obtained in different testing conditions in the past, a maximum working pressure of 10^{-6} torr has been established as necessary. This low pressure is needed to eliminate mass entrainment effects and to reveal unexpected operational difficulties that may occur in a very high vacuum environment. In order to obtain this working pressure it has been necessary to make some improvements in the totally insulated vacuum facility. A second stage diffusion pump has been added to reduce the backstreaming of vacuum pump oil from the main diffusion pump in the unbaffled vacuum chamber. Special observation windows which can be changed without opening the vacuum tank have been developed. Possible methods of improving the vacuum level using cryogenic systems are under investigation. Techniques have been developed for introducing test equipment into the vacuum environment (and withdrawing equipment from the environment) without altering the pressure level in the test chamber. This greatly reduces the testing time needed when parts must be frequently removed for weighing or alteration. Equipment has been installed which allows tests with and without thrust measurement to be conducted separately, thereby allowing better utilization of the vacuum facility. Special tools for improved manipulation of materials under vacuum have been developed. Difficulties experienced in the measurement of the ambient pressure, especially during an operative pulse, have led to extensive studies of more elaborate pressure measuring instrumentation. With the refinements that have been adopted so far, it has become possible to conduct all of the tests at pressures of 10^{-6} torr or better.

The use of very low impedance quasi-steady thrusters led to the adoption of electrolytic capacitors as the principal source of laboratory energy storage. It has been found necessary to use carefully designed pulse generating networks of compact construction to permit operation on the thrust stand at the desired energy levels. Studies have been conducted to reduce the resistance of the connecting circuit elements while maintaining the inductance needed to shape the pulse by careful use of mutual inductance effects. It is well

known that the main drawback of electrolytic capacitors used in high current discharge is their characteristically high internal resistance. With energy densities about two orders of magnitude higher than equivalent paper capacitors, the losses associated with this high internal resistance produce overheating which becomes excessive for very rapid duty cycles. However, experimental studies of this condition show the electrolytic capacitors can be used to advantage for laboratory operation with a moderate duty cycle. The results of a study on possible ways of matching the low impedance of the arc also favors use of the electrolytic capacitor. The production of one millisecond pulses having a peak power of two to three megawatts has been satisfactorily obtained with up to 70 percent of the initially stored energy being transferred to the arc electrodes. Capacitor banks capable of producing peak power three to four times higher are being studied.

The techniques used to measure the electrical characteristics of the pulse have been improved permitting a reliable evaluation to be made of the important variables. Coaxial shunts have been developed which can be used with currents up to 50 kiloamps. The measurement of the net arc voltage has presented some difficulties which have not yet been completely resolved. Auxiliary instrumentation has been used to count the number of pulses, control the operation and simplify the conduction of the tests. The complete package containing the capacitor network is enclosed in a cylindrical canister maintained at atmospheric pressure while operating in an ambient pressure of 10^{-6} torr. Additional automatic accessories are planned for improving the precision and speed of the measurements. During thousands of discharges the operation of the pulse shaping network has been reliable with no failures experienced.

The use of electrode vapor as the propellant was an outgrowth of the experience with more conventional gas-fed arcs where electrode erosion appeared as a spurious and troublesome complication.[2] Carbon has been selected as an exceptionally attractive consumable electrode material because of its high vapor pressure, high operating temperature, low molecular weight, good sublimation characteristics, etc. A detailed analysis supporting the selection is presented. The difficulties connected with the vaporization process and the emission of submicron particles are reviewed. The variation of the thermal and electrical characteristics along the various crystallographic axes appears to be an area of interest for further study. The possible use of pyrolytic types of graphite is considered, and the influence of the lattice orientation is examined. A study of thermodynamic properties of carbon vapor has been initiated and suggestions for further work to support theoretical analysis of thruster performance have been made. A relatively simple computer program is anticipated.

A number of practical designs for the arrangement of electrodes in plasma heads are illustrated using a variety of triggering systems with high and low voltages. The results of a simplified system where the electrodes are brought together by electromagnetic action producing the discharge without a separate triggering circuit are reported. Advantages

and disadvantages of the various triggering circuits are examined on the basis of test experience. The experiments include the design and test of numerous electrode types which evolved during a long test period. Tables including dimensions, geometries, and types of material used for various front, back and triggering electrodes are presented. Among the types tested, conical electrodes with radial current feed seem to offer the best metal to graphite contact and the minimum voltage drop due to resistance in the graphite. Various commercial graphites have been considered with densities between 1.6 to 1.9 g/cm^3, resistivities between 0.6 to 5.0 milliohm/cm and purities ranging from 6 to 500 parts per million.

The measurement of electrode evaporation rates as a function of geometry, material, and power required a large fraction of the testing time. These tests were made at the specified vacuum level and required a large number of pulses (normally from 50 to 1000) to be made so that precision measurements of weight could be taken before and after operation. The results are tabulated for an initial capacitor bank charge of 400 volts corresponding to an average arc power of 1.5 to 5.0 megawatts for one millisecond. Evaporation rates range from 0.5 to 2.0 milligrams per pulse. The results at lower voltages and powers are not included because the measurement of the change of the weight at these low powers requires different procedures. The precise measurement of small evaporation rates requires the use of a precision analytical balance and dehydration of the samples before and after the tests. Tests now in progress are concerned with plasma heads that use low voltage triggering systems. With these configurations it has been found that the electrode evaporation rate is strongly affected by the spacing of the electrode, the type of triggering system used, and the electrode polarity. An understanding of these effects will require further work.

The total energy expended in the millisecond part of the discharge appears to range from 40 to 70 percent of the energy stored in the capacitors, but further tests are needed to accurately establish a breakdown of energy losses. The heat of vaporization of carbon (about 50 joules per milligram) appears as only a small fraction of the total pulse energy. A substantial number of tests is contemplated to understand and optimize the evaporation rate.

The last major section of the report is concerned with the measurement of impulse, which is of basic interest in all our experiments. A torsional ballistic pendulum calibrated with a weight and pulley system is used. The difficulties encountered in the development of a reliable system capable of operating in the high vacuum environment are described. The need for frequent weighing and replacing of the evaporating electrodes consumed a large amount of test time and required the development of unconventional techniques for speeding up the operation. These are described and the problems which still require solutions are pointed out. Plasma heads can now be installed on the torsional ballistic pendulum or removed to the outside of the chamber without disturbing the high vacuum level. The tests

for each operating point include a series of 100 identical pulses to establish the propellant consumption rate as well as a shorter series (in some cases a single pulse) for determining impulse. At the end of the series the plasma head is withdrawn (without affecting the vacuum level) and the weight losses are determined to permit the calculation of the specific impulse. This method is very precise and requires a relatively small total amount of time. However, when numerous secondary variations are required without basic changes in the plasma head, it has been found convenient to use two identical heads, one suspended on the pendulum for the measurement of thrust and the other attached to a separate mounting base for the measurement of electrode evaporation rates. This procedure has been used frequently since it permits a substantial increase in the number of tests that can be conducted in a given time. The scale to read the pendulum deflection is calibrated in degrees and minutes of arc. It moves with the pendulum and is read against a luminous index mark. The calibration is conducted under vacuum by direct weight application. The actual sensitivity obtained is around 32 minutes deflection per gram second. A one gram weight was used with a typical application period of about ten seconds. A reduction of this weight would be desirable to permit an increase in the time of application, but this would require that the friction of the pulley be reduced in proportion. A system to eliminate the pulley has been tested with good results and will probably be applied in the future.

The extremely low pendulum damping in vacuum suggested the use of a procedure which we have termed "resonant pulsing." A single pulse is applied precisely at the zero point of each oscillation until the desired amplitude is attained. This eliminates the correction factors that are required when all of the pulses are applied during a single swing. The repeatability and absence of damping effects in the instrument have been checked by adding and subtracting a given number of impulses which consistently returns the pendulum to its initial amplitude. While the development of operating methods is continuing, it is already apparent that a torsional ballistic pendulum which contains the complete propulsion system is a reliable instrument for pulsed thrusting devices.

At the time this report was concluded, a test series at 100, 200, 300, and 400 volts initial capacitor charge had been completed for just one plasma head. The measurements showed good reproducibility and are believed qualitatively accurate, although further refinement in the mass measurements may change the detailed values somewhat. The impulses produced fell between 0.05 and 2.0 gram-seconds per pulse. The corresponding mass consumed per shot ranged from 0.02 to 0.60 mgm, which implies specific impulses in the range of a few thousand seconds, and was quite repeatable at any voltage. The thrust scaled as the square of the current, but was only about one-third of the ideal electromagnetic value. The $J^2/\dot{m}$ parameter was nearly constant, but of the order of 10^3, much higher than the values for gas-fed arcs. The efficiency of energy transfer from the capacitor line to the electrodes reached 70 percent, but the overall thrust efficiency was quite low, as anticipated from the lossy and un-optimized electrode configuration employed in this series.

In summary, the program to date has largely been concerned with the development of thrusters and testing equipment that can be used to obtain satisfactory performance measurements. Initial performance results show that quasi-steady thrusters using consumable electrodes can operate in an attractive specific impulse range. Although the losses are high with present designs, it is evident that substantial reductions in at least some of the losses should result from careful design modifications. Further work is expected to concentrate on an evaluation of thruster performance as a function of thruster design, pulse energy and power levels, and environmental conditions, with the goal of establishing the performance potential of consumable electrode quasi-steady thrusters.

2.0 THE VACUUM ENVIRONMENT

2.1 Maximum Acceptable Operating Pressure

The importance of an appropriate environment in experimenting with space propulsion is well established. The advantages of working under high vacuum conditions were recognized a number of years ago[3] and have been confirmed by recent experimental investigations both in steady state and in pulsed operation. A detailed description of our vacuum facility consisting basically of a 25- by 10-foot vacuum chamber made of insulating material and connected to a 48-inch diffusion pump can be found in the referenced literature.[4] The next section will report on improvements that have recently been introduced in the facility. However, before describing these improvements, we would like to explain how a value was arrived at for the maximum acceptable operating pressure. Results of recent experiments make it evident that for conclusive tests of a thruster destined to operate in space the actual ambient pressure should be closely simulated. Considering the graph of Figure 1 it is evident that even for modest altitudes the task is not trivial and can easily become completely infeasible when a small mass flow is introduced. Some degree of compromise is therefore necessary. For reasons which will be discussed next, a limit of 10^{-6} torr has been established as an operating condition that is attainable and can also give useful results. This corresponds to a modest altitude of 220 kilometers which is far from the desired simulation for most projected applications. However, it can be shown

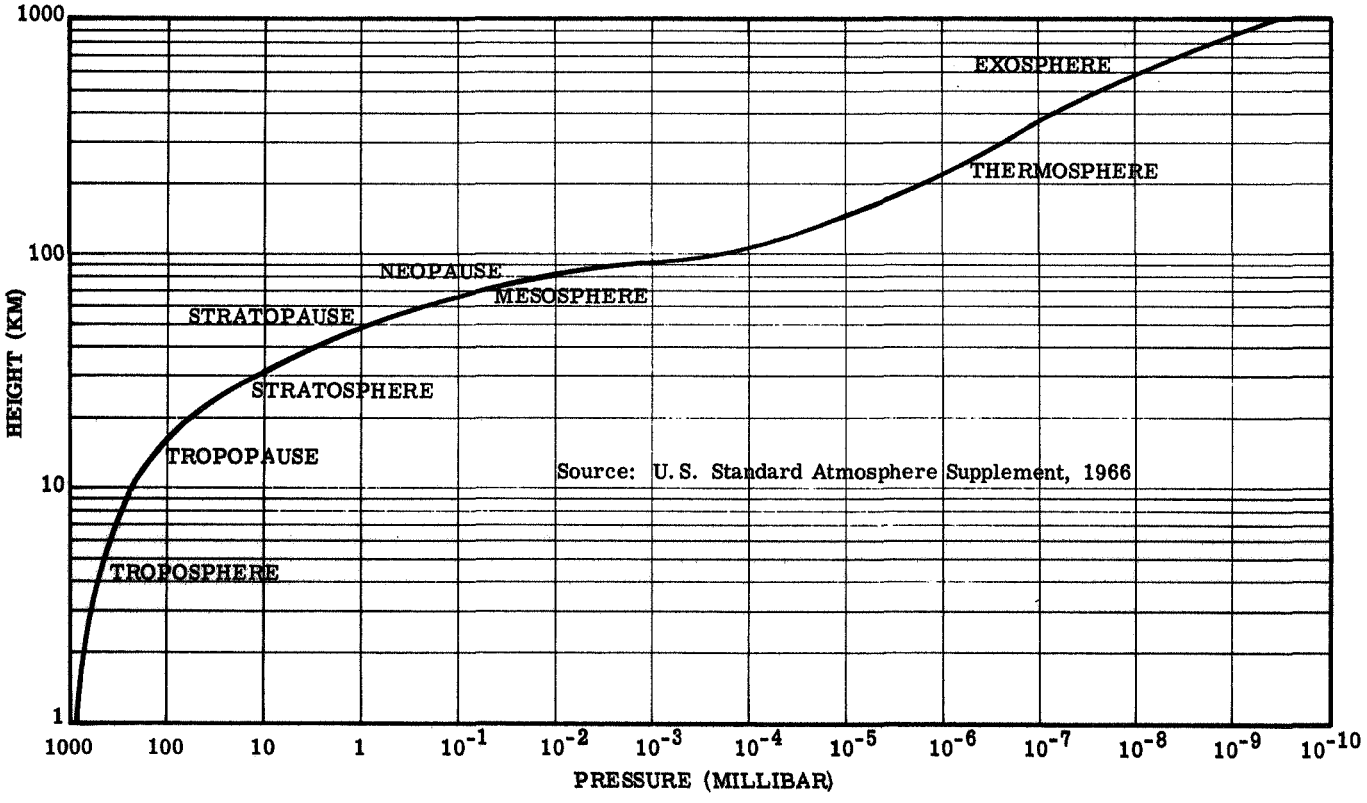

Figure 1. Atmospheric Pressure in Millibars to 1000 Kilometers Altitude

to be quite difficult to maintain even this vacuum level in typical test conditions. (To give an idea of the difficulty, it is sufficient to say that the maximum mass flow of hydrogen that could be handled by a 48-inch diffusion pump at this pressure is about 1/100 of a milligram per second - see Figure 2.) The primary reason for working at pressures under 10^{-6} torr is associated with the effects of mass entrainment (i. e. recirculation of the ambient gas). This action is evidently responsible for most of the erratic measurements obtained in the past. The effect appears to be reduced to a tolerable value when working in this pressure range. In any event, the Knudsen number for the plume falls well within the free molecular flow regime which reduces the risk of extrapolating measurements to lower pressures.

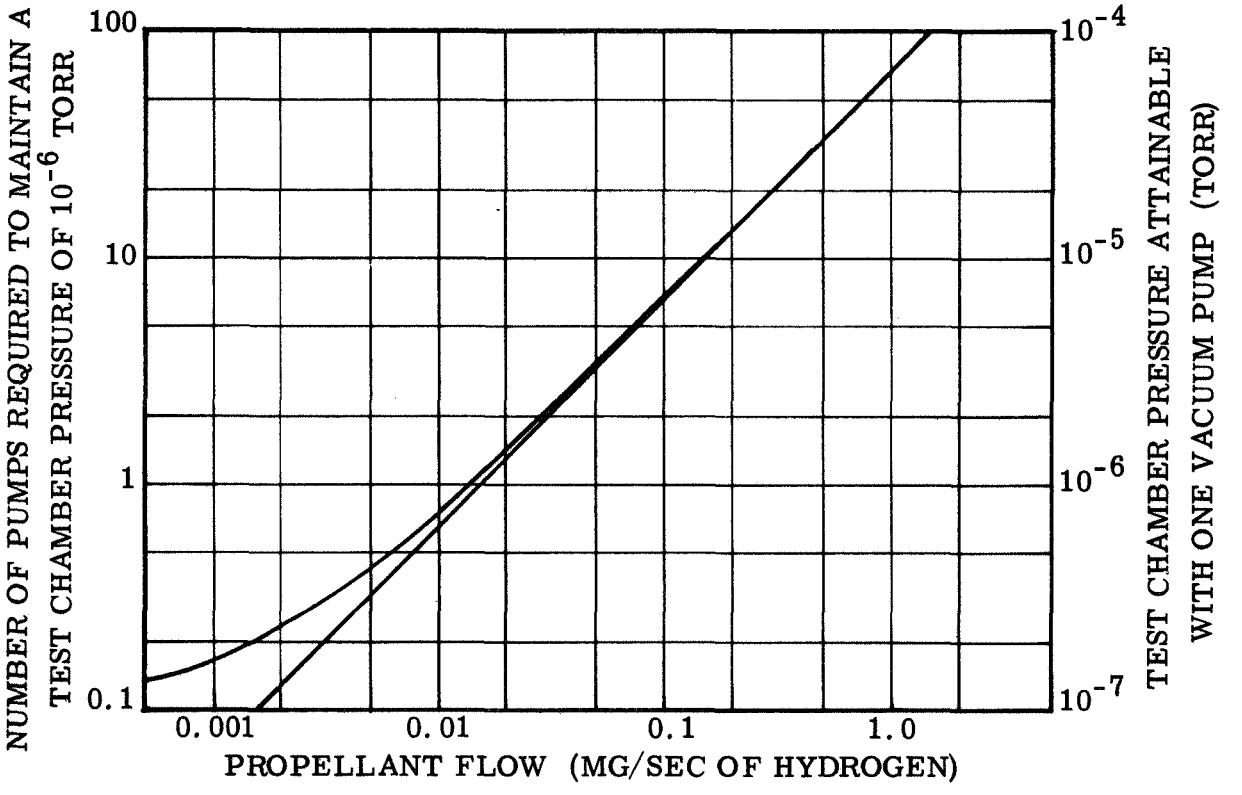

Figure 2. Number of 140,000 liter/sec Pumps Required for 10^{-6} Torr Versus Mass Flow; or One Pump Pressure Attainable Versus Mass Flow

The second reason for working at pressures under 10^{-6} torr is that the stability of operation of the arc is markedly improved in a higher environmental pressure. A thruster tested successfully at higher pressure could turn out to be a complete failure when real space pressure is simulated.

A third situation where higher environmental pressure can alter the test results has been found in the repetitive triggering of pulsed discharges. At very low pressures

an extremely high voltage is sometimes required to initiate the pulse and prevent irregular operation. Again, a successful test at higher pressure could be misleading.

A final reason to operate at pressures under 10^{-6} torr is found in the increased electrode evaporation that occurs when the pressure is very low. This can have an influence on electrode life as well as thruster performance. It is expected that many other effects will be discovered when the limit of 10^{-6} torr is adopted as extensively by other laboratories.

As will be discussed in more detail in Section 4, "The Plasma Head," steady state operation with a continuous flow of propellant requires a very elaborate pumping system to provide the 10^{-6} torr pressure level. When a substantial continuous mass flow is required, cryogenic pumping becomes necessary with the full surface of the vacuum chamber participating in the pumping operation. This approach, which is certainly the most efficient and desirable, reaches its maximum complexity when hydrogen is used as a propellant and liquid helium is consequently needed. On the other hand, it becomes extremely simple when vapors that condense easily at room temperature are used, as for example evaporated solid substances (again see Section 4).

In all these cases it is evident that the evacuation system becomes greatly simplified if pulsed operation is adopted as was done in this investigation, because in the intervals between pulses the vacuum system can provide the necessary pumping to maintain the 10^{-6} torr level. The condensation of the pulsed propellant on the cold walls of the vacuum chamber is particularly convenient in the case of pulsed operation because the extended dimensions of the cold chamber surfaces participate to eliminate reflection of the sudden pressure wave produced by the pulse of evaporated mass (see Section 4).

Because of the foregoing, a strong effort has been devoted to maintaining a working pressure that does not exceed 10^{-6} torr during all tests that relate to this investigation.

2.2 Improvements in the Vacuum System

Our insulating vacuum chamber described in detail elsewhere has been used extensively in recent years and is normally kept in operation 24 hours a day. The facility has given excellent service and to date has required no modifications. The facility consists of a vacuum chamber of fiberglass about 10 by 25 feet connected to a 48-inch diffusion pump (140,000 liters/sec of hydrogen) with the possibility of using various forepumps (from a few hundred to a few thousand liters/sec). For economy reasons the facility does not have a main (48-inch) valve, a main door, or a cryogenic baffle.

The lack of these important accessories produces some important drawbacks in the operation. In particular, backstreaming due to absence of a baffle introduces a certain quantity of oil vapor, making it difficult to reach the minimum pressure during hot days;

while lack of a main valve and a large door add to the difficulty of servicing the test setup. However, estimates of the costs of introducing these desirable accessories are so high that it will not be possible to have them in operation for some time. In the meantime, methods have been found to remedy these deficiencies partially without incurring excessive expense.

Because of the duty cycle adopted with pulses separated by fairly long intervals relative to the pulse length, it has been thought that increasing the forepump vacuum level would produce a reduction in the residual oil vapor. Accordingly, a small diffusion pump has been connected between the main diffusion pump exhaust and the forepump inlet. This improved the forepressure of the main pump at least an order of magnitude, with an appreciable reduction of the oil dispersion. Since this small pump produced satisfactory results, a new diffusion pump has been procured with higher pumping capacity. It is to be installed together with the existing one to obtain a further reduction of oil vapor in the testing chamber.

The use of condensable propellants, together with a small amount of oil vapor in the chamber atmosphere, produce a gradual condensation of film deposits on the windows of the vacuum chamber. The film becomes heavy enough to affect seriously the quality of photographs taken through the windows. Since the chamber is in nearly continuous operation, the deposits are difficult to clean out. To remedy this deficiency, a special window (Figure 3) has been designed which permits the rapid exchange of the transparent quartz

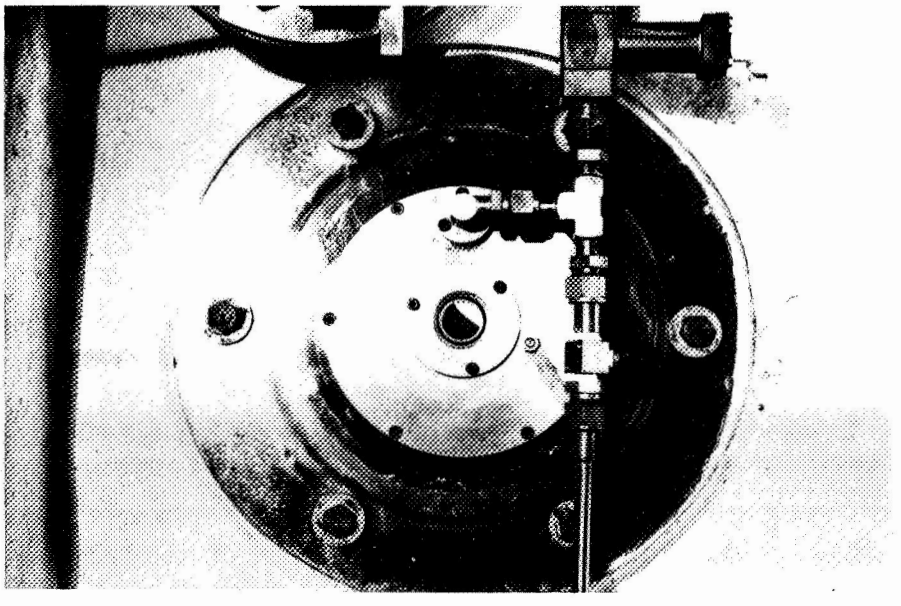

Figure 3. Quartz Window That Can be Cleaned or Replaced Without Affecting the Vacuum Level in the Test Chamber

window which is normally exposed to the interior environment without opening the tank and without influencing the high vacuum level (see Section 4). The design is a simple one involving a flat valve which can be closed on the interior side of the window. It has been in service for over a year and has given very satisfactory results.

Studies have been made of the use of a cryogenic baffle and of methods for cooling the external walls of the chamber, and it is planned eventually to incorporate these features in the facility. An intermediate solution using a plastic tube to be wound around the fiberglass tank carrying a refrigerating mixture has been designed and will be put into operation as soon as time is available. This solution is also expected to have a beneficial effect on the condensation of the residual oil vapor as mentioned before, and on the vaporized propellants as discussed in Section 4.

2.3 Improvements in the Vacuum Manipulations

The test procedure being used requires that the thruster be disassembled so that its components can be measured and weighed after each test or series of tests. This normally makes it necessary to open the vacuum tank and withdraw the thruster. The immediate consequence is the loss of many hours, and even days, before a second test can be initiated because of the long time required to outgas the chamber and reach again the very low vacuum level (around 10^{-6} torr) required. This problem, which appeared early in the program, has been solved with a system which can withdraw the thruster without opening the vacuum tank. The system, which is now in use and giving satisfactory service, is described and illustrated in Reference 1.

The concept is to reach the thruster inside the vacuum tank with a cylindrical tool which can slide through a vacuum-tight conduit with an "O" ring seal. The thruster is disconnected from the thrust stand and clamped to the cylindrical tool with special wrenches controlled from a distance. It is then removed from the tank simply by removing the cylindrical tool, which is larger in diameter than the thruster. A vacuum valve is used to close the opening before the tool is withdrawn past the "O" ring seal. This operation is illustrated on page 40 of the above-mentioned reference. The reverse of this operation permits installation of a new thruster inside the vacuum tank while full vacuum is maintained.

The full operation takes a number of minutes, which is an extremely short time compared to what is necessary when the complete tank must be opened. However, there is still a considerable time loss when hundreds or even thousands of samples must be tested.

To reduce this loss of time, the testing has been divided into two categories; i.e. with and without the measurement of thrust. The first requires a longer installation time but constitutes only a small percentage of the total number of test runs, so a substantial gain of testing time is obtained. To permit this subdivision of the testing, two different

vacuum testing stations have been designed, each one complete and capable of receiving the same thruster geometry.

Special outlets have been installed in the insulating vacuum tank at various angles to the chamber axis as illustrated in Figure 4. These permit rapid installation and removal of the thruster under test and the determination of all performance parameters except thrust. Each outlet is equipped with a large vacuum valve and an "O" ring seal in the cylindrical passage which permits a large "vacuum plug-in probe" with the thruster mounted on its end to be inserted without losing vacuum in the test chamber. Connections to a small vacuum pump permit evacuation of the space between the seal and the valve before the valve is opened. The installation of a thruster to be tested in one of these outlets requires only 60 seconds, and a number of vacuum plug-in probes are available to permit a test sequence using different thrusters to be conducted quite rapidly. The advantage is that a thruster can be taken in and out of the chamber many times to determine electrode consumption rates at different power levels without an excessive loss of time.

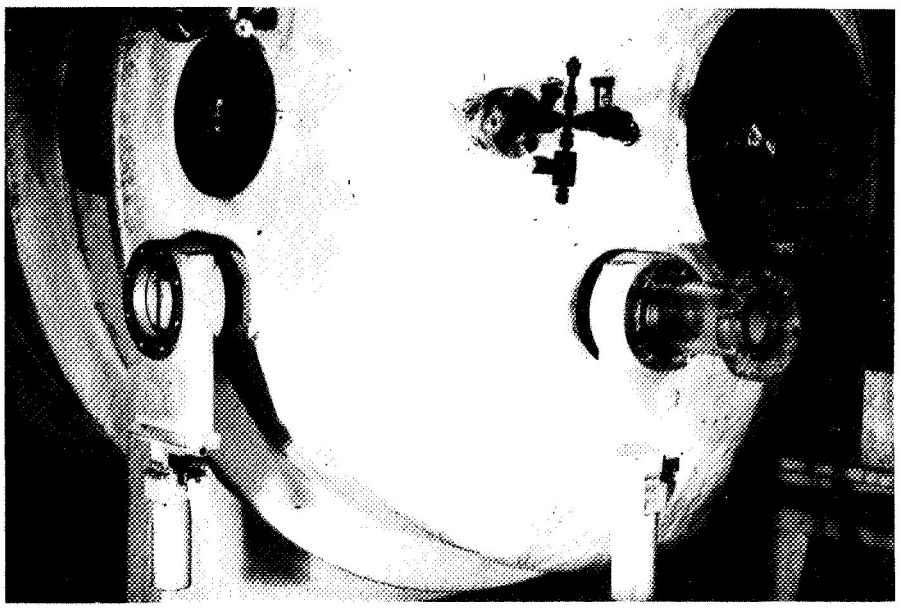

Figure 4. View of the Test Chamber Showing the Outlet Used for Rapid Installation of Plasma Heads When the Measurement of Impulse is Not Required

When thrust must be measured, the thruster is mounted on the regular suspended enclosure which operates as a ballistic pendulum (this is a self-contained unit as described in Section 5). Following the methods described in Reference 1, page 40, a time of about

10 minutes is required, most of which is needed to assure a stable electrical contact between the thruster with its socket. To reduce that time, a new socket arrangement has been developed to assure a very good contact in a fraction of that time. By separating the portion of the test in which thrust is measured, it is possible to install the thruster on the ballistic pendulum once and measure impulse for all of the desired test conditions before removing it again.

Other connections of a similar type have been made to the vacuum chamber to permit rapid introduction and removal of other equipment and instrumentation that must be taken in and out of the tank at frequent intervals. This approach has resulted in a substantial reduction in testing time.

2.4 Calibration and Measurements

The measurement of the vacuum chamber pressure before, during and after the pulse in a range from 10^{-5} to 10^{-7} torr is extremely difficult. Some of the problems involved are listed below.

The test chamber pressure is measured with an ionization gage. The measurement of pressure "before" the pulse involves the least difficulty because conditions are steady at room temperature and the composition of the residual atmosphere of the tank can be estimated or if necessary evaluated using a mass spectrometer type of instrument. The residual atmosphere of the tank is composed of a mixture of gases and vapors which poses a problem since the calibration of the instrument is sensitive to the composition of the tank fluid. Unfortunately, instruments of this kind have not been calibrated in sufficient detail to cover the required range, but it seems likely that this deficiency can be corrected in the future by extending our knowledge of the response of existing instruments.

The most difficult measurement is one needed to determine the variation of tank pressure during the pulse period. In this case the sudden "explosion" of the vaporized propellant introduces a series of new parameters which can influence the measurement; for example, the increase in temperature, the presence of ionization and the expansion of completely different gases due to vaporization. These and perhaps other transient parameters present a continuously changing pattern in an interval lasting a fraction of a millisecond and make the detection and recording of the variation of the tank pressure a very sizable task.

The same situation is encountered to a lesser extent after the pulse period during the gradual return to pre-pulse conditions. The recording of the pressure during this time can provide interesting information on the completion of the cycle and the recondensation of the vaporized propellant.

Our work in the recording of the vacuum chamber pressure and its variation during the pulsed cycle is still in a primitive stage. The effects of the sudden increase of temperature, ionization and vaporization during the pulse have been observed, but not interpreted quantitatively. Results, which are reported in the last part of this section, are subject to the uncertainties discussed above.

The ionization gages are normally connected to the vacuum chamber through a liquid nitrogen trap to reduce the formation of deposits on active elements of the gage. Their indication is directly observed or recorded. To follow the variations during the pulse the use of a regular cathode ray oscillograph is contemplated. Further work along these lines is considered useful for studying detailed characteristics of the pulse.

2.5 Test Results on the Vacuum Chamber

As mentioned earlier, the vacuum facility has been performing satisfactorily with nearly continuous operation during several years of service. An average vacuum level of 4×10^{-7} torr has been obtained and maintained repeatedly during periods when propellant is not added. During the night and the periods of non-testing activity, the main diffusion pump is operated in a standby position with the 100 liters/sec diffusion pump left in operation followed by a 50 cfm mechanical pump. The vacuum level in the chamber remains practically unchanged with this configuration. During the summer when the temperature in the room containing the vacuum tank rises above 30°C, the vacuum level in the chamber is reduced to about 1×10^{-6} torr. To avoid this, an economical cooling system for the vacuum chamber is contemplated for future applications.

During pulsed operation, it has been found that the pressure in the vacuum chamber increases as the amount of electrical energy discharged in each pulse is increased (see Section 5.6). Quantitative measurements of this behavior will be attempted as soon as preparation of a high speed oscillographic recording system is completed. Measurements of the distribution of the chamber temperature before, during, and after the pulse will also be attempted.

The practical use of the "vacuum plug-in" probes has been tested successfully on hundreds of occasions with no incidents of vacuum loss. An automatic system is continuously in operation to provide an alarm and switch off of the pumping system if vacuum should be lost. The facility has been in operation to date for 1600 hours in full power and for 10,000 hours in standby.

3.0 THE POWER SUPPLY

3.1 The Energy Storage Medium

The purpose of this program is to learn as much useful information as we can about the operation of quasi-steady MPD thrusters in a limited time period and with a limited investment. From this point of view, some of the components selected may not represent an optimum choice for practical applications. This may possibly be the case in the selection of electrolytic capacitors for the main energy storage system. In Reference 1, Section 2.2, some discussion of the reasons for their choice can be found, but we would like to underline here again the main considerations that led us to their selection.

The classical length of a quasi-steady pulse has been fixed somewhat arbitrarily at around one millisecond. One of the program goals is to operate with energies ranging from 250 to 20,000 joules per pulse, which gives a peak power varying from 0.25 to 20.0 megawatts. Considering an arc impedance around 5 milliohms and a similar total circuit resistance, the currents will vary between 5 and 50 kiloamps and the voltages between 25 and 200 volts. Having decided to avoid the use of a coupling transformer to match the power supply to this extremely low impedance load, the most suitable energy storage media appear to be flywheel generators, storage batteries and electrolytic capacitors. For the sake of simplicity, economy and availability on the market, the last solution was adopted. It is evident from the nature of the electrolytic capacitor that their adoption entails certain drawbacks including high internal resistance, limited maximum voltage, presence of an electrolyte, limited working temperature, leakage current, etc. It is clear also that these drawbacks would preclude use of electrolytic capacitors (at the present state of the art) for routine space applications, except in particularly favorable cases.

However, their choice has proved to be quite advantageous from the standpoint of providing compact packages ranging from a few hundred to tens of thousands of joules at voltages ranging from 50 to 500 volts and with currents from 1 to 100 kiloamps, all from standard components available on the market on relatively short notice. After several years of testing it is also evident that for the moderate duty cycle used, their working conditions are conservatively rated. Not a single failure has been recorded. For these reasons the original favorable opinion on the use of electrolytic capacitors for laboratory testing in low impedance pulsed operation is confirmed and their use can be recommended for future applications with similar goals.

It is necessary, however, to be sure that the duty cycle selected will not result in overheating of the capacitors due to their high internal resistance. To establish practical duty cycle limits, small capacitor banks were tested in special calorimeters and the capacitor temperature variation was determined as a function of the energy per pulse and the pulse series duration. These tests are described in Sections 3.3 and 3.5.

It is interesting to compare the volumes of the electrolytic and paper capacitors for the same operating voltages of 450 volts and energy storage of 100 joules as illustrated in Figure 5. The graphs of Figures 6 and 7 compare the specific weight and volume of electrolytic and paper capacitors as a function of voltage.

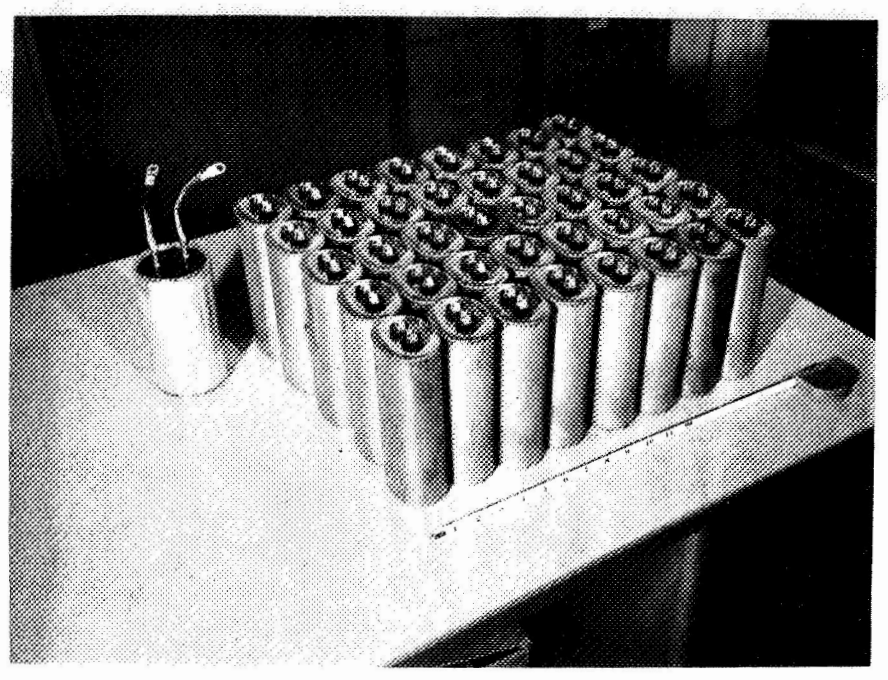

Figure 5. Volume of Electrolytic and Paper Capacitors for the Same Energy Storage

The net superiority in weight and volume of the electrolytic capacitor cannot be considered as an advantage for practical applications until some of the drawbacks of the electrolytic type have been eliminated. While a substantial improvement may be considered as likely as the state of the art advances, a major difficulty that will remain using either type of capacitor at the very high current levels required, is the high resistive losses that occur in the connecting circuit. Reduction of these losses is an important task and will be considered in the next section.

1) General Electric 86F161M - 32,000 μF at 40 V
2) Sangamo DCMX658023 - 5000 μF at 100 V
3) Sangamo Type 500 - 4800 μF at 200 V
4) Sprague Powerlytic 36D - 2500 μF at 350 V
5) General Electric 86F246M - 1250 μF at 450 V
6) Sprague Compulytic 32 D - 900 μF at 450 V
7) General Electric 49F 1930G5 - 25 μF at 330 V a. c. (say 500 V d. c.)
8) Aerovox P8292 ZN31 - 1 μF at 600 V

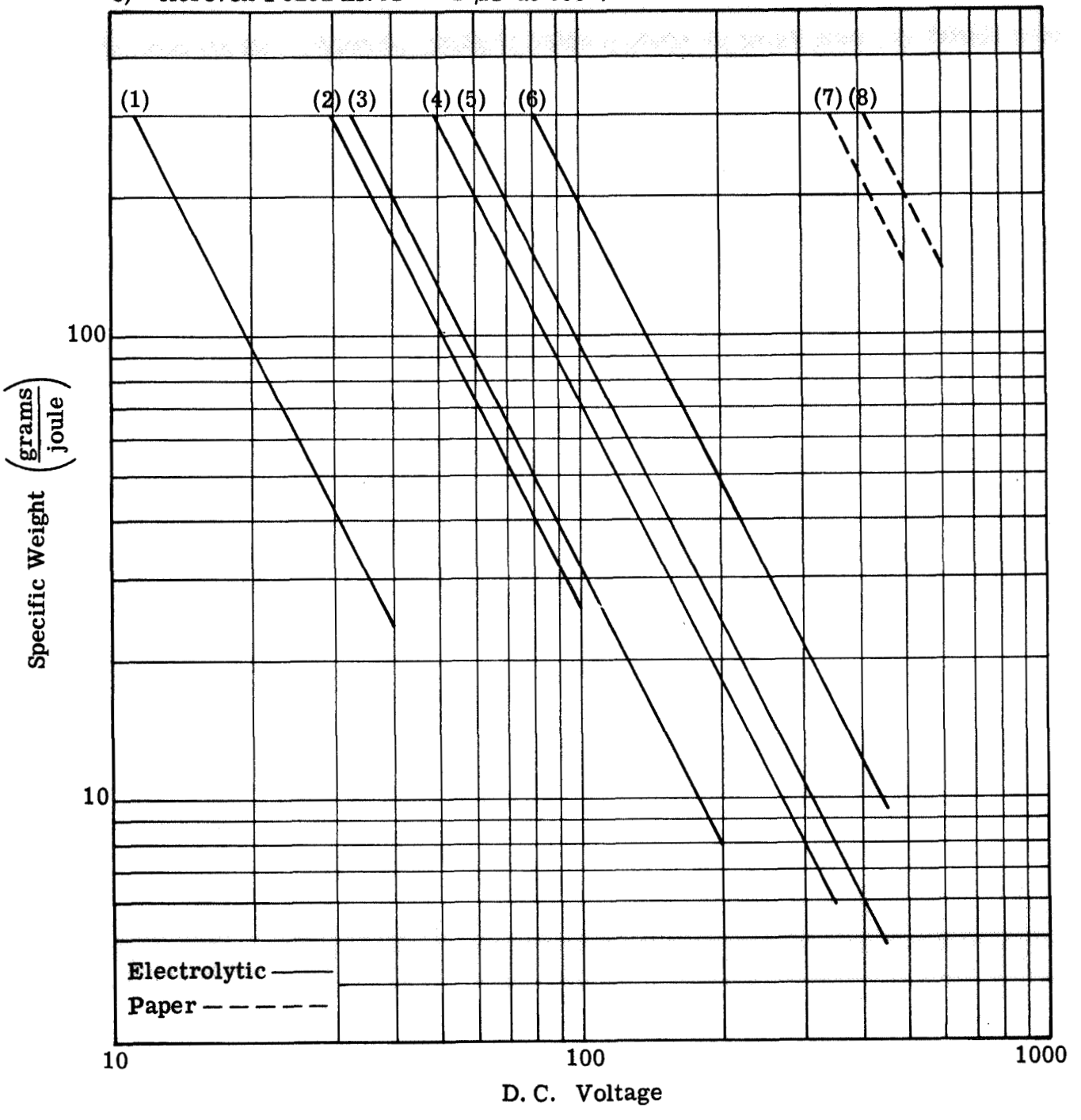

Figure 6. Comparison of Specific Weights of Some Electrolytic and Paper Capacitors

1) General Electric 86F161M - 32,000 μF at 40 V
2) Sangamo DCMX 658023 - 5000 μF at 100 V
3) Sangamo Type 500 - 4800 μF at 200 V
4) Sprague Powerlytic 36D - 2500 μF at 350 V
5) General Electric 86F246M - 1250 μF at 450 V
6) Sprague Compulytic 32D - 900 μF at 450 V
7) General Electric 49F1930G5 - 25 μF at 330 V a.c. (say 500 V d.c.)
8) Aerovox P8292ZN31 - 1 μF at 600 V

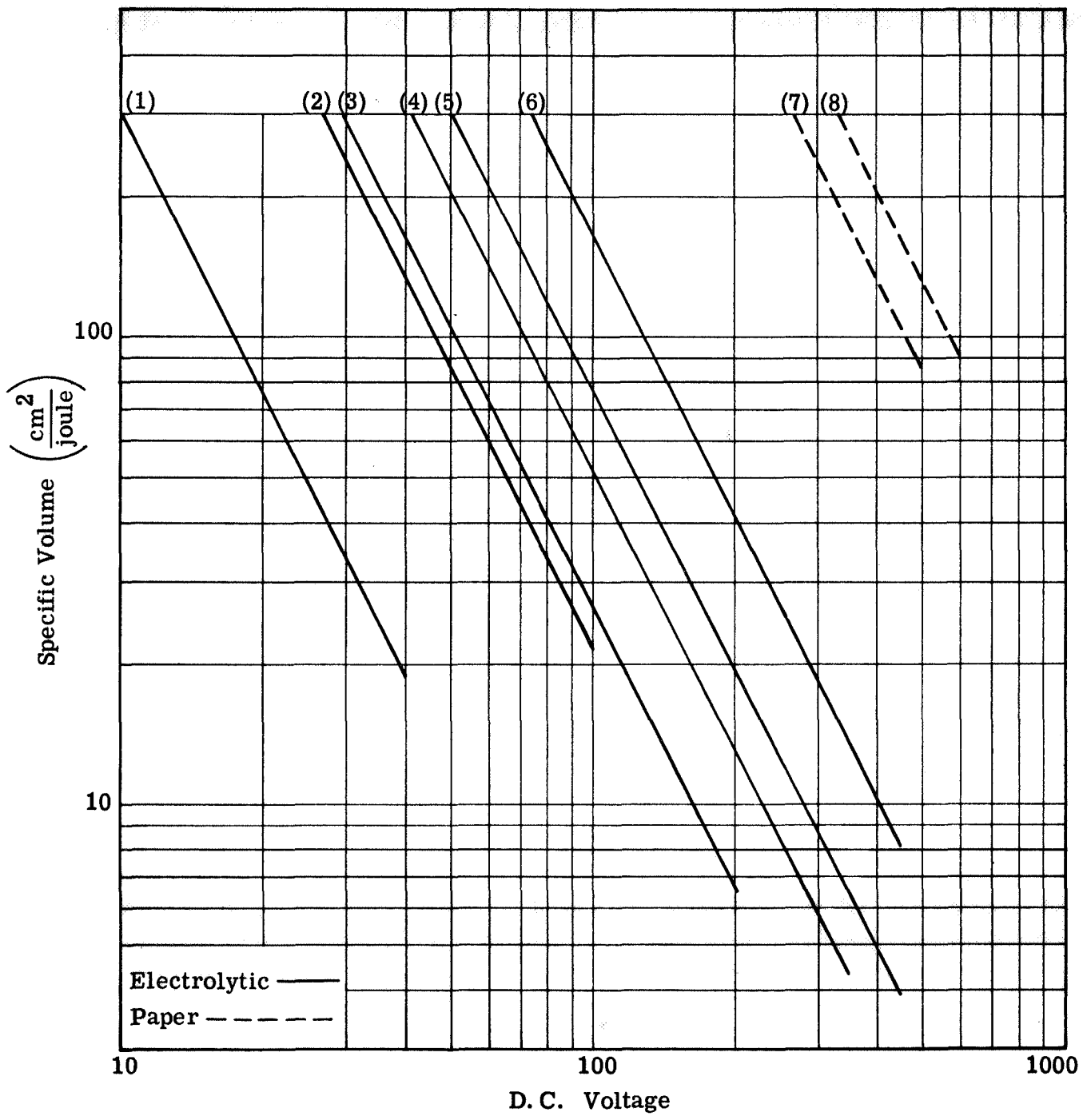

Figure 7. Comparison of Specific Volumes of Some Electrolytic and Paper Capacitors

3.2 The Pulse Generating Network

Experimental work with pulse generating networks has continued fairly steadily during this program. Although there are existing techniques for designing networks to generate desired pulse shapes, we have an unusual requirement in the respect that the network must be exceptionally compact and light so that it can be mounted directly on the torsional ballistic pendulum. A large amount of energy must be stored to assure that the full potential of quasi-steady MPD thrusters is realized (high power operation for a long enough period to establish steady operating conditions). In line with the philosophy of determining the performance potential of this type of thruster as rapidly as possible, innovations have been introduced to permit high energies to be stored in a small light package. Electrolytic capacitors housed in a pressurized canister were introduced in the initial phase of the program.[1] Since that time, the study has focussed on reducing the large heavy induction coils used to shape the pulse with minimum resistive loss. To do this, a departure has been taken from the conventional ladder type network.

The circuit inductance and capacitance required is determined by the arc impedance, and the pulse duration desired. For an ideal network with matched impedance, the following relations apply;[5]

$$T = 2\sqrt{L_N C_N}$$

$$Z_{arc} = \sqrt{\frac{L_N}{C_N}}$$

which are sufficient to establish L_N and C_N if T and Z_{arc} are known. From self field theory, arc impedance depends primarily on specific impulse, and can be expected to be reasonably constant if propellant flow is proportional to power (which tends to be the case when the propellant is electrode vapor). Test observations confirm that the average arc impedance is nearly constant for this type of thruster. It follows that the power level is simply a function of network voltage when the pulse is initiated, and does not affect the desired circuit characteristics. The desired network inductance and capacitance are fixed quantities for a given thruster, and the network size can be reduced only by reducing the size of the elements that provide the inductance and capacitance.

In a ladder type network, separate induction coils are used between each condenser. Ideally, a wave travels down the ladder, discharging the condensers in sequence. Most of the coils see either full current or zero current. Induction effects are important only in the region near the capacitors that are discharging. Large heavy coils are needed to supply the required inductance without flux linkages between them. On the other hand, if the circuit is deliberately designed to give maximum mutual inductance, it has been found

possible to obtain the required circuit inductance without using any coils. The bus bars connecting the capacitors can be arranged to provide enough inductance with little more conductor length than is needed to connect the capacitors. The result has been a substantial reduction in size and weight combined with a simultaneous reduction in resistive power loss. Although the new circuits depart from the original ladder type of geometry, it has been found possible to maintain pulse shapes very close to those given by the earlier networks. This has been accomplished by a largely experimental approach.

If we have a given length of conductor available, increased inductance is obtained if the leads are arranged so that the current in all of the leads circles about a center point in the same direction. Figure 8 illustrates how this would be accomplished in a simple case with three rows of capacitors. The flux linkage between the inner pair and the outer pair of conductors provides a mutual inductance effect that adds to the circuit inductance. Notice that the current in all of the leads circulates in a clockwise direction, and the highest current is in the outer pair of leads. Some experimental networks which were designed in a similar manner are shown in Figure 9.

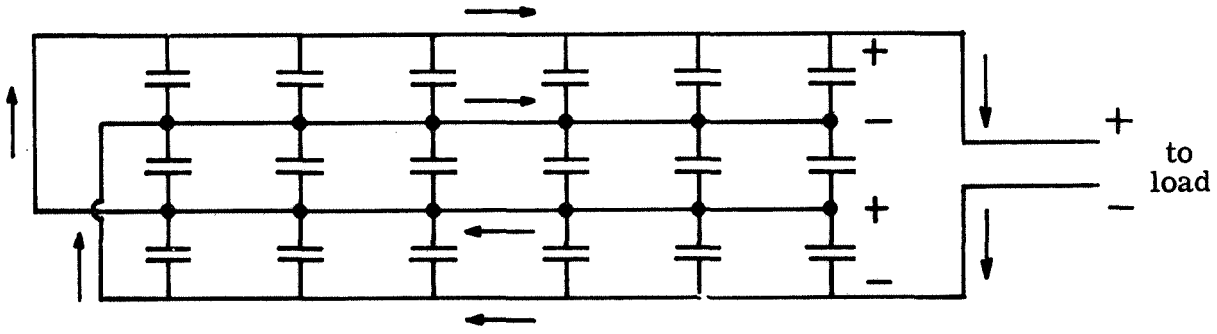

Figure 8. Arrangement of Conductors Connecting Three Rows of Capacitors in a Manner that Increases Network Inductance

The shape of the loops formed by the conductors is also of importance. Approximate expressions for the inductance of single coils is given, for example, in Reference 6. From these relations, the inductances of rectangular coils with the same perimeter but different length to width ratios were calculated and are shown in Figure 10 expressed as a ratio of the inductance of a circular coil having the same number of turns, coil cross section, and conductor length. This curve illustrates the desirability of arranging the capacitors in a pattern that allows the conductor loops to be nearly square - or better still, nearly circular.

Another conclusion can be drawn by examining the form of the above equations. In both expressions the inductance is seen to be proportional to the size, or a characteristic

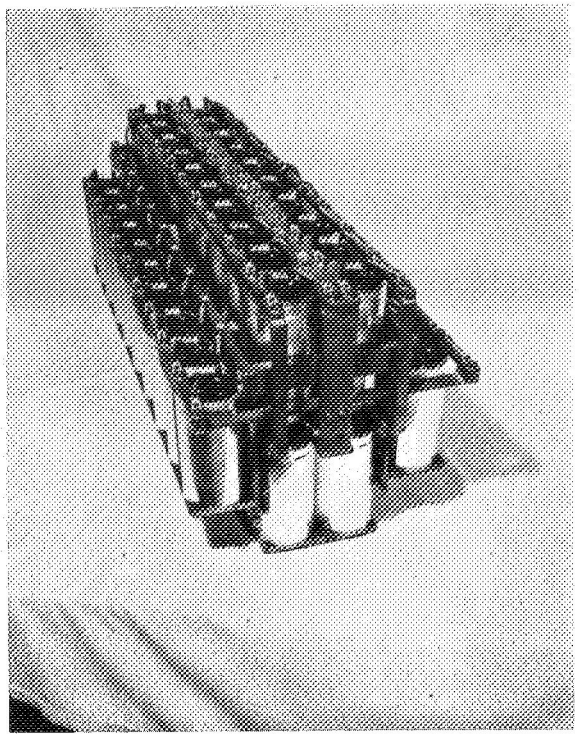

Top Front View

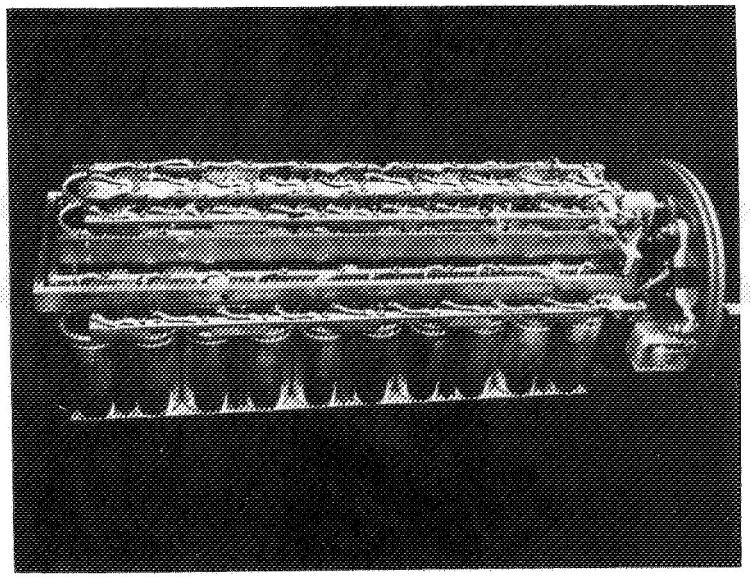

Side View

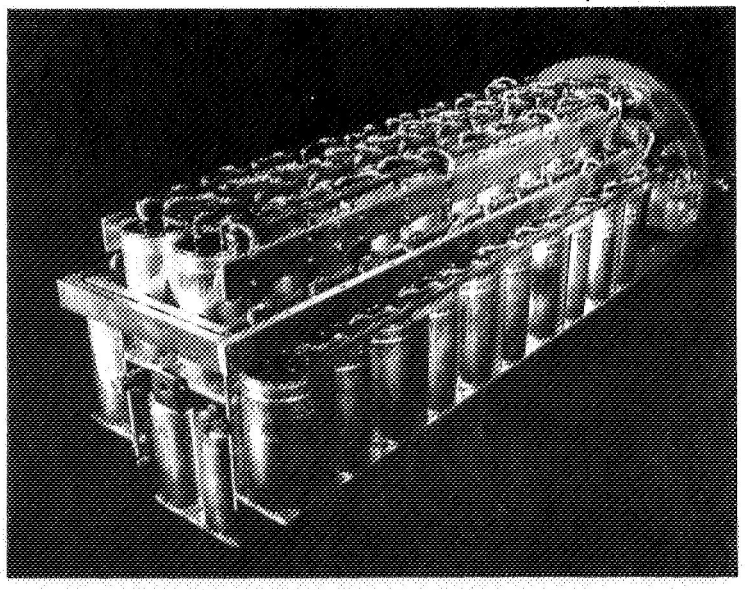

Back Side View

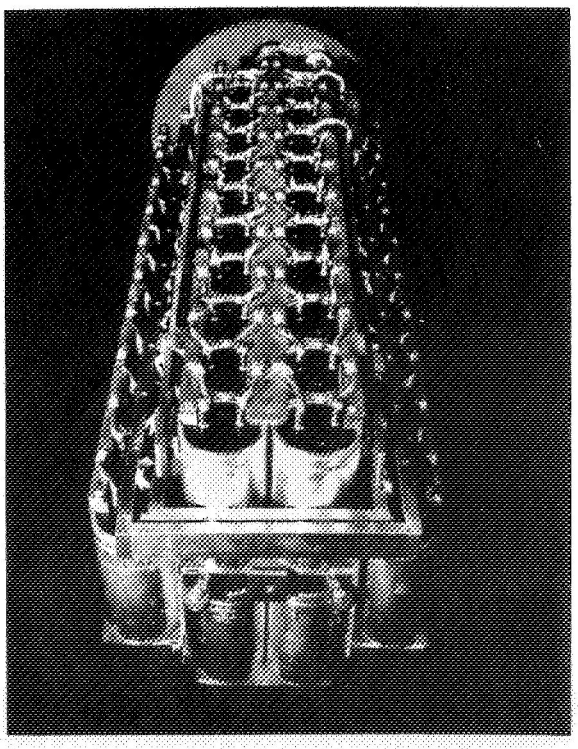

Top Back View

Figure 9. 5000-Joule Capacitors Packages Showing Connections for Variations of Inductance

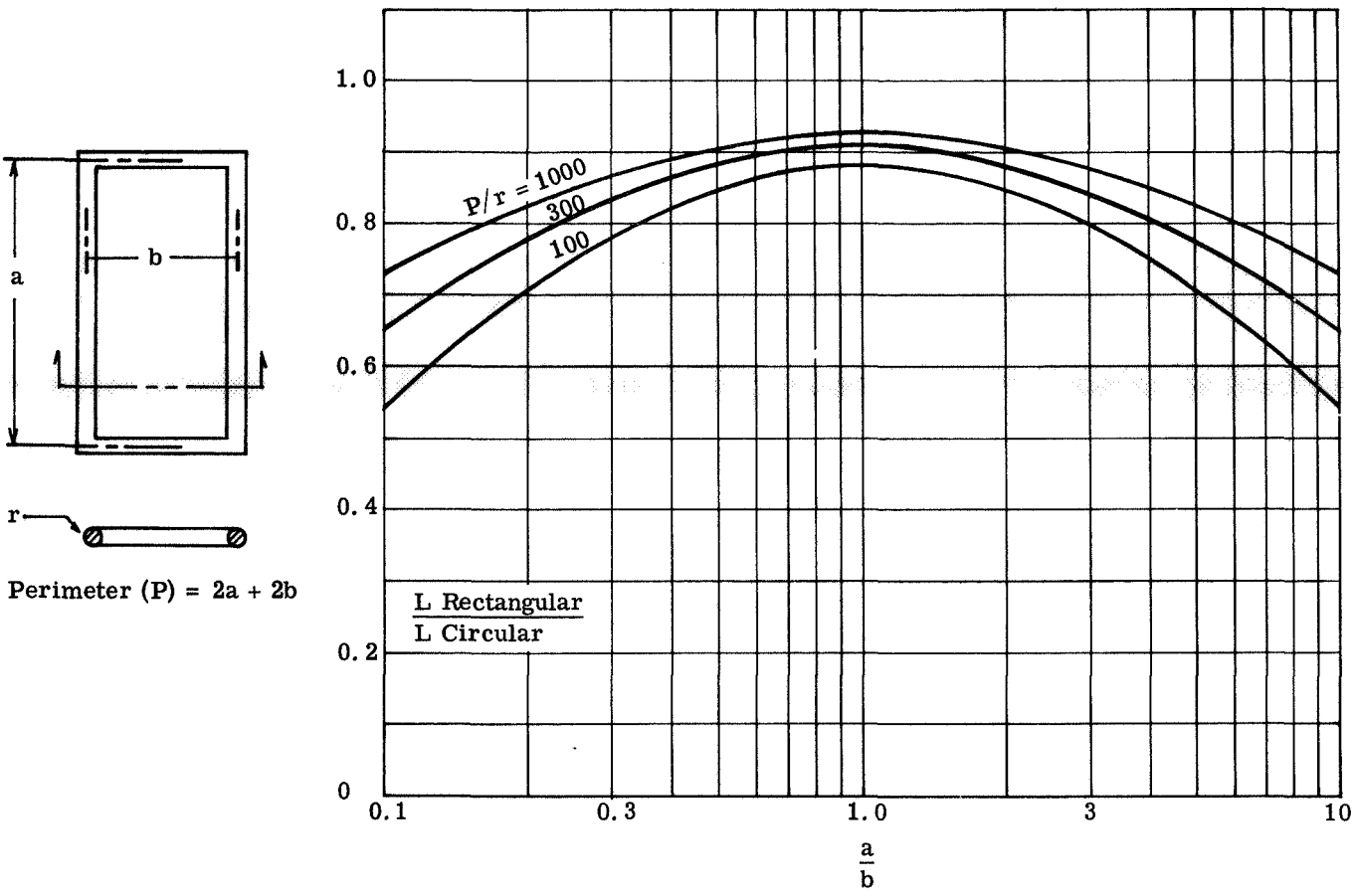

Figure 10. Effect of Coil Shape on Inductance (Compared to a Circular Coil of the Same Cross-Section, Perimeter and Number of Turns)

dimension of the coil, while at the same time it is proportional to the square of the number of turns. By stacking the capacitors as closely together as possible, it may be possible to reduce the size of the loops with a corresponding increase in the number of turns that are used in forming the connections. The result would be a net increase in inductance. An experimental network using a closely packed spiral pattern of capacitors is shown in Figure 11. With circuits that depend on the bus bar geometry for inductance, pulse shaping is accomplished by moving the connection point of the flexible capacitor leads to different locations on the bus bar. When the connection spacing is widened, more of the bus bar is utilized for inductance in that particular mesh. The action is similar to that obtained with the rail and slide type of adjustment used with ladder type networks and reported in Reference 1. The effect is, of course, complicated by mutual induction and would be tedious to evaluate analytically; however, the experimental approach was found to be reasonably tractable.

The value of the impedance of the arc discharge is typically around 5 milliohms or less. To avoid excessive resistive loss, it is necessary for the total circuit resistance to

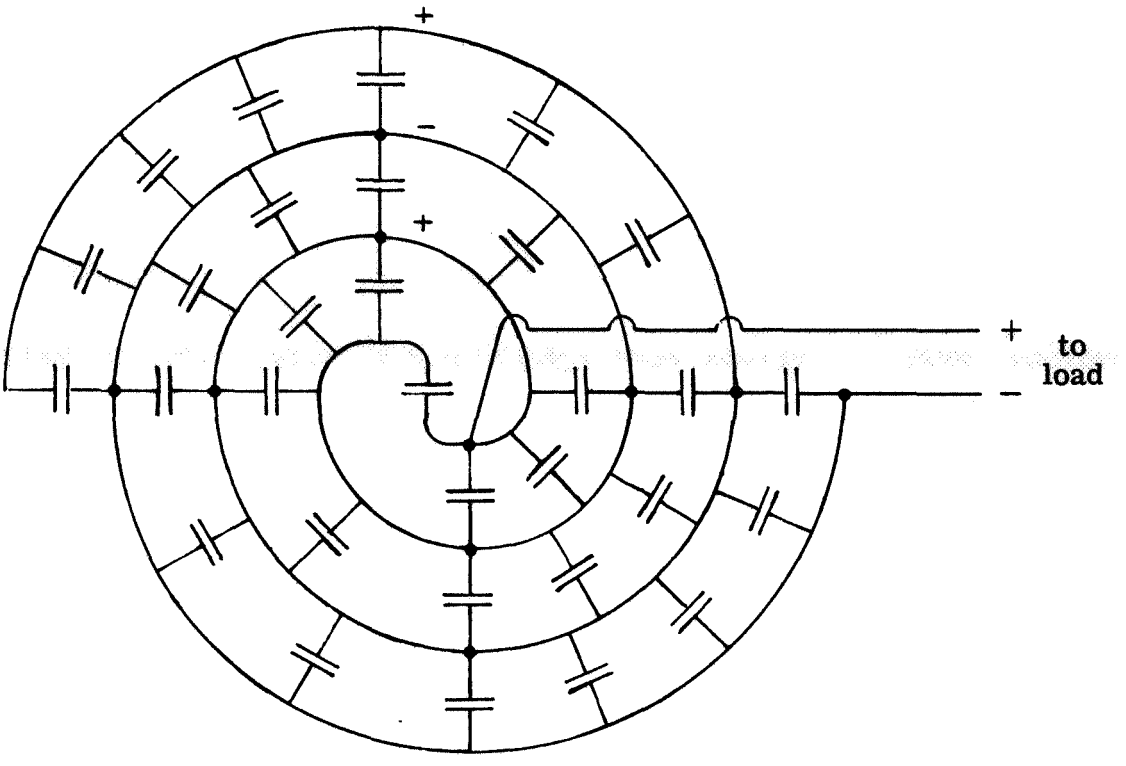

Figure 11. An Experimental Pulse Generating Network With Capacitors Closely Packed in a Spiral Pattern to Allow Connections that Increase Bus Bar Inductance

be a small fraction of that value. To accomplish this, heavy conductors are required. The weight of the pulse generating network as well as its volume can be reduced substantially by carefully designing the circuit to minimize the length of conductor required to join the capacitors and provide the necessary inductance. The importance of the copper bus bar weight can be shown best by an example. Consider a bank of 60 capacitors with a conductor length between capacitors of 10 centimeters. The total length of the positive and negative conductor (with no separate induction coils) is 1200 centimeters. Taking a resistance of 0.25 milliohms for the conductor (5 percent of the arc impedance at the least), the cross section of copper needed is given by:

$$A = \frac{\sigma \ell}{R} = \frac{1.724 \times 10^{-6} \text{ ohms cm } 1200 \text{ cm}}{0.25 \times 10^{-3} \text{ ohms}} = 8.28 \text{ cm}^2$$

which for a constant area bus bar would give copper weight equal to;

$$\text{weight} = 1200 \text{ cm } 8.28 \text{ cm}^2 \; 0.00889 \; \frac{\text{kg}}{\text{cm}^2} = 88.3 \text{ kg}$$

For comparison, the capacitors weigh 0.86 kg each or a total of 52 kilograms. The capacitor bank must fit into a canister of limited size (it must be passed through a 20-inch port for installation). This requirement, combined with the large mass of copper required to keep the losses acceptable, has made it necessary to make a rather careful study of the design of the pulse generating network.

The fact that better thruster performance can be expected at high power levels is probably the primary reason for experimentation with quasi-steady MPD thrusters. Accordingly, a strong effort has been made to increase the range of power levels that can be used during a pulse so that the effect of power on performance can be assessed. Power can be increased either by shortening the pulse duration or by increasing the size of the capacitor bank (and its operating voltage). Since the quasi-steady philosophy requires a pulse duration of the order of one millisecond to provide steady operating conditions for a large fraction of the pulse duration, it was decided to enlarge the capacitor bank. The initial experiments reported in Reference 1 used a capacitor bank of about 20,000 microfarads, and a compact arrangement has been developed so that the enlarged bank can still be housed in the gas tight canister that serves as the inertia element of the torsional ballistic pendulum.

Actually, capacitors are on hand to provide a four-fold increase in pulse energy (200,000 microfarads), but it has been found impractical to mount a network this large on the platform of the pendulum. It is essential to house the capacitors in a pressurized enclosure to prevent shortened capacitor life and reduced vacuum capability due to evaporation of the electrolyte, and to avoid accidental arcing between leads. A pressure of one atmosphere is used which requires a compact cylindrical canister to withstand the pressure difference. There is a practical limit to the size of network that can be housed in this canister. Work is continuing on the setup for testing with a 200,000 microfarad capacitor bank. Initial tests will be made without impulse measurement. Details on this work can be found in Section 5.3.

A major part of the work on the pulse generating network has been directed toward developing a package that gives the required pulse shape and is still compact enough that a 60,000 microfarad unit will fit into the canister.

3.3 Improvements in the Instrumentation

The power supply package must operate in a sealed envelope suspended in the vacuum tank, as will be described in a later section. Numerous flexible leads transmit information on the principal operating parameters from the sealed package to the instrument panel, as for example the charging current and voltage, the inside pressure and temperature, discharging current and voltage, the number of pulses, the triggering signals and their values, etc.

Some of these connections are straightforward while others are more critical, depending primarily on the level of the output signal. Difficulties have been encountered with low level signals (such as the millivolt signal from the discharge current shunt) because of radio interference and parasitic circulation between the grounded parts. This particular circuit required a considerable amount of experimental work before the desired accuracy was achieved. Most of the measurements must, of course, be conducted during the high current discharge period when high frequency oscillations, over-voltages and strong induction effects are present. Attention was therefore directed to increasing the strength of the signals as much as possible and improving the grounding and shielding of the instrumentation circuits. Although further improvements can be made, the quality of the measurements obtainable with the present circuiting is sufficient to assure reproducible readings.

Most of the delicate readings are taken with cathode ray oscillograph recorders, working quite far from the position where the signals originate. These instruments have their own ground connection, and some difficulties have been found in the inevitable unbalance of these grounds. Balanced symmetrical and ungrounded oscillograph connections would have been preferable, but it was not possible to procure new instrumentation. This obliged us to eliminate the ground at the remote side whenever possible.

Another important difficulty which was not completely solved is the measurement of discharge voltage at the tip of the electrodes. This measurement would have required multiple connections located in the hot region of the discharge. To obtain an accurate determination with the existing connections, a correction factor must be applied taking into account the drop of voltage in the last part of the arc circuit, most particularly along the carbon electrodes themselves.

When it is desired to measure the current in very short electrical pulses, a common technique is to use a current transformer or Rogowski coil[7] to give a signal proportional to the rate of change of current. In essence, interference effects are utilized to provide the measurement, so the effects do not have to be eliminated. A disadvantage is that the signal must be integrated to determine the value of current. This complicates the circuitry and can introduce additional errors - particularly near the end of a long pulse. A conventional shunt is therefore more satisfactory when one can be used without difficulty. With quasi-steady thrusters the pulses are long enough that it is practical to obtain accurate measurements with a shunt. The decision was therefore made to concentrate on developing shunts and circuit arrangements that will minimize the response of the current signal to high frequency components.

Figure 12 shows the original shunt used. This is a standard 500-amp, 50-millivolt unit. A momentary 10,000-amp discharge there produces a signal of one volt. This resistive loss is acceptable and the pulses are short enough that the shunt does not overheat. The advantage of the high resistance shunt is a greatly improved signal to noise ratio.

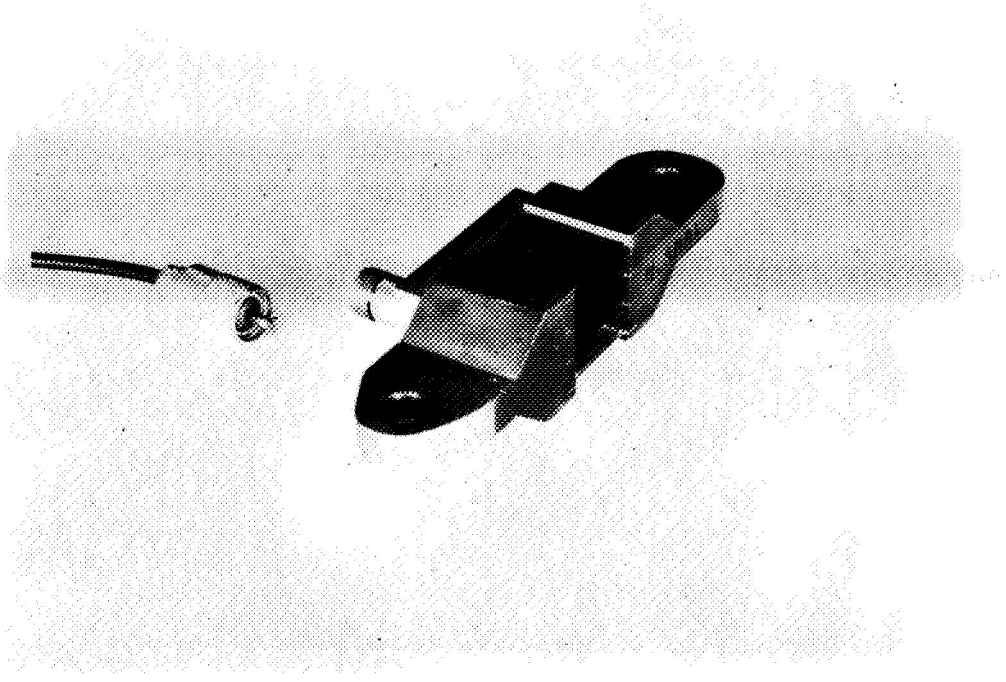

Figure 12. Conventional Shunt Adapted for Attachment of Coaxial Cable

The disadvantage is that the high resistance of the shunt enters as an appreciable percentage in the total connecting network resistance increasing the total losses somewhat. Other solutions are therefore being considered. The brass bar attached to the shunt is a fitting for connecting a coaxial lead. The bar also completes the circuit joining to the other side of the shunt and forming a loop of minimum size. Some interference is picked up by this remaining loop.

Recent studies[7, 8] have demonstrated that shunts can be constructed with extremely low inductance. To further refine the pulse current measurement, the coaxial shunt shown in Figures 13 and 14 was constructed. The arrangement is basically identical to that shown in Figure 6 of Reference 7. The current to be measured passes up through the outer cylinder and back through the inner cylinder. The inner cylinder is the active element of the shunt. It is constructed of constantan to minimize temperature effects and has a resistance of 2×10^{-4} ohms producing a signal of 2 volts when the current is 10,000 amps. The instrumentation leads are coaxial and pass down the center of the inner cylinder connecting to either end of the shunt section. This forms a torus shaped conducting path resembling a current transformer between the connections. The two cylinders carrying current in opposite directions have the effect of cancelling the magnetic field produced in the space occupied by the instrumentation leads so that with truly uniform current distribution no interference effects would result. True symmetry of the coaxial elements would also lead to

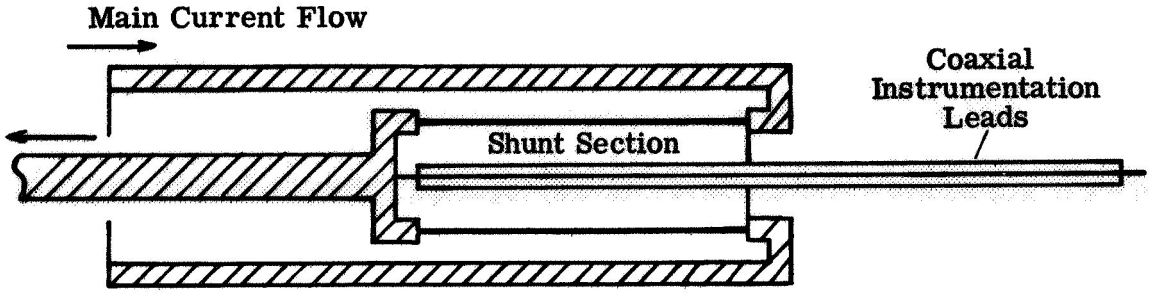

Figure 13. Schematic Arrangement of the Coaxial Shunt

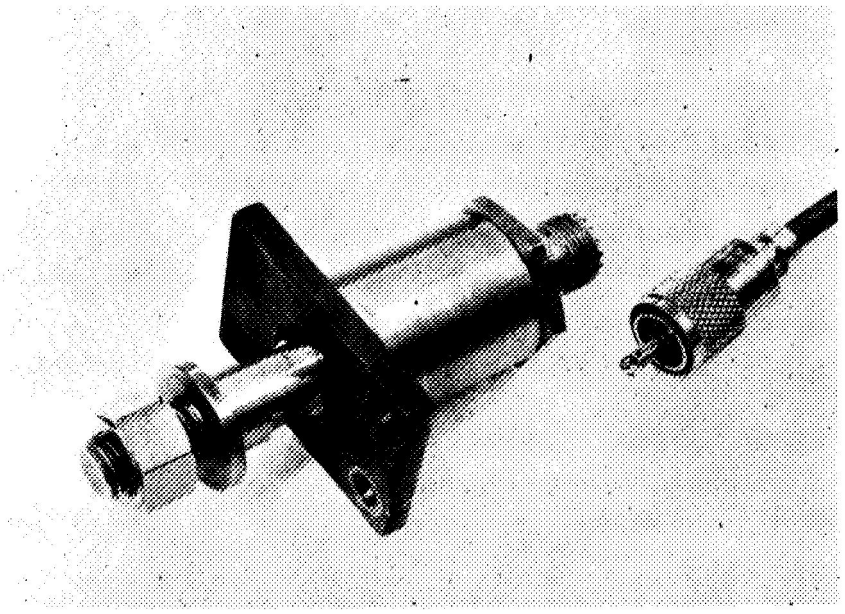

Figure 14. The Coaxial Shunt

insensitivity to changing magnetic flux originating in other (unsymmetrical) parts of the circuit. To minimize possible residual effects, the shunt terminals are arranged so that connecting conductors can be branched in a pattern that is symmetrical about the shunt axis.

As pointed out in Reference 7, it is desirable to have the resistive element of the shunt thin compared to the skin depth so that the shunt resistance will be essentially independent of frequency. This consideration can set the shunt diameter since large diameter thin cylinders have reduced skin effect for the same resistance (see Figure 12-154 of Reference 6). For example, if we want reasonable response with a frequency of 10,000 cycles per second, we find:

$$\text{skin depth} = \frac{1}{2\pi}\sqrt{\frac{10^9\rho}{\mu f}} = \frac{1}{2\pi}\sqrt{\frac{10^9\ (44.1 \times 10^{-6}\ \text{ohm cm})}{1.00\ (10,000\ \text{cycles/sec})}} = 0.334\ \text{cm}$$

An examination of the relations between resistance ratios and conductor geometries shows that a thin walled cylindrical conductor with wall thickness equal to the skin depth would introduce an error of about 10 percent, while the use of half that thickness would reduce the error to around 2 percent. In our application this accuracy can be obtained in combination with the desired shunt resistance by using a tube 3 cm long, 1.43 cm in diameter and 0.167 cm in thickness. Thin foil type shunts are not required for the measurement of pulses one millisecond in duration.

Leads for sensing arc voltage are connected directly to the thruster electrodes to minimize line drop errors, which are appreciable with the high pulse currents. Interference effects are less of a problem for this set of leads because the signal is the full arc voltage (25 to 120 volts). Nevertheless, coaxial leads are used except for the short section needed to span between the electrodes. Since the voltage level is moderate and the RC response time of the leads is short compared to the pulse duration, there are no unusual problems associated with the measurement of pulse voltage.

Current and voltage signals during the pulse are recorded by photographing the screen of a dual trace oscilloscope. The sweep of the oscilloscope is triggered from the arc triggering circuit which gives satisfactory timing. It was found that a signal from the pulse generating network starts the sweep a little late so that part of the slope of the initial rise is lost for each pulse. On the other hand, a signal from the circuit that initiates the pulse would start the sweep too soon because of the time delay in the electromechanical arc triggering device. A signal from the arc triggering circuit is obtained using a ring type transformer around one of the conductors in that circuit.

As pointed out in Section 3.1 (page 14), it is considered desirable to measure the losses and heating rates for the electrolytic capacitors used in the pulse generating network. Two approaches have been adopted: 1) a separate calorimeter (as described below), and

2) a direct measure of the temperature rise of the capacitors in the suspended canister of the ballistic pendulum.

In the first case, the capacitor (or capacitor bank) to be tested is enclosed in a calibrated calorimeter (Figure 15) and repetitively discharged under particular working conditions. The frequency of discharge is one cycle per second and any of the four standard voltages (100, 200, 300, 400 volts) are used. The discharge is made across a low resistance, low inductance circuit without attempting to simulate quasi-steady conditions. For this reason, the discharge is shorter with a higher peak current and somewhat more severe heating than would be expected in actual service. The rise in temperature after a certain elapsed time or after a certain number of discharges is correlated with the rise of temperature produced by internal resistors under steady known d. c. power. Results allow pulse duty cycles to be selected that will not result in excessive heating of the capacitors. At the same time, information is obtained on the fraction of the pulse generating circuit loss that can be attributed to the capacitors. Tests have also been made comparing losses generated by electrolytic and paper capacitors so that a comparison can be made of efficiencies obtainable with the two types of capacitor banks.

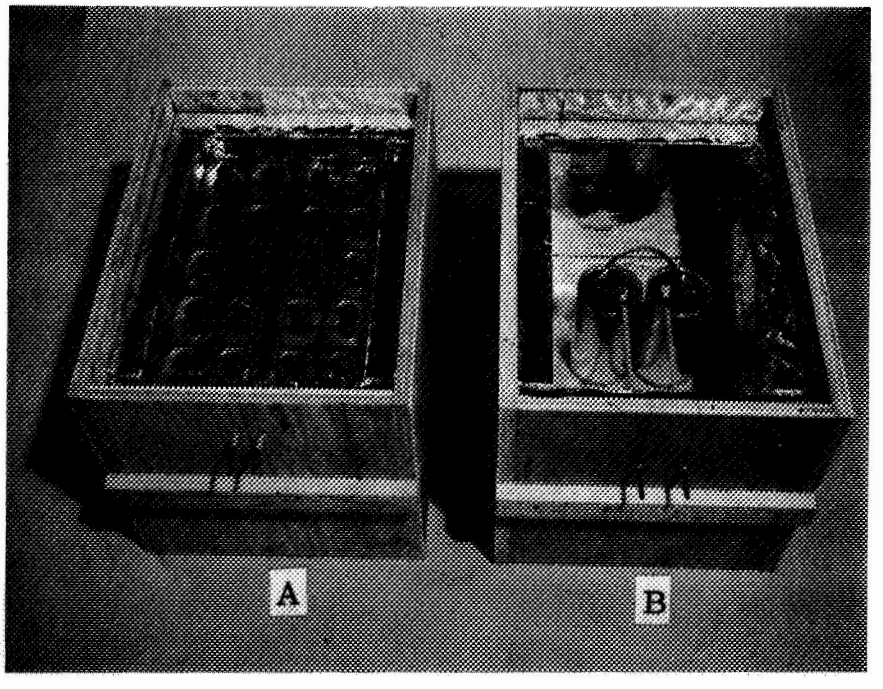

Figure 15. Calorimeters to Compare Total Losses of Paper (A) and Electrolytic (B) Capacitors (500 Microfarads)

With the second method the canister itself is used as a calorimeter with internal temperature sensors. In this case the real quasi-steady working conditions are used. Initial results of these tests are presented in Section 3.5.

A number of thermocouples are distributed in strategic points in the bank of capacitors and are used to follow the temperature rise during operation. An improved setup has been designed for future work with each capacitor having a thermocouple taped to its surface. A timed rotating switch connects the various thermocouples to a single external lead in a repeating sequence. In this way it is possible to monitor the behavior of each capacitor, and eventually will permit differences in the operating current in various parts of the pulsing network to be detected.

At present, the charging current and voltage is read visually from meters on the panel. The voltage at the time that the pulse is initiated is determined by the operator who presses a button when the capacitor bank voltage reaches the desired value. The interval between pulses is controlled by regulating the charging current which is done with a variable resistor, so the measurement of charging current at the beginning of each cycle is a useful parameter for setting up reproducible test conditions. Since the interval between pulses is never more than a few seconds, a certain amount of operator skill is required in pressing the triggering button at precisely the same voltage for each pulse in a series. It is planned to substitute an automatic system to perform this function in the near future to improve repeatability and allow a more precise determination of capacitor bank voltage when the discharge is initiated.

The structure of the power supply block is extremely rigid, but the electrodynamic forces during the maximum power discharge are also quite appreciable. A series of tests have been programmed to study the mechanical deformation of the canister during discharges and to minimize its effects.

The charging power supply consists of two 320-volt, 12 kilowatts continuous duty rectifiers in series. Even at the designed maximum discharge rate of one second these units have more than adequate capacity. A variable power resistor is provided in series with the rectifiers to permit precise regulation of the charging time. With the present circuitry, the charging current is limited by heating of the flexible connections to the rotating canister which is only 1.0 millimeter in diameter to reduce disturbing effects on the damping of the pendulum.

3.4 Calibration and Measurements

The most time consuming work done in this section was for obtaining the desired shape of the pulse discharge. This was done by testing various arrangements of the electrolytic capacitors with their connecting leads. This work resulted in the selection of a complete package that gives satisfactory performance (see Figure 9).

First of all, a single electrolytic capacitor was considered with a nominal capacity at 450 volts of 900 microfarads. Since the capacity of electrolytic capacitors increases as the working voltage is lowered and since our maximum testing voltage is 400 volts, we have usually considered the average capacity to be 1000 microfarads for calibration and testing.

Four standard testing and calibrating voltages have been selected at precisely 100, 200, 300 and 400 volts which provides approximately a doubling of the energy stored between one value and the next. The first tests were made using a single capacitor directly connected to the discharging head in vacuum with little intermediate inductance. The behavior at the four fixed voltages with two oscilloscope sweep speeds (50 and 20 microseconds) is shown in Figure 16. Figures 17 through 19 show the same behavior for 2, 4 and 8 capacitors in parallel, all having the same intermediate inductance.

Next, six groups of ten capacitors, with each group connected in a parallel line and joined in the manner previously described to increase mutual inductance, were tested at the same four fixed voltage levels of 100, 200, 300 and 400 volts. The resulting discharge curves for voltage and current are illustrated for 200 and 100 microsecond sweeps in Figure 20. The change in scale to 10 kiloamps/cm for current and 200 volts/cm for voltage should be noted. Figures 21 through 23 illustrate the effect of increasing the inductance of the network by modifying the connecting lines for the same group of capacitors.

Finally, the distribution of small groups of capacitors was altered to further improve the shape of the discharge. This gave the pulse shown in Figure 24. It should be noted that while the scale for current remains unchanged at 10 kiloamps/cm, the scale for the recorded voltage has been 100 volts/cm while its origin has been shifted to the lower baseline (the same as used for the current trace). Additional improvements in the pulse shape could be obtained by further refining the distribution of inductance, but for reasons of time, the curve illustrated was considered acceptable. The repeatability of these recordings has been good enough to permit small differences in the shape of the discharge to be detected. The right column shows the discharge obtained with Plasma Head No. 3 while the left column shows the discharge obtained with Plasma Head No. 1, as described in Section 4.

Tests to determine reproducibility have been conducted and the recorded curves are superimposed so exactly that it has been concluded that it is only necessary to make one recording for each series during a performance test.

The voltage recorded in the preceding pictures must be corrected to allow for the IR drop in the electrodes between the points where the instrumentation leads connect and the arc attachment points. The size of the correction depends on the electrode shape and the current.

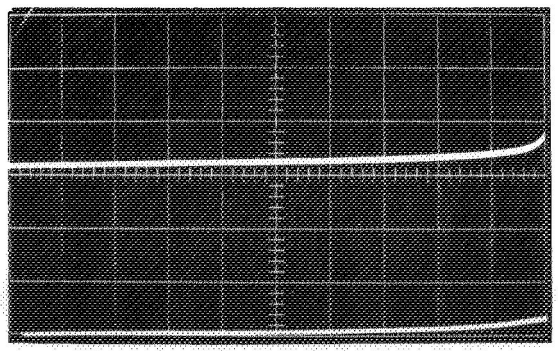

a. 100 Volts, 50 μS/cm

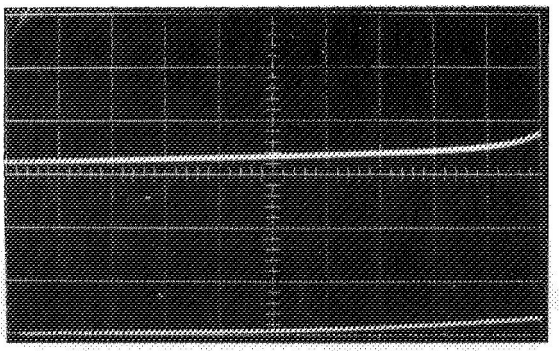

a1. 100 Volts, 20 μS/cm

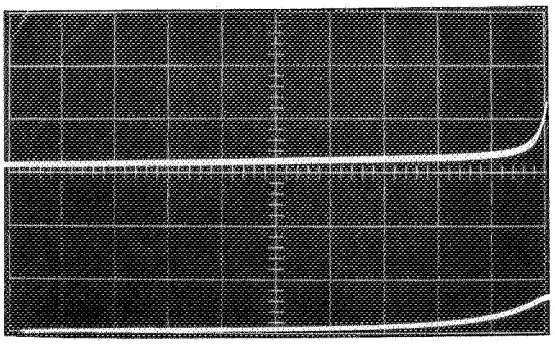

b. 200 Volts, 50 μS/cm

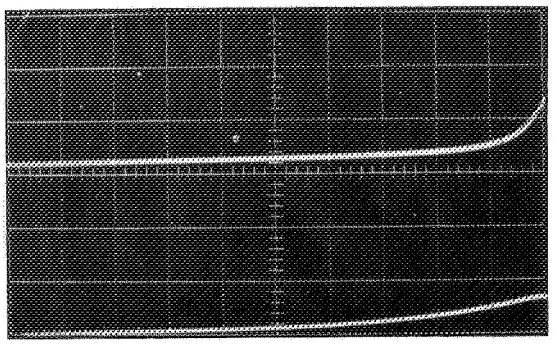

b1. 200 Volts, 20 μS/cm

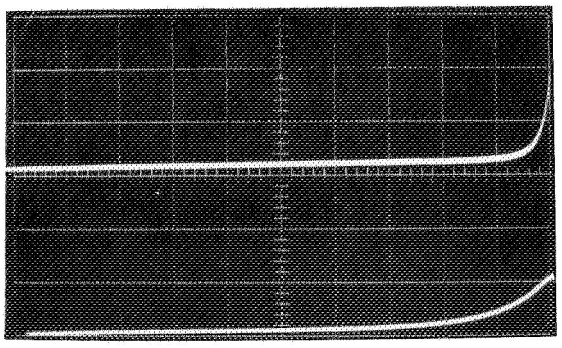

c. 300 Volts, 50 μS/cm

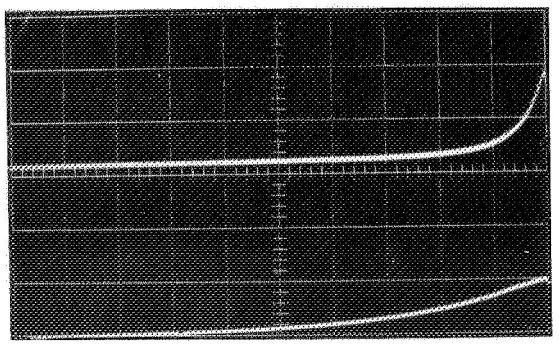

c1. 300 Volts, 20 μS/cm

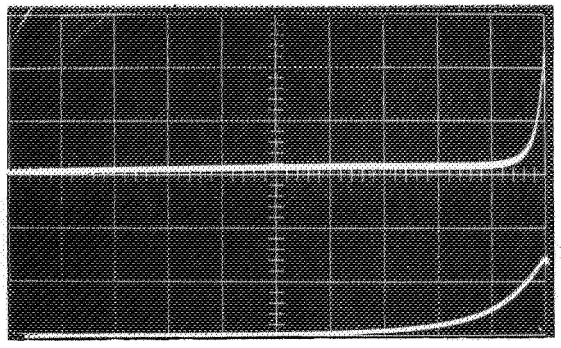

d. 400 Volts, 50 μS/cm

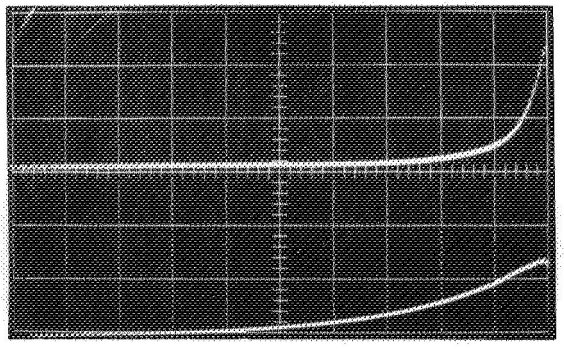

d1. 400 Volts, 20 μS/cm

Figure 16. 1000 μF Current vs Voltage at 100, 200, 300, 400 Volts (50 and 20 μS/cm) Voltage 100 V/cm (Upper Curve), Current 5000 A/cm (Lower Curve)

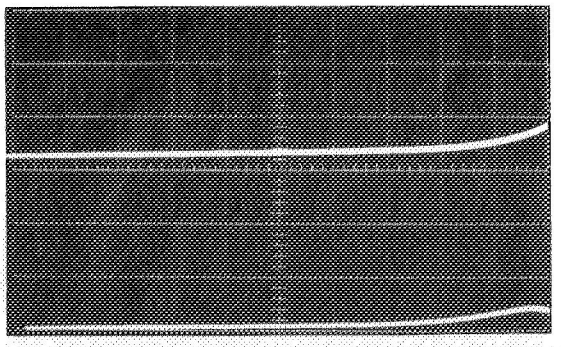

a. 100 Volts, 50 μS/cm

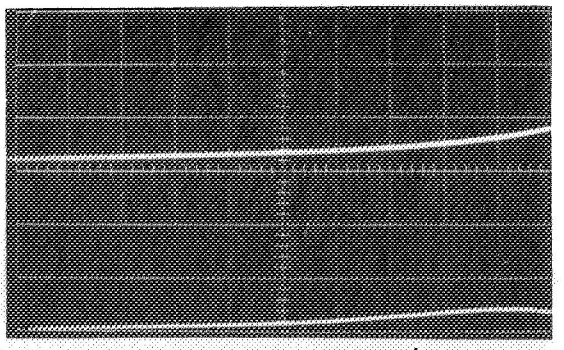

a1. 100 Volts, 20 μS/cm

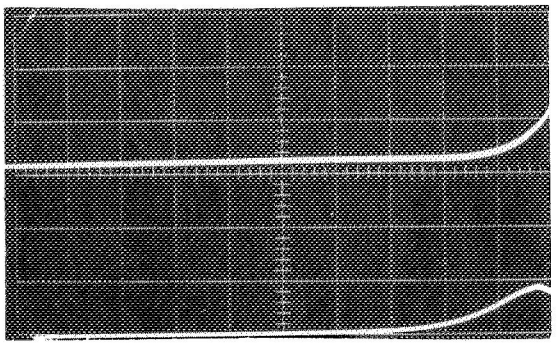

b. 200 Volts, 50 μS/cm

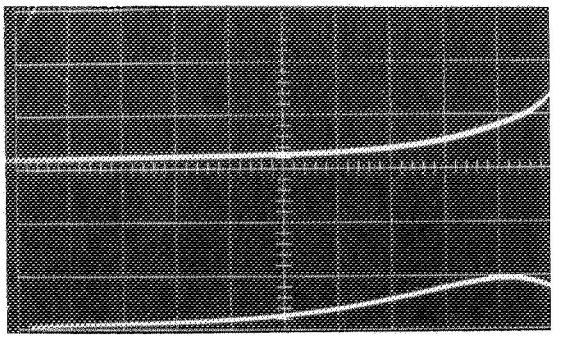

b1. 200 Volts, 20 μS/cm

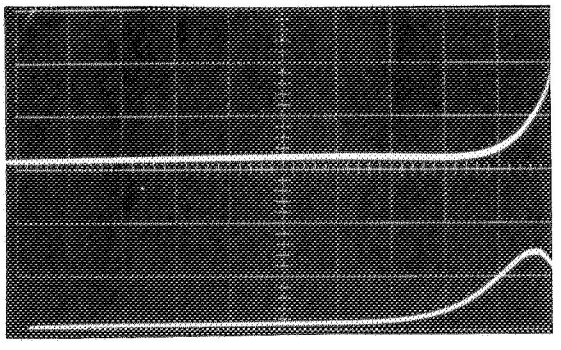

c. 300 Volts, 50 μS/cm

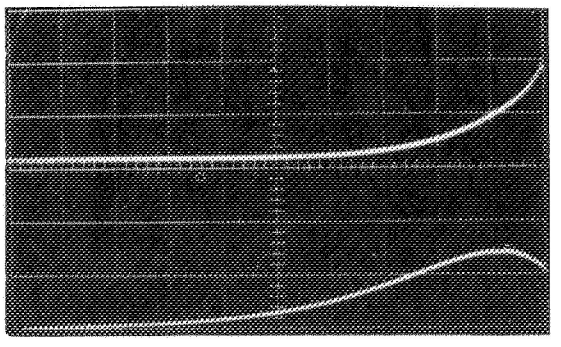

c1. 300 Volts, 20 μS/cm

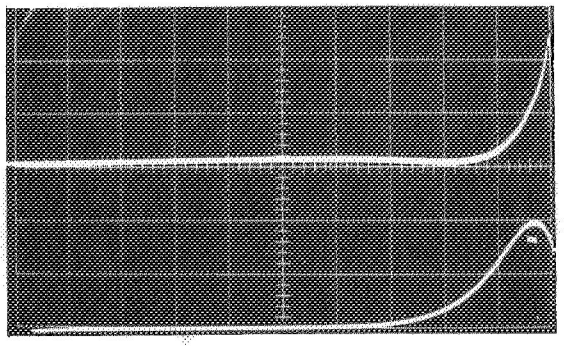

d. 400 Volts, 50 μS/cm

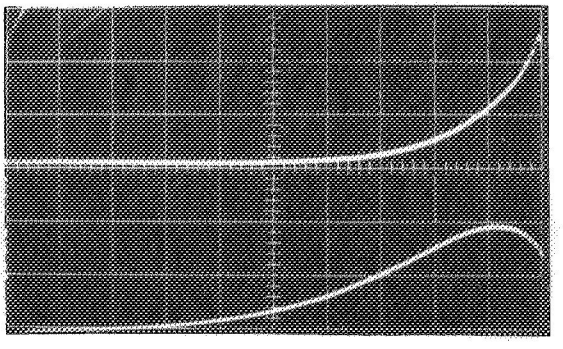

d1. 400 Volts, 20 μS/cm

Figure 17. 2000 μF Current vs Voltage at 100, 200, 300, 400 Volts (50 and 20 μS/cm) Voltage 100 V/cm (Upper Curve), Current 5000 A/cm (Lower Curve)

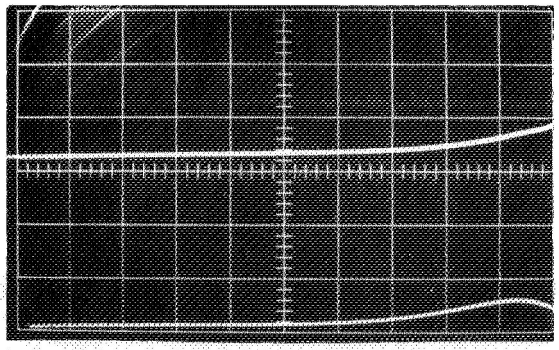

a. 100 Volts, 50 μS/cm

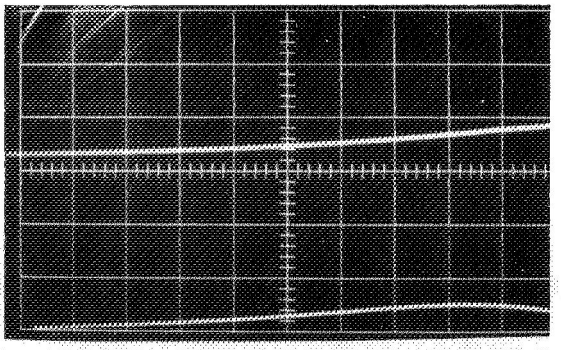

a1. 100 Volts, 20 μS/cm

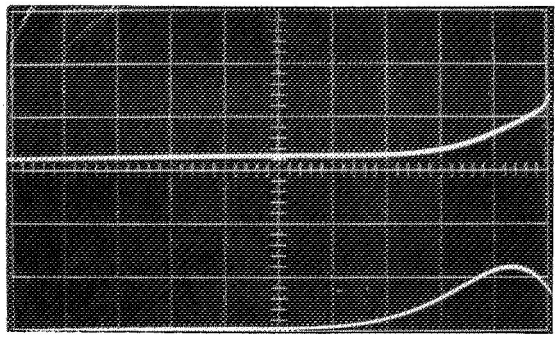

b. 200 Volts, 50 μS/cm

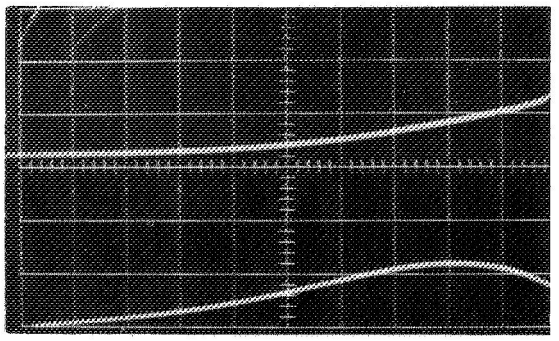

b1. 200 Volts, 20 μS/cm

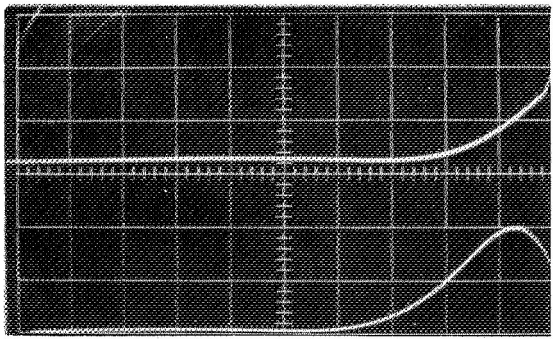

c. 300 Volts, 50 μS/cm

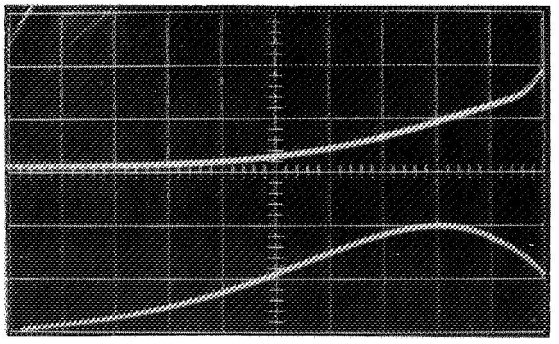

c1. 300 Volts, 20 μS/cm

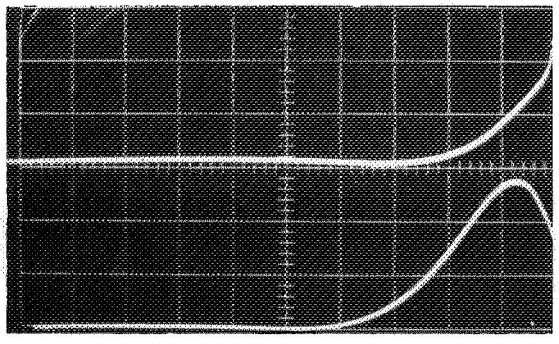

d. 400 Volts, 50 μS/cm

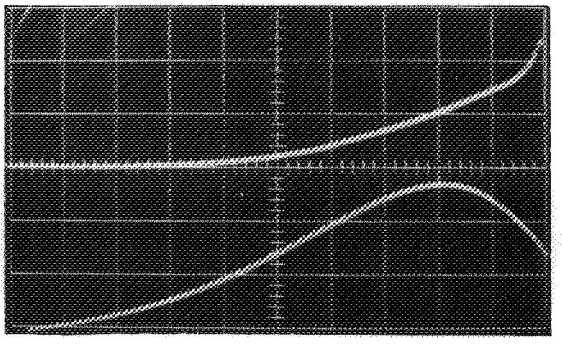

d1. 400 Volts, 20 μS/cm

Figure 18. 4000 μF Current vs Voltage at 100, 200, 300, 400 Volts (50 and 20 μS/cm) Voltage 100 V/cm (Upper Curve), Current 5000 A/cm (Lower Curve)

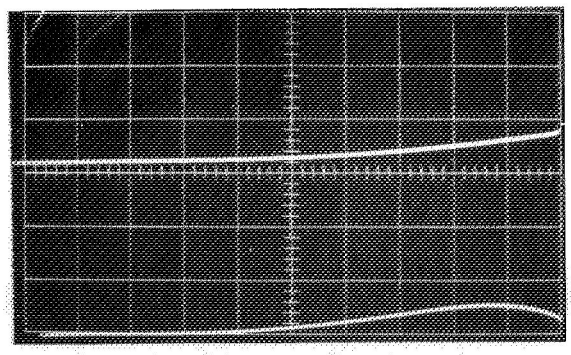

a. 100 Volts, 50 μS/cm

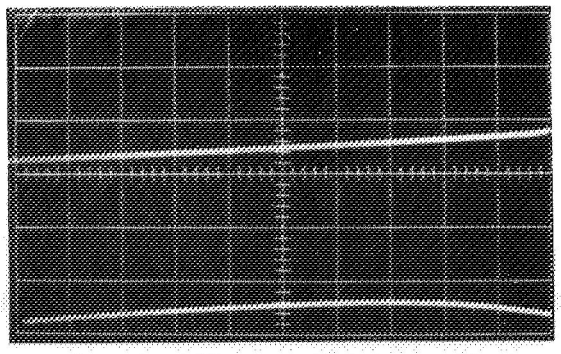

a1. 100 Volts, 20 μS/cm

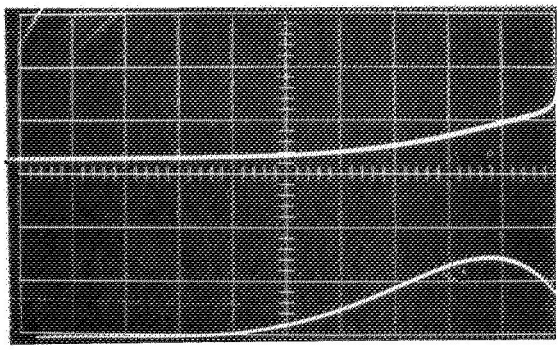

b. 200 Volts, 50 μS/cm

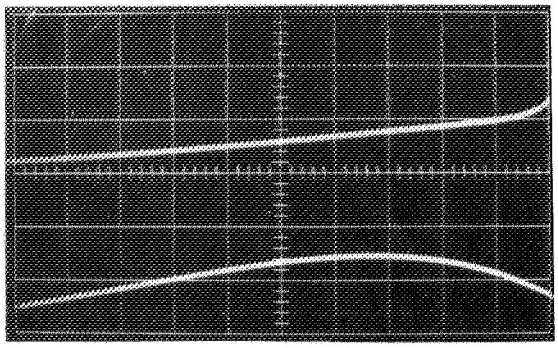

b1. 200 Volts, 20 μS/cm

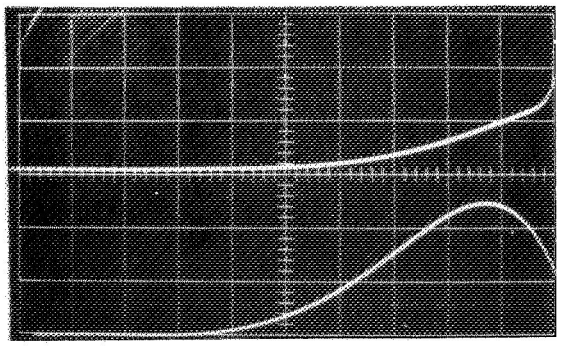

c. 300 Volts, 50 μS/cm

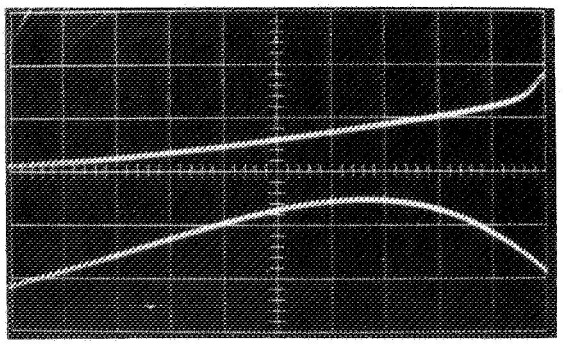

c1. 300 Volts, 20 μS/cm

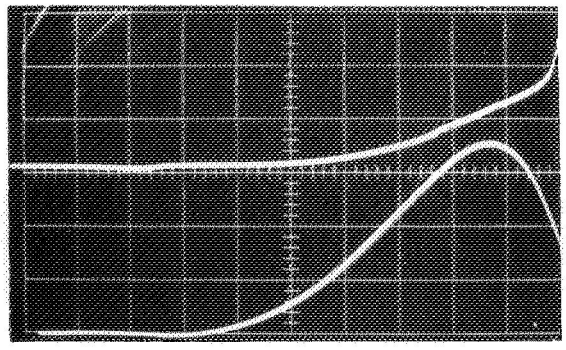

d. 400 Volts, 50 μS/cm

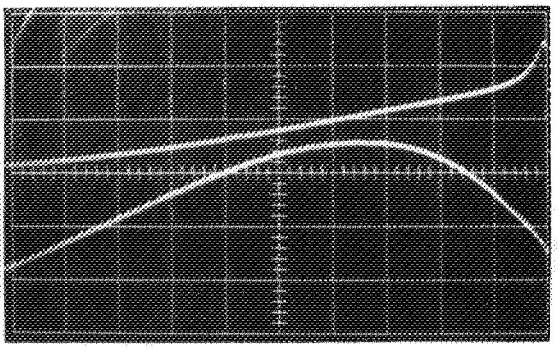

d1. 400 Volts, 20 μS/cm

Figure 19. 8000 μF Current vs Voltage at 100, 200, 300, 400 Volts (50 and 20 μS/cm) Voltage 100 V/cm (Upper Curve), Current 5000 A/cm (Lower Curve)

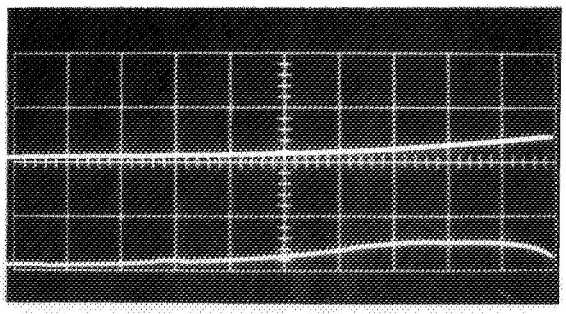

a. 100 Volts, 200 μS/cm

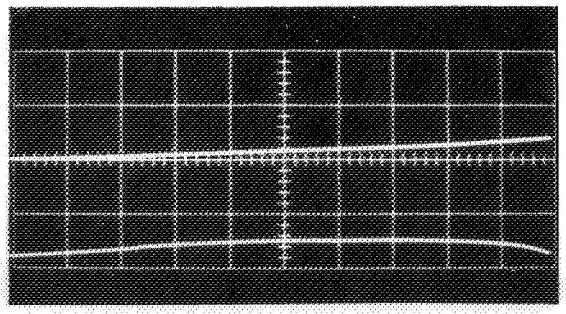

a1. 100 Volts, 100 μS/cm

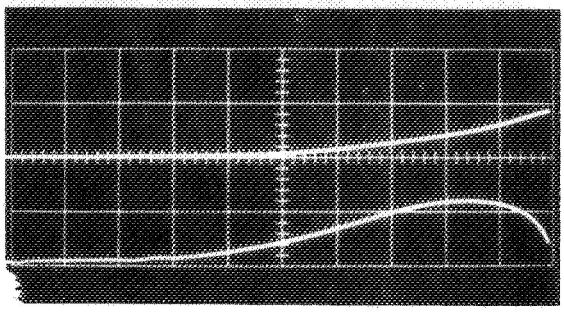

b. 200 Volts, 200 μS/cm

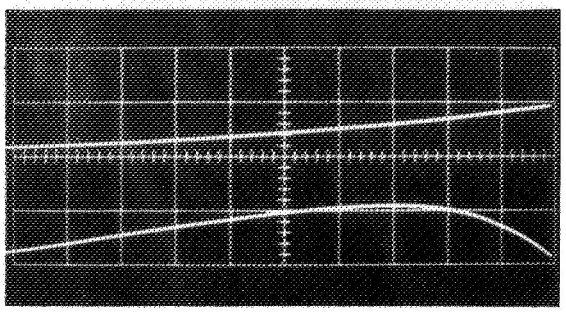

b1. 200 Volts, 100 μS/cm

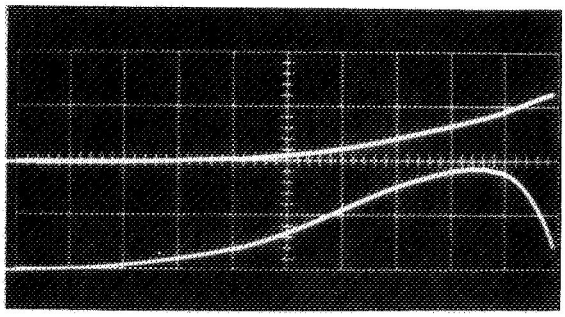

c. 300 Volts, 200 μS/cm

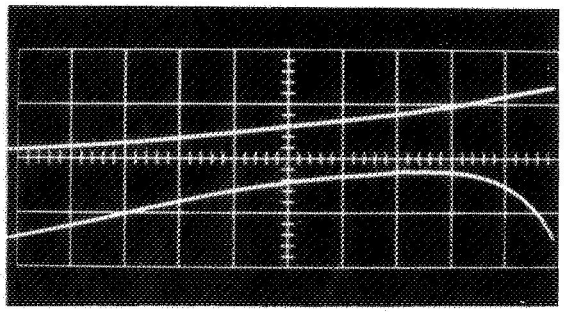

c1. 300 Volts, 100 μS/cm

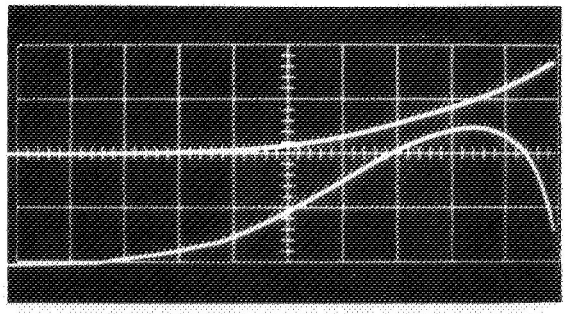

d. 400 Volts, 200 μS/cm

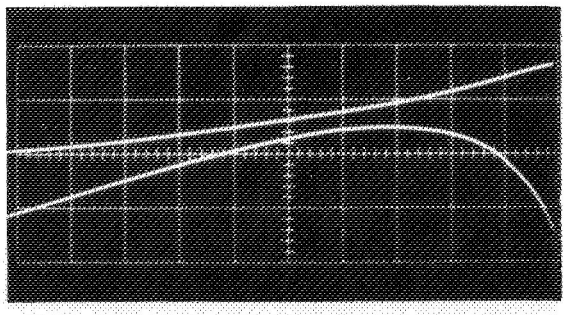

d1. 400 Volts, 100 μS/cm

Figure 20. 60,000 μF (L_5) Current vs Voltage at 100, 200, 300, 400 Volts (200 and 100 μS/cm)
Voltage 200 V/cm (Upper Curve), Current 10,000 A/cm (Lower Curve

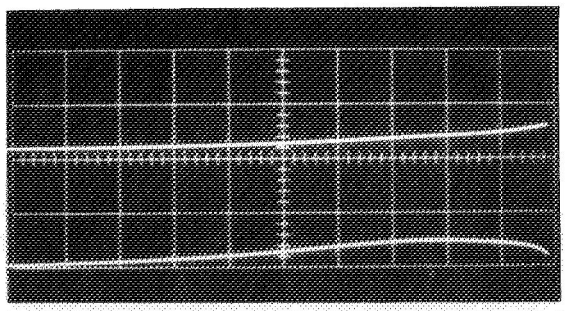

a. 100 Volts, 200 μS/cm

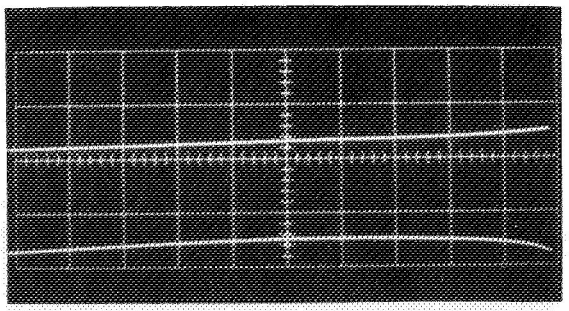

a1. 100 Volts, 100 μS/cm

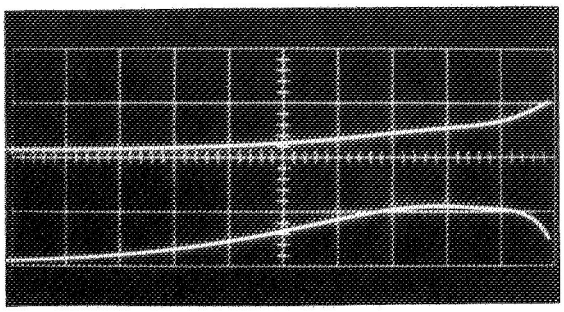

b. 200 Volts, 200 μS/cm

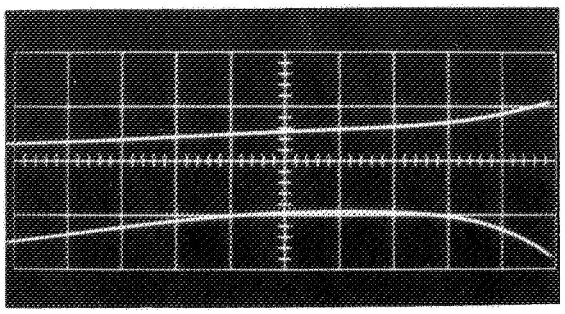

b1. 200 Volts, 100 μS/cm

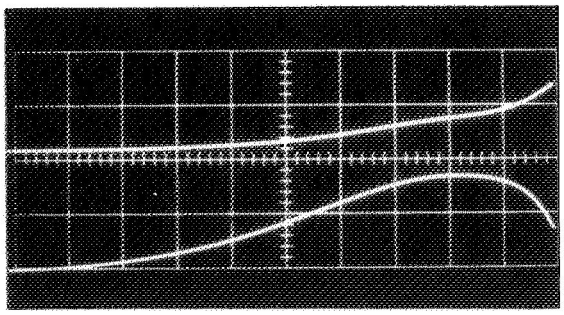

c. 300 Volts, 200 μS/cm

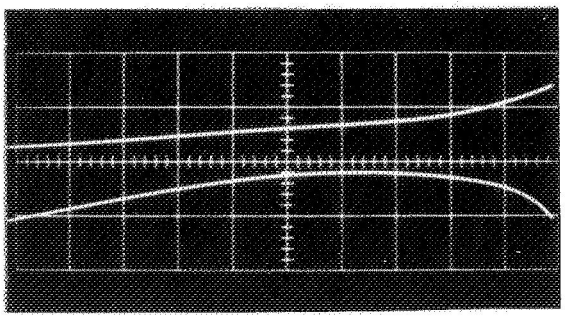

c1. 300 Volts, 100 μS/cm

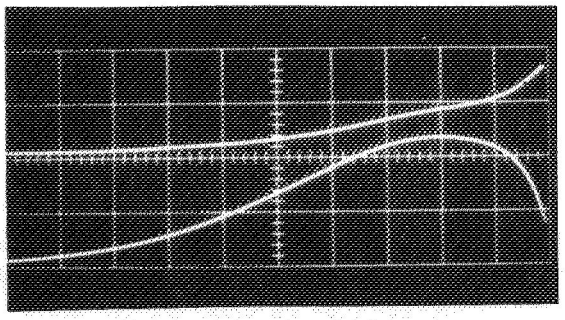

d. 400 Volts, 200 μS/cm

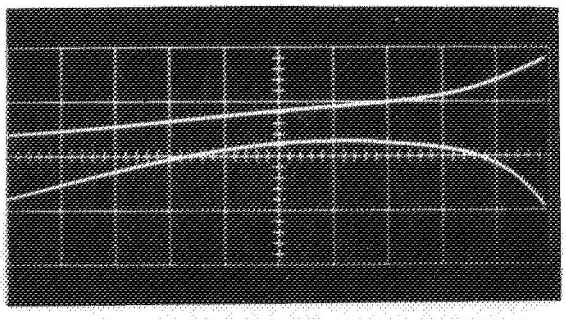

d1. 400 Volts, 100 μS/cm

Figure 21. 60,000 μS (L_4) Current vs Voltage at 100, 200, 300, 400 Volts (200 and 100 μS/cm)
Voltage 200 V/cm (Upper Curve), Current 10,000 A/cm (Lower Curve

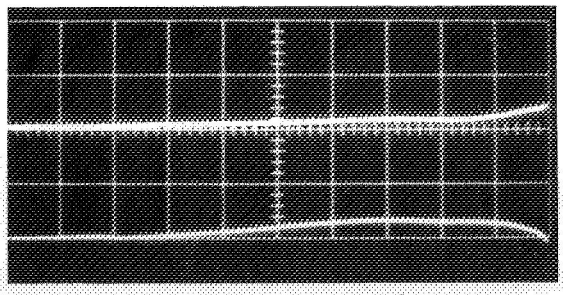

a. 100 Volts, 200 μS/cm

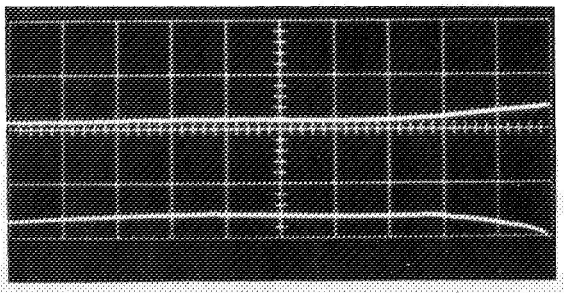

a1. 100 Volts, 100 μS/cm

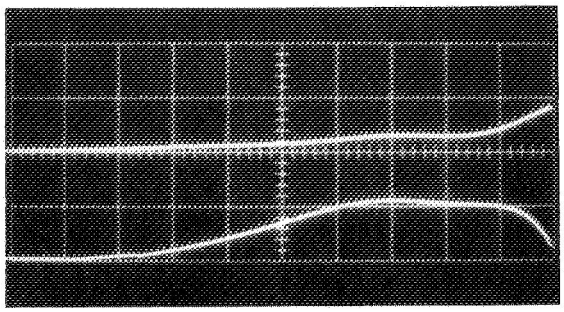

b. 200 Volts, 200 μS/cm

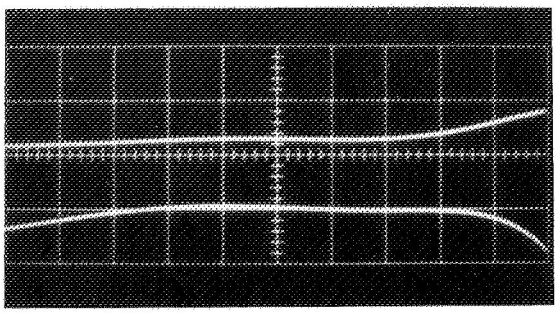

b1. 200 Volts, 100 μS/cm

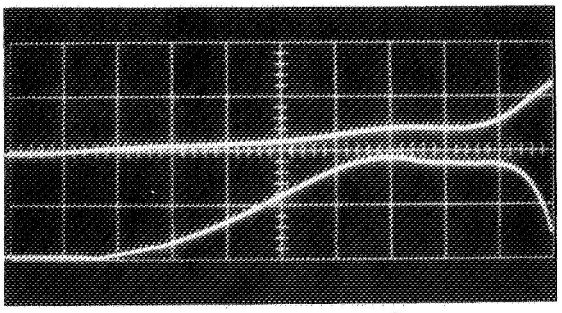

c. 300 Volts, 200 μS/cm

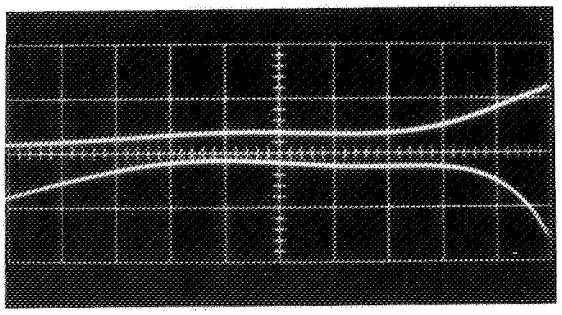

c1. 300 Volts, 100 μS/cm

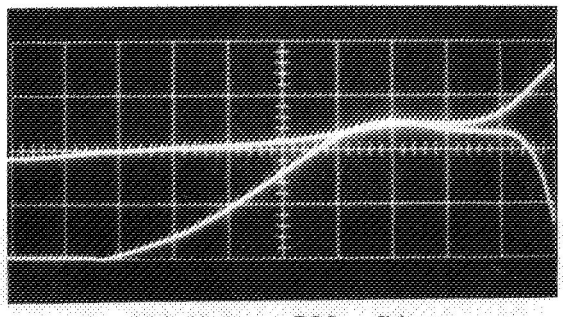

d. 400 Volts, 200 μS/cm

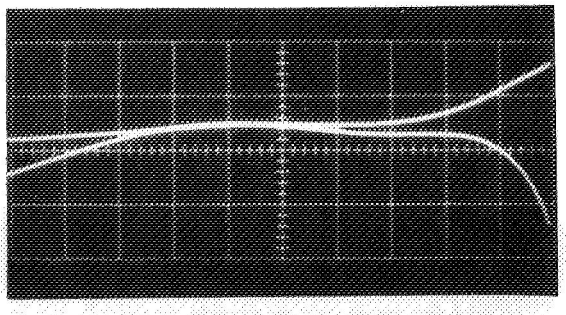

d1. 400 Volts, 100 μS/cm

Figure 22. 60,000 μF (L_9) Current vs Voltage at 100, 200, 300, 400 Volts (200 and 100 μS/cm)
Voltage 200 V/cm (Upper Curve), Current 10,000 A/cm (Lower Curve)

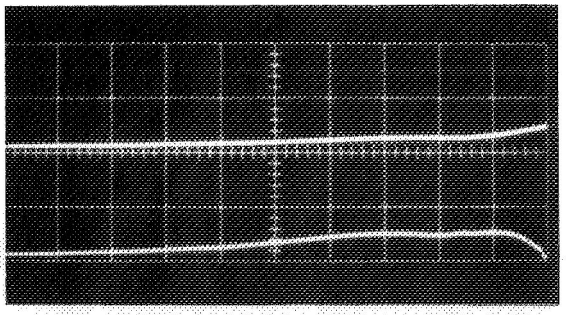

a. 100 Volts, 200 μS/cm

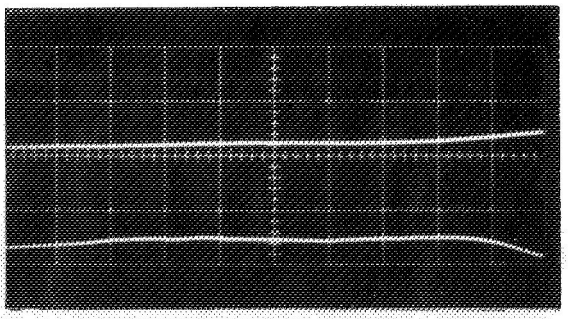

a1. 100 Volts, 100 μS/cm

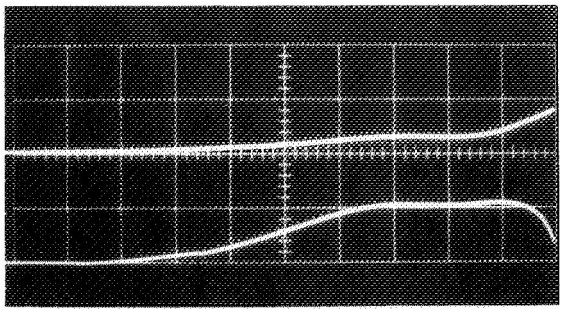

b. 200 Volts, 200 μS/cm

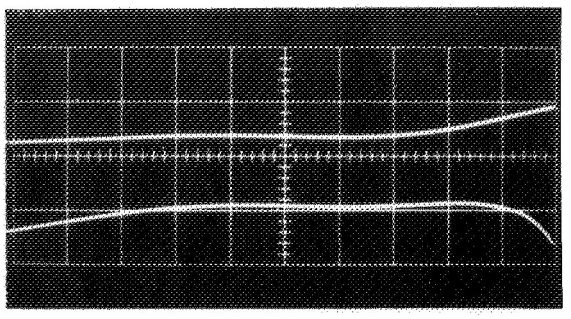

b1. 200 Volts, 100 μS/cm

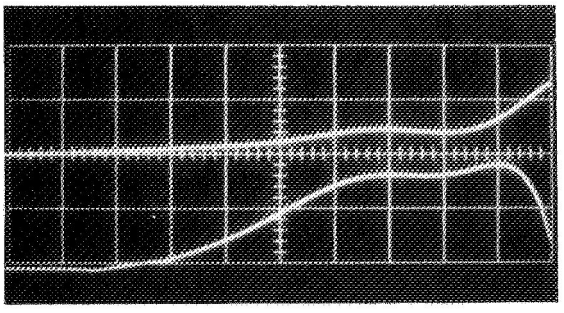

c. 300 Volts, 200 μS/cm

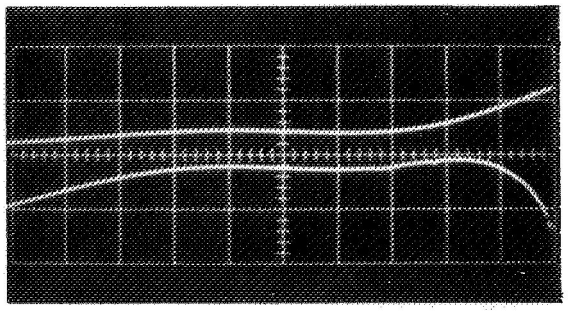

c1. 300 Volts, 100 μS/cm

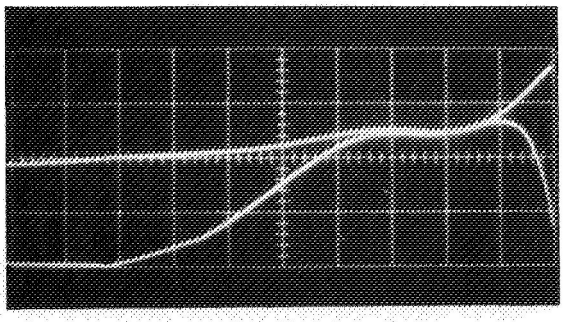

d. 400 Volts, 200 μS/cm

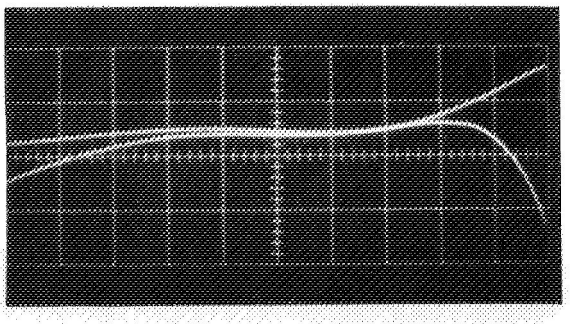

d1. 400 Volts, 100 μS/cm

Figure 23. 60,000 μS (L_{11}) Current vs Voltage at 100, 200, 300, 400 Volts (200 and 100 μS/cm)
Voltage 200 V/cm (Upper Curve), Current 10,000 A/cm (Lower Curve)

Plasma Head No. 1 Plasma Head No. 3

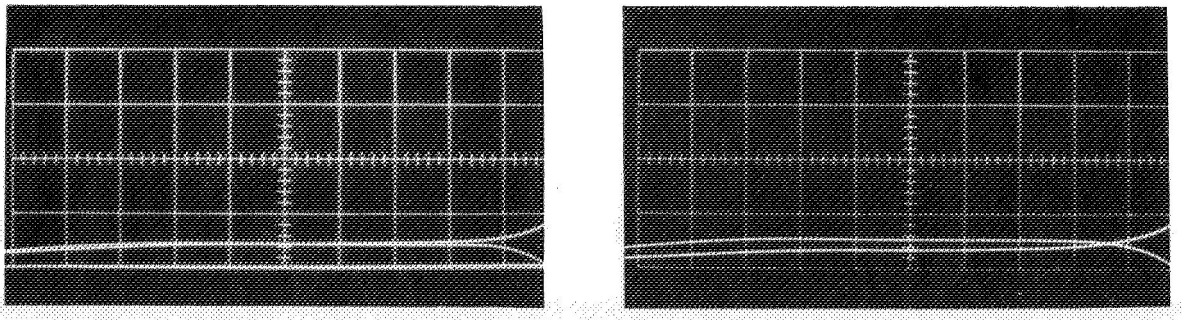

a. 100 Volts, 100 μS/cm

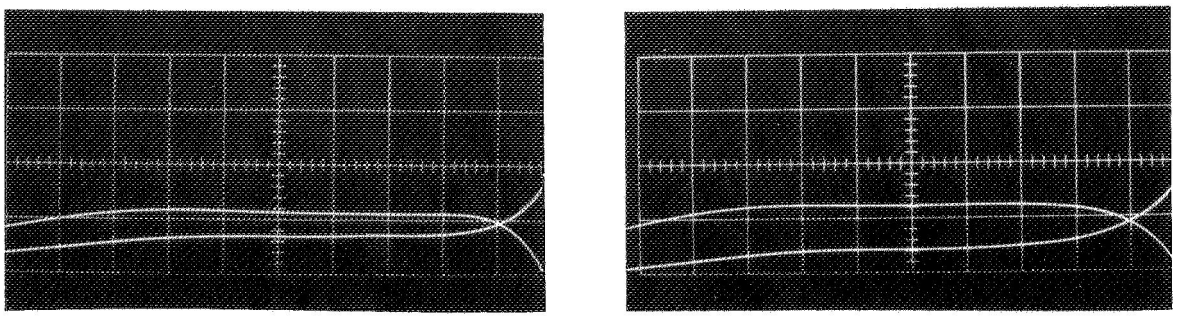

b. 200 Volts, 100 μS/cm

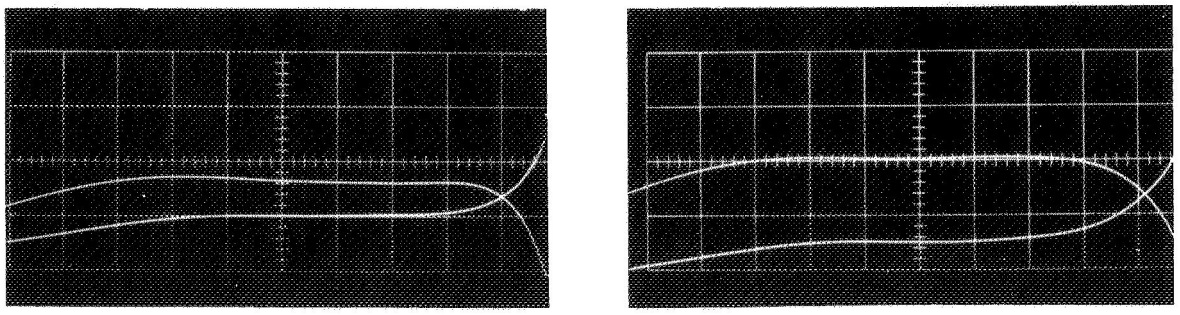

c. 300 Volts, 100 μS/cm

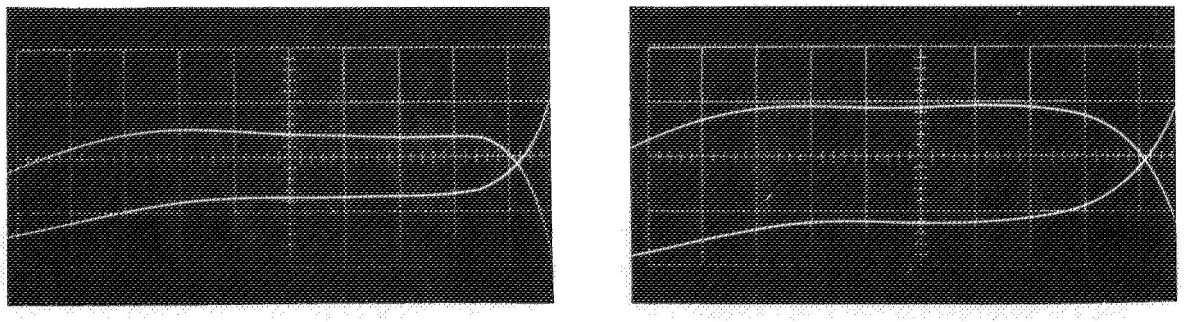

d. 400 Volts, 100 μS/cm

Figure 24. 60,000 μF (L_{50}) Current vs Voltage at 100, 200, 300, 400 Volts Voltage 100 V/cm, Current 10,000 A/cm

Until the commutator for the thermocouples becomes available to permit the measurement of the temperature of any single capacitor, the temperature is being measured at the top of the suspended canister and in the central zone where capacitor temperatures are believed to be highest. The thermocouple readings are referenced to an ice bath.

The inside pressure of the canister is initially the ambient atmospheric pressure and is read with a precision absolute aneroid gage. The variation of the pressure gives an idea of the internal ambient temperature and of possible leakage from the canister. The measurement of the currents and voltages used to charge the main and triggering capacitors are performed in a normal manner and do not present any problems. A system is being designed to initiate triggering of the main discharge automatically as soon as the desired test voltage is reached during the charging period.

The measurement of the signal that triggers the oscilloscope sweep is useful to permit accurate regulation of the strength of the signal. This assures a consistent response from the oscilloscope as plasma head characteristics are changed.

3.5 Test Results on the Power Supply

The total weight of the quasi-steady power supply for the nominal 5000-joule discharges is about 140 kilograms (308 pounds). Its final dimensions when enclosed in the protective atmosphere canister are a length of 107 centimeters (42 inches) and a diameter of 48 centimeters (18 inches). The weight and dimensions of the propellant and thrust generating head are not included but are considered in Section 4.5.

During about one year of continuous testing, the number of discharges at full voltage exceeded 10,000 with no evidence of variations in the performance of the system. Voltage and current traces taken now are essentially identical to those recorded when the system was first put in service provided the same discharge head design is used. During this period no failure has been detected in any component, which speaks well for the reliability of the electrolytic capacitors used.

With an initial charge of 400 volts, the discharge current varies between 25 and 30 kiloamps for a good portion of a millisecond, depending on the geometry of the electrodes used. A standard test series consists of 100 discharges, and during such a series the maximum temperature in the canister is very small. With the calorimeter setup described in Section 3.3, extensive tests have been conducted to obtain the increase in temperature of the 1000-microfarad electrolytic capacitor used in our pulsing network. Repetition rates from 1/4 second to 4 seconds have been included. The tests are continuing to cover different capacitors and a wide range of operating voltages. When operating at one pulse per second, and at charge levels of 200, 300 and 400 volts, the number of pulses required to reach a temperature of 50°C was 4500, 1200 and 700, respectively.

4.0 THE PLASMA HEAD

4.1 Use of Electrode Vapor for Propellant

To date all plasma propulsion experiments (we can say all plasma acceleration experiments) have unavoidably used a mixture of propellants instead of a single one. In general, the propellants are: 1) the main or nominal propellant (generally a gas) injected in known quantities in the arc zone, 2) the residual atmosphere in the vacuum environment where the tests are conducted, 3) the vapors ablated from the electrodes in varying proportions depending on power density and geometry, and 4) the vapors ablated from the solid insulation separating the electrodes. The proportions of these four often extremely different propellants depends on the test parameters in a manner that is difficult to predict. For many years this has introduced serious difficulties in the measurement of performance, and made the confirmation of related analytical work nearly impossible. To avoid the great number of variables involved, the ideal solution would be to eliminate the parasitic propellants, 2, 3 and 4, and use only the main propellant, 1. However, this is extremely difficult to accomplish, particularly when the power input is at a high level. Even for low power tests the following steps are necessary: the first propellant must be metered with good precision; a vacuum environment at pressure not over 10^{-6} torr (possibly 10^{-7} torr) must be used to eliminate the second propellant; highly refractory electrode materials with very low current density and extremely good cooling must be used to eliminate the third propellant; and ceramic insulation located as far as possible from the plasma zone, protected from radiation and very well cooled must be used to eliminate the fourth propellant. But even when all these precautions are taken, it is evident that some undesired material will remain. Consider, for example, the precise metering of the first propellant, assuming for the time being the successful elimination of all the other propellants. While the quantity of the first propellant fed to the thruster can be metered with the required precision, two reasons to question the performance measurements remain: 1) not all the gaseous propellant fed to the thruster goes through the heating zone, but part escapes and diffuses in the vacuum environment through other paths, and 2) when pulsed operation is necessary, the synchronization of the pulse of gas with the pulse of current (in the microsecond range) is extremely difficult.

Regarding the elimination of the second propellant (i.e. the recirculation of the residual chamber atmosphere) by maintaining a pressure level under 10^{-6} torr, the problem becomes more complicated when a flow of gas is admitted to the vacuum chamber. To maintain a pressure level of 5×10^{-7} torr with an average flow of one milligram of hydrogen per second requires either a cryogenic pumping system using liquid helium or about 100 large diffusion pumps, each having a capacity of 140,000 liters per second (see Section 2.1). The capacity needed increases in proportion as higher flow is used. Studies have shown that the cryogenic solution is the most practical when a large flow is necessary and becomes more attractive when the propellants used in the tests are more condensable. It

is evident that the maximum economy and efficiency can be achieved with propellants that are easily condensable at room temperature (i. e. those with high vaporization temperature). The need to eliminate the influence of residual chamber atmosphere during thruster tests is becoming more widely recognized. In our opinion, it is essenital if useful performance measurements are required.

The complete elimination of the third propellant (i. e. the vapor emitted by the hot electrodes) is also a difficult problem to solve and practically no solution is possible when very high power density is used. When the electrodes contact extremely hot gases, continuous evaporation of the conducting surfaces next to the high temperature plasma, takes place. The consumption of the electrodes in these cases is such a common event that the "life" of the entire system is normally related to the electrodes' ablation. Only at extremely low power levels and with elaborate cooling of the electrodes it is possible to eliminate the metal vapors from the operative picture. Spectrographic records invariably show the presence of electrode material in the jet and give evidence of the difficulty of completely eliminating these vapors.

Nearly complete elimination of the fourth propellant (i. e. of the vapor emitted by the insulating material separating the electrodes) can be achieved without serious difficulties. A thruster is needed that is carefully designed to keep the insulators in a region of lower temperature. The use of highly refractory insulating materials such as quartz or ceramics can also be helpful. However, a careful analysis is required. It is well known that some insulating materials, such as "Teflon," are so easy to evaporate under plasma thermal action that practical propulsive systems using Teflon vapor as propellant have been developed and successfully used. A completely opposite technique must be followed to eliminate completely vapor emitted by the insulating material.

To obtain reliable data on the performance of plasma thrusters fed with gaseous propellants (propellant number one), we see that it is necessary to essentially eliminate the presence of the environmental atmosphere (propellant number two), the electrode vapors (propellant number three), and of the insulator vapor (propellant number four). Clearly this can only be accomplished with great technical difficulty. It is evident, however, that any one of the four mentioned propellants can be considered as the main propellant which would require the elimination of the other three. An example of this possibility is offered by the practical utilization of the Teflon vapor as a propellant. The following table indicates the degree of difficulty involved in eliminating the other three propellants when each of the four is selected as the main propellant.

The table shows that less difficulty would be expected with propellant three than with propellant two, and that either of these propellants should be easier to use than propellants one or four. Because the practical use of the environmental atmosphere as propellant would be limited to low altitudes, it appears that electrode vapor is the most attractive

TABLE I

Main Propellant	Propellants to be Eliminated (x Easy, ₀ Very Difficult, o Difficult)		
1. Gas	o Environmental	₀ Electrode vapor	x Insulating vapor
2. Environmental	x Gas	₀ Electrode vapor	x Insulating vapor
3. Electrodes	x Gas	o Environmental	x Insulating vapor
4. Insulators	x Gas	₀ Electrode vapor	o Environmental

choice. Its use permits the elimination of the remaining three propellants with minimum difficulty. Further effort has therefore focused on the use of electrode vapor.

The main feature that distinguishes the work described in this report from experiments with quasi-steady MPD thrusters being conducted at other laboratories is that the activities described here are concerned with thrusters that use electrode vapor for the propellant. Emphasis will therefore be placed on thruster characteristics that result from this feature. There are a number of advantages that evidently result from the use of consumable electrodes aside from those that have just been discussed. These include improved performance and the possibility of longer electrode life via more uniform ablation and continuous electrode replenishment by external feed, as well as the ability to essentially eliminate extraneous interaction effects that seriously reduce the confidence that can be placed in test results.

Since the electrodes are cooled ablatively, the electrode cooling problem is relieved. Electrode fall losses serve the useful function of vaporizing the propellant rather than simply introducing more heat that must be disposed of by a cooling system. Some cooling capacity is needed to permit attachment of electrodes to cooler insulators and power leads, and to regulate the rate at which propellant is vaporized so that the desired specific impulse can be maintained. Consumable electrodes provide an effective means for introducing highly storable propellants into the arc. In fact, the vapor is introduced precisely at the hottest region of the arc foot, a feature that would be impractical to provide with other propellant feed systems. The advantages of this feature will be discussed later. As the electrodes erode, they are continuously replenished by a feed system so that an extended thruster life is readily achieved. A final and very important advantage of ablative cooling is the marked reduction in thermal stress that results from the fact that the heat is largely absorbed at the location in which it is released. The amount of conductive cooling required can be kept low so that the temperature gradients and thermal stresses for steady state conditions will be moderate. Transient thermal stresses can also be minimized by preheating the electrodes or by increasing power in a programmed manner when the arc is started.

The use of electrodes that ablate is believed to be particularly advantageous whenever difficulty is experienced in maintaining adequate and uniform ionization of the propellant. For example, in devices designed to have most of the electrical discharge outside of the thruster (no enclosed arc chamber) it has been found difficult to maintain a discharge that is entirely in the external gas because the propellant is not readily ionized after it is released in the low density space surrounding the electrodes. Even when a stable discharge can be maintained, only a fraction of the gas stream is ionized by the cathode emissions. Remaining portions are not contained by the magnetic nozzle or accelerated by electromagnetic effects. This gas spreads rapidly and escapes from the active region with a minimum contribution to thrust.

4.2 Graphite for Evaporating Electrodes

One of the problems encountered, especially at high energy levels, is that the electrode material expelled as propellant tends to be only partially vaporized leaving in the jet a fraction of the material in the form of minute particles at temperatures lower than the melting point (spitting). The velocity of these particles is not comparable to the velocity of the vaporized portion and the test measurements show a corresponding reduction in overall performance. To circumvent this difficulty, it has been decided to concentrate on the use of materials that vaporize by sublimation.

The advantage of using a material that sublimes and has good thermal shock resistance was clearly illustrated in a series of comparative tests conducted during the preceding report period. Figure 5 of Reference 1 shows electrodes of a number of materials following operation for identical duty cycles. The graphite electrodes show much less erosion and retain their original smooth geometry much better than any of the other electrodes tested.

Based upon numerous tests, graphite appears to be one of the best materials for this purpose. It has been found to sublime without conspicuous spitting at the highest levels of discharge energy. Figure 25 shows the plume during a pulse with tungsten electrodes in use while Figure 26 shows the plume obtained at the same energy level with graphite electrodes. High speed motion pictures of the electrodes have shown that the spitting observed with tungsten or copper electrodes is caused by the formation of droplets of molten metal that are carried downstream before they can vaporize. This mechanism is eliminated when graphite electrodes are used.

It is difficult to judge the fraction of material lost as solid praticles from observations of the plume. A comparison of measured impulse and measured jet velocity could give an indication, but usable data of this type are not available at present. However, plausible limits can be established by simple calculations. The maximum particle size used in the formation of the graphite for the electrodes is 0.001 inch (25 microns). Judging from the pore size quoted (0.2 to 0.7 microns), it is inferred that gaps must be filled

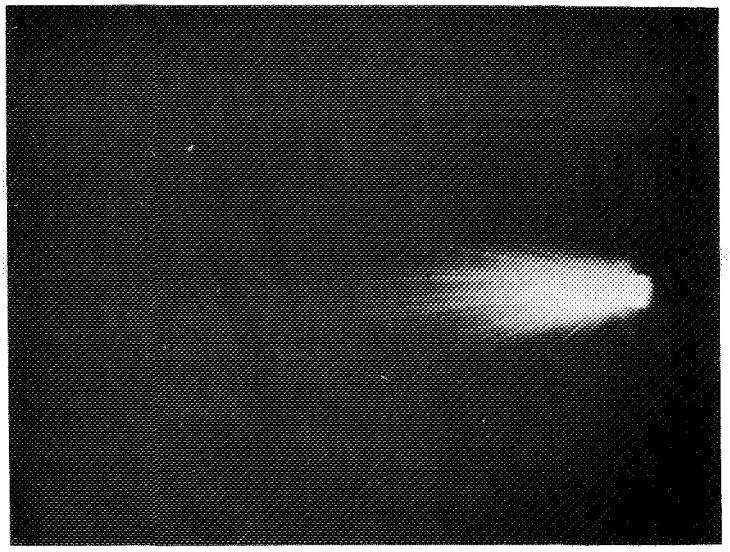

Figure 25. Plume From Tungsten Electrodes Showing Sputtered Particles

Figure 26. Plume From Carbon Electrodes Showing Blue Color of Carbon Gas

by smaller particles ranging from 1.0 to 5.0 microns for the minimum size. If the spitting observed in the carbon vapor plume is assumed to all be formed of particles of the maximum size (25 microns) a mass of 18.5×10^{-6} milligrams is estimated for each particle. Even if a hundred particle traces were observed during a pulse, the total mass represented would be only 0.00185 milligrams which is a fraction of one percent of the material expended during the pulse.

As an alternate example, it is assumed that a clump of particles may be ejected as a unit after thermal stresses form fractures at the electrode surface. Pieces formed in this way could be considerably larger in size. Assuming that half of the total mass used during a pulse (about 0.5 milligram) is ejected in the form of 10 solid pieces, the average dimension of each piece would be about 0.35 millimeter. White hot pieces this large would produce bright traces in the plume. Since the actual traces observed with graphite electrodes are relatively inconspicuous, it is concluded that the mass lost in solid form is small.

Graphite in particular has some exceptionally favorable properties. At a pressure of one atmosphere, it sublimes at a temperature of around 3550°C (168°C above the melting point of tungsten). Since no melting occurs, the erosion takes place smoothly with little spitting, and a uniform electrode geometry is maintained which is essential if the electrodes are to be progressively fed.

The life of graphite electrodes is enhanced by unusually good resistance to thermal shock. This results primarily from low values of the modulus of elasticity and the coefficient of thermal expansion. In a section on thermal shock in Chapter 5, Reference 9 states that, "Of all the temperature resistant nonmetallic materials available, carbon and graphite have the best overall thermal shock resistance." Reference 10 reports that graphite specimens at about 1560°C have been quenched in water without damage, but that spalling has been obtained by quenching in liquid sodium. The same reference shows values of the parameter $kS/\alpha E$, where

k = thermal conductivity,

S = tensile strength,

α = coefficient of thermal expansion, and

E = modulus of elasticity

for graphite and a number of refractory oxides and carbides. On this basis, graphite is shown to be superior to the next best material (titanium carbide) by a factor of 166. When a similar comparison is made between graphite and tungsten, the parameter is found to be nearly the same for the two at room temperature. The comparison is more favorable to graphite at higher temperatures because graphite increases while tungsten decreases in strength. However, the application of the parameter to metals is questionable. Although

brittle at room temperature, tungsten develops fairly good ductility when heated, and can probably undergo a greater amount of yielding to relieve thermal stresses. The major advantage of graphite over tungsten from a thermal stress standpoint is that graphite may be cooled by ablation and is therefore not subject to the high thermal stresses that result from the strong conductive cooling necessary in tungsten electrodes. This feature is undoubtedly the principal reason for the very successful history of graphite electrodes in commercial arc furnace and light source applications.

The advantages of consumable electrodes can be fully realized only if the normal electrode losses come close to supplying the heat needed to provide the flow of electrode vapor required for propellant. Power and propellant flow cannot be independently controlled except in an indirect manner by regulating the heating or cooling of the electrodes. An electrode material with a low value for the heat of vaporization would provide a large flow of vapor and would tend to operate at a low specific impulse unless the electrodes were heavily cooled. On the other hand, electrodes with a high value for the heat of vaporization would tend to provide high values of specific impulse. The heat of vaporization of graphite is on the high side, so this material is most suitable when a specific impulse of high value is desired. This fact is illustrated in Figure 6 of Reference 1 which shows the ratio of the heat of vaporization to the kinetic energy in the jet as a function of jet specific impulse for a number of materials. Although many materials have heats of vaporization that would be suitable for lower specific impulse operation, none have been found with characteristics that would make them as appropriate as graphite for use as consumable electrodes. If operation at low specific impulse is required, the use of graphite with an additive propellant may be preferable to the substitution of an alternate electrode material. However, in most cases it is expected that a high purity graphite will be preferable, both from the standpoint of achieving a high specific impulse and to provide a fairly uniform vaporization rate during the pulse. Graphite is commercially available with only five parts per million of impurities and may be obtained in spectroscopically pure grades if required.

Returning to the subject of space simulation, graphite has an exceptionally low vapor pressure, and can be expected to condense readily on the cool walls of the test chamber and vacuum system. Figure 27 shows vapor pressure as a function of temperature for tungsten and the elements in the first two rows of the periodic table. Carbon is seen to rival tungsten in vaporization temperature, and to be well above the other low atomic weight elements. Actually, it is believed that any of the solid elements shown would permit operation of the vacuum system at the desired low pressure levels. Experience with lithium as a propellant shows that a large fraction of the propellant expended collects on the chamber walls rather than being carried into the vacuum pump. Unfortunately, the accumulation of electrode vapor deposits will eventually affect the insulating characteristics of the test chamber. It will undoubtedly be necessary to clean the interior walls of the chamber periodically.

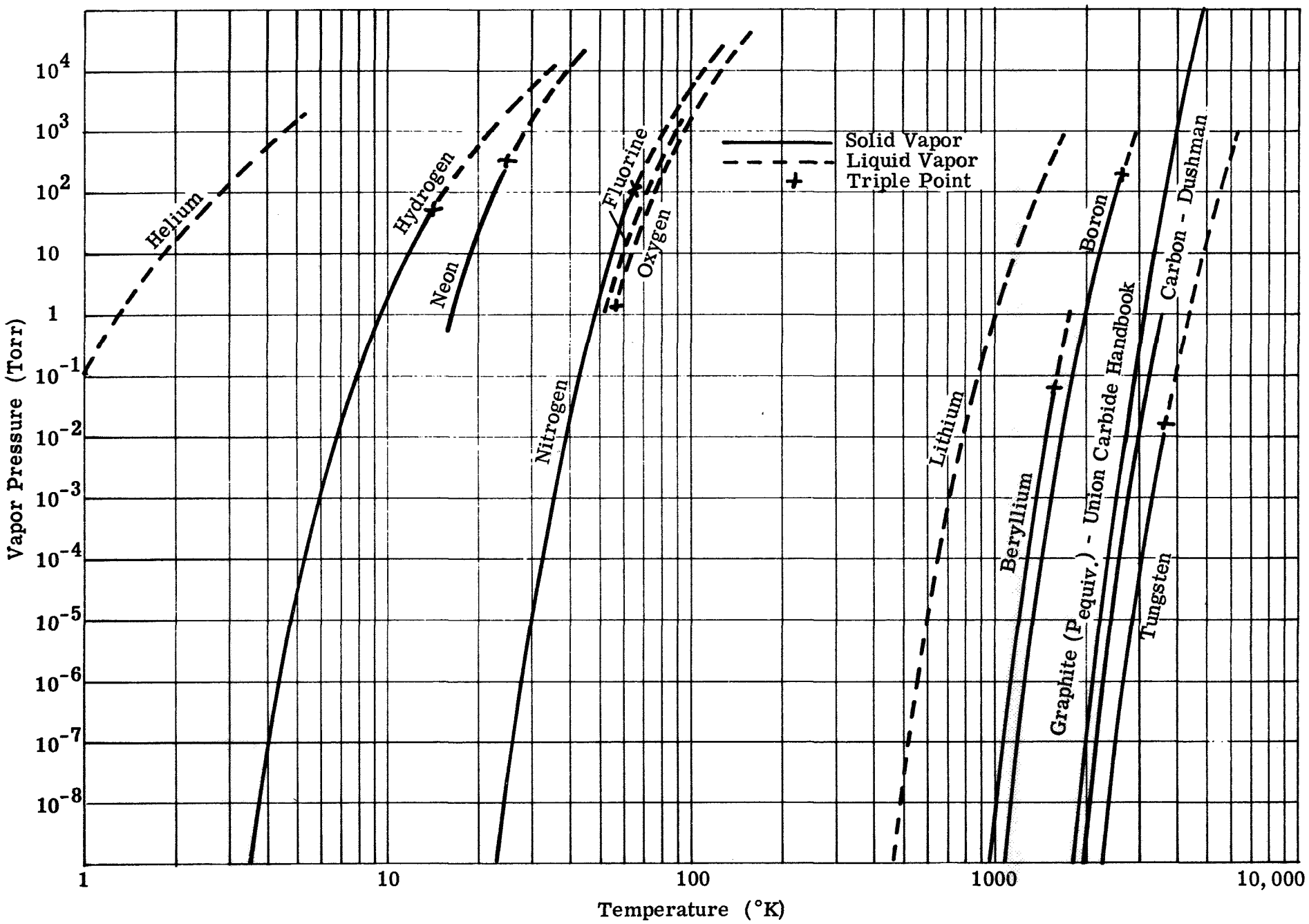

Figure 27. Vapor Pressure of a Number of Possible Propellants

Carbon has other important advantages of a less glamorous nature. The material is inexpensive, readily available, and easily machined. Its properties are well known and documented, and there is an extensive background of experience with graphite electrodes. Unless inhaled in quantities experienced by coal miners, the material presents few threats to health or environment. Finally, having an atomic number of 6, it has a relatively low atomic weight which may be of some advantage for operation in a wide range of specific impulse.

Graphite is available in numerous grades of varying density and purity and covering a wide range of physical properties. Several grades have been used in the test program to date and significant variations in the spitting that can be observed in the plume have been noted. It is believed that continued studies will be useful in determining which grades give the greatest electrode life. The thermal conductivity of graphite is of particular interest since this property affects the temperature gradients and thermal stresses that develop in the electrode as well as the heat loss to the electrode and the amount of heat remaining for vaporization of propellant. Electrodes with high thermal conductivity will provide more cooling and will operate at lower specific impulses. For this reason, pyrolytic graphite appears to be a material that should be carefully investigated.

Pyrolytic graphite provides a wide range of thermal conductivities - normally a factor of several hundred to one, depending on how the crystal structure is oriented. However, the thermal conductivity parallel to the planes decreases fairly rapidly with increasing temperatures. Figure 28 shows estimated temperature profiles near the end of cylindrical electrodes with the end maintained at vaporization temperature for a pulse duration of one millisecond. Profiles are shown for a conventional high density graphite and for pyrolytic graphite oriented in two ways. The cooling between pulses is assumed to be adjusted for each case so that the initial electrode temperature is 2000°C below the temperature of vaporization. It is shown that the temperature gradient and the amount of heat flowing into the electrode during a pulse may be varied by a factor of five or six by choosing the orientation of pyrolytic graphite. For example, for an electrode one-half inch in diameter, the heat loss associated with the temperature profiles shown is about 178 joules per pulse when the heat flow is parallel to the lattice planes, but reduces to 32 joules per pulse when the heat flow is normal to the lattice planes. Since the heat given up in the electrode fall region is expected to be several hundred joules, a substantial amount of heat remains for vaporizing the electrode tip to produce propellant gas. The choice of electrode material and geometry can be used to control the amount of material vaporized and therefore the specific impulse at which the unit will operate.

The temperature profiles shown were obtained from Chart 1 of Reference 11. The calculation involved the simplifying assumptions of uniform thermal properties throughout the material, the sudden application of vaporization temperature uniformly across the end of the electrode, and negligible dimensional change due to erosion during the pulse. This

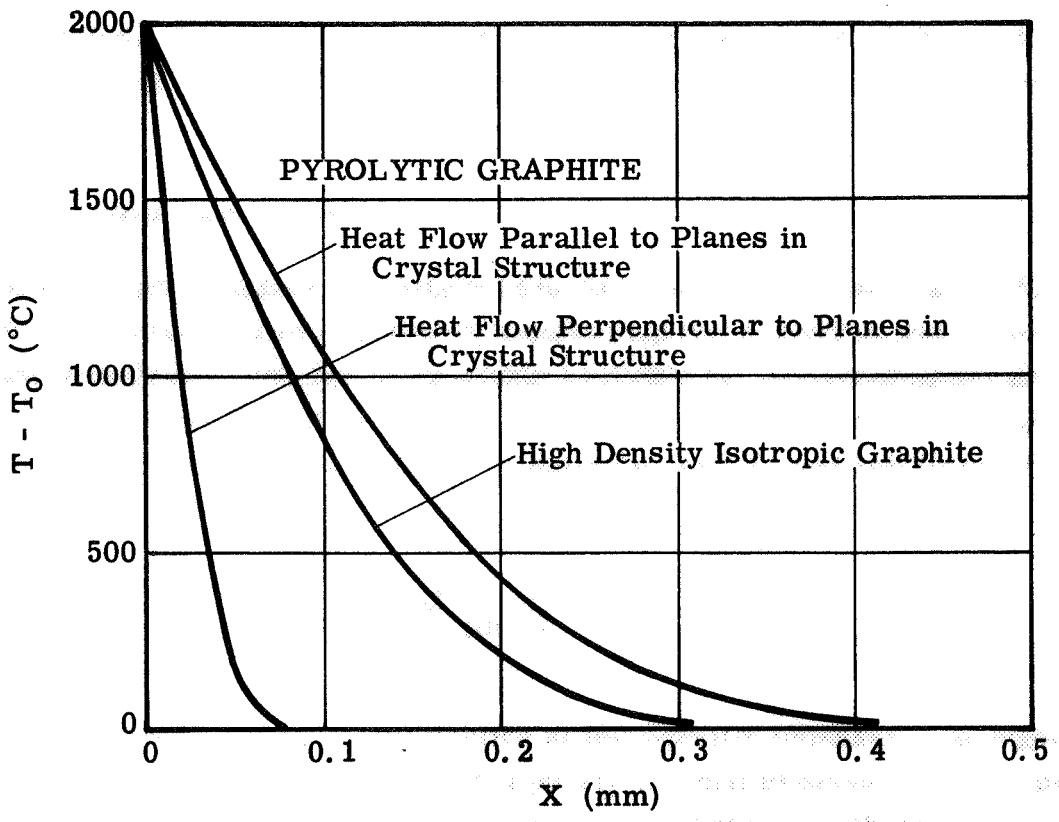

Figure 28. Estimated Temperature Variation in Cylindrical Graphite Electrodes at the End of a One-Millisecond Pulse

simplified model is presented to illustrate trends rather than as a precise representation of conditions.

Although the use of pyrolytic graphite may have advantages, there would also be complications. The material must be deposited on a mandrel and the thickness to diameter ratio is limited by thermal stresses that develop as the material cools and shrinks unevenly along its principal dimensions following deposition. It is often difficult to form parts of the desired shape and lattice structure and it is sometimes necessary to clamp small machined segments together to achieve the desired results. It would probably be necessary to find a configuration in which the thermal stresses that develop during thruster operation tend to cancel rather than adding to pre-stresses that originate as a result of the high temperature deposition process. The possible use of electrodes made of pyrolytic graphite is a subject for further study. The desired goal is to find a design that provides good electrical conductivity in the direction of current flow, low thermal stress during a pulse, and control of the thermal conductivity so that the desired amount of propellant is vaporized during a pulse. The most difficult requirement occurs when high electrical conductivity and low thermal conductivity are needed simultaneously. These conflicting requirements can be satisfied to some extent by using pyrolytic graphite and carefully selected

electrode geometries. To a first approximation, the heat loss can be limited to the value that occurs unavoidably due to flow along the path followed by the electrical current (see Section 4.4).

4.3 Electrode Vapor Acceleration

The potential performance advantages associated with the use of consumable electrode vapor for propellant can be clarified by considering the manner in which velocity is imparted to the propellant. The two mechanisms available for accelerating the propellant in an MPD thruster are thermal effects which involve heating the gas to a very high temperature followed by expansion in a physical or magnetic nozzle; and self field effects, which are given by the relation

$$F = \frac{\mu J^2}{4\pi}\left[\ln\left(\frac{r_a}{r_c}\right) + \frac{3}{4}\right]$$

The thermal effects are normally most effective at low specific impulses. As higher energies are required, the losses associated with a purely thermal expansion become prohibitive. However, these losses become less on a percentage basis at high power levels and might be dramatically reduced if an effective magnetic nozzle could be developed. Exceptionally high power levels are certainly available in pulsed MPD thrusters, and there is reason to believe that an effective magnetic nozzle action is obtainable from the self field alone in thrusters that use electrode vapor as the propellant. There is therefore a renewed interest in the feasibility of thermal acceleration effects in high performance thrusters.

In thrusters that use electrode vapor as the propellant, the vapor is introduced directly into the hottest part of the arc foot. This has the advantage that the propellant enters at high temperature and is exposed to the arc discharge immediately which provides for relatively uniform ionization of the material, improves the stability of the discharge at low pressures, and improves the effectiveness of electromagnetic forces. A second advantage is that the material evaporating from the cathode surface enters a high pressure region of the arc. The electrical discharge is highly concentrated in the cathode spot region which leads to a strong pinch effect and a high initial pressure. As the gas moves into a lower pressure region, the expansion converts thermal energy to directed kinetic energy which augments the acceleration due to self field forces. In effect, a very concentrated magnetic nozzle action is provided by the self field in a very localized region near the cathode spot. An external field coil is not required, but the gas pressures generated can be much higher than would be feasible even with large heavy external fields. However, the self field magnetic nozzle action can be fully utilized only when the propellant is introduced directly into the arc foot where pressure from the pinch effect is greatest.

At this point it is necessary to recognize that thrust produced by a self field magnetic nozzle is closely related to the usual self field forces. In fact, the thrust forces produced by the nozzle are identical to the self field forces, and are already included in the self field force equation. The only distinction is that the magnetic nozzle action recovers energy that went into ohmic heating (a resistive voltage drop in the arc) while the remaining thrust is produced by purely electromagnetic action which increases the arc voltage by the back emf effect. It is useful to make this distinction as it permits the feasibility of recovering thermal energy to be recognized.

To take full advantage of the magnetic nozzle action it is necessary for most of the propellant to be introduced from the cathode rather than the anode. This is because the cathode spot has a high current density and a strong pinch effect, while the anode foot tends to be more diffuse. Experiments with consumable electrodes show that the amount of propellant evaporated from the anode can be controlled over a wide range by modifying the electrode geometry, while the contribution of the cathode tends to be independent of electrode geometry. Thermal effects are therefore most effective at high specific impulses when they may be needed less. This situation might be remedied by using cathode additives with a lower heat of vaporization, or by using a geometry with reverse polarity and introducing a mechanism for concentrating the current density at the anode foot. Focused laser beams or electron beams might provide a means for increasing the conductivity of the gas in the anode fall region in a limited surface region. Notice that concentration of the arc foot for the center electrode is also shown to be advantageous in the self field force equation. A small arc foot is equivalent to a small inner electrode radius which increases the radius ratio term which in turn results in increased thrust force.

To assist in evaluating the importance of thermal effects, preparations are being made to calculate ideal nozzle performance with carbon gas assuming equilibrium conditions at the nozzle inlet, frozen flow through the nozzle, and no losses in the nozzle. Some information is available on the thermodynamic properties of carbon gas (see, for example, References 12 and 13), but since magnetic nozzles can operate at very high temperatures, it may be desirable to extend the calculations to higher temperatures. If this is found to be the case, calculations of thermodynamic properties will be extended to higher temperatures than those for which data are now available in the literature. Depending on the inlet temperature, carbon will be present in various states of molecularity, and each of these, as well as various levels of ionization, must be included in the calculations.

4.4 The Plasma Head and Triggering System

The thrusters tested so far on this program have used the conventional coaxial electrode geometry. In the future the need for extremely long life (and consequently of continuous feeding of the electrodes) may suggest other configurations. However, during this first phase of the work the proven coaxial geometry has been retained.

A coaxial plasma head is illustrated schematically in Figure 29 with a front electrode generally used as an anode (A) and a back electrode generally used as a cathode (C). The energy storage unit is connected across these two terminals and its discharge or triggering can be obtained in a great variety of ways going from a direct short circuit of two terminals to low voltage, high voltage, high frequency or even laser discharge initiation. In many of these cases a third electrode called the triggering electrode is used as shown schematically in Figure 30.

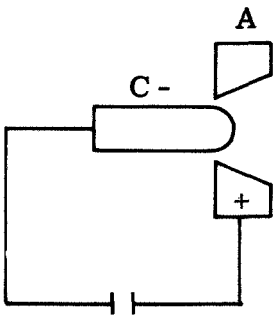

Figure 29. Schematic of a Coaxial Plasma Head

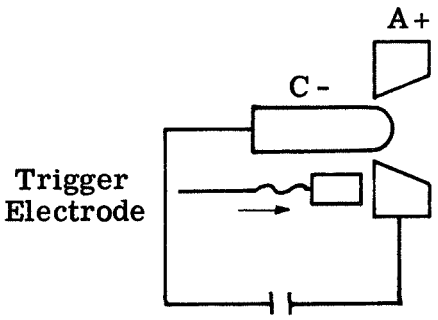

Figure 30. Schematic of a Coaxial Plasma Head With Triggering Electrode

The practical design of these plasma heads is not very different from conventional units with the exception that for an experimental program with pulsed operation the thrusters are designed to carry very high instantaneous currents and to accommodate a large variety of electrodes with the minimum amount of modification. Figures 31 through 35 illustrate the design of the five plasma heads that have been used for most of the tests. The electrodes of these units are capable of operating with currents greater than 50 kiloamps. Figure 31 (Plasma Head No. 2HV) uses a high voltage triggering signal and has no moving parts; Figure 32 (Plasma Head No. 2) requires movement of the triggering electrode to form a contact and cause the discharge of an auxiliary low voltage capacitor; Figure 33 (Plasma Head No. 1) is the same geometry as Figure 32 but of reduced dimension and shortened electrodes; Figure 34 (Plasma Head No. 3) operates without a trigger electrode using an electromagnetic actuator to push the two main electrodes together; Figure 35 (Plasma Head No. 4) shows the same geometry as Figure 34 but with a triggering electrode. A detailed description of the various triggering systems will follow in this same section.

Although systems have been available for triggering the arc discharge since tests were initiated, there has been a continuing need for improvement; not because it was particularly difficult to start the arc, but because of various interface problems that arose as attempts were made to refine the test procedure and to operate with repeated pulses for extended time periods. Vacuum levels of the order of 10^{-7} torr are possible between

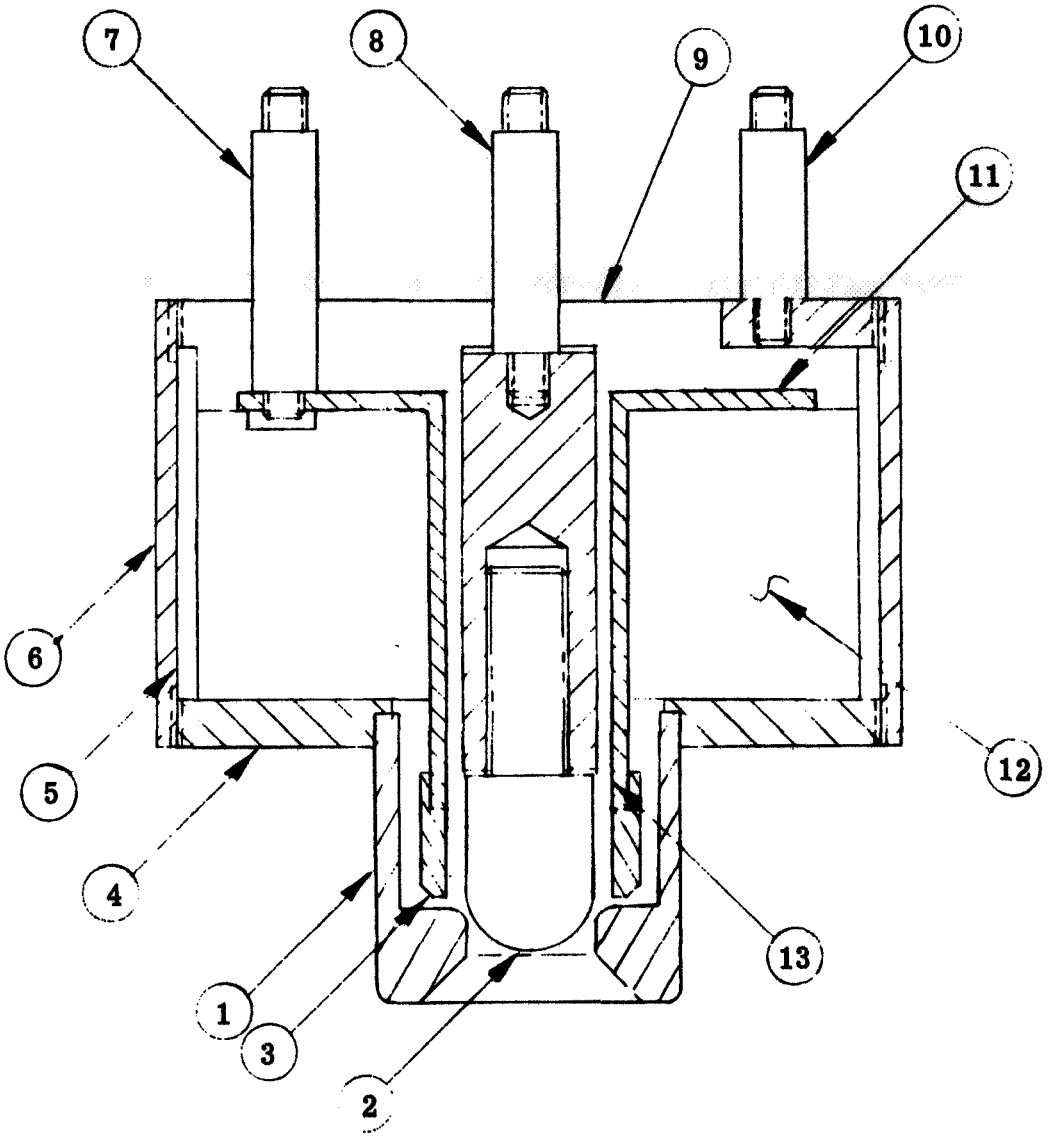

1. Anode Carbon Tip
2. Cathode Carbon Tip
3. Trigger Carbon Tip
4. Anode Front Plate
5. Insulator
6. Outside Anode Connection
7. HV Trigger Terminal
8. Cathode Terminal
9. Insulator
10. Anode Terminal
11. Trigger Base
12. Insulator
13. Trigger Tip Support

Figure 31. Plasma Head No. 2HV

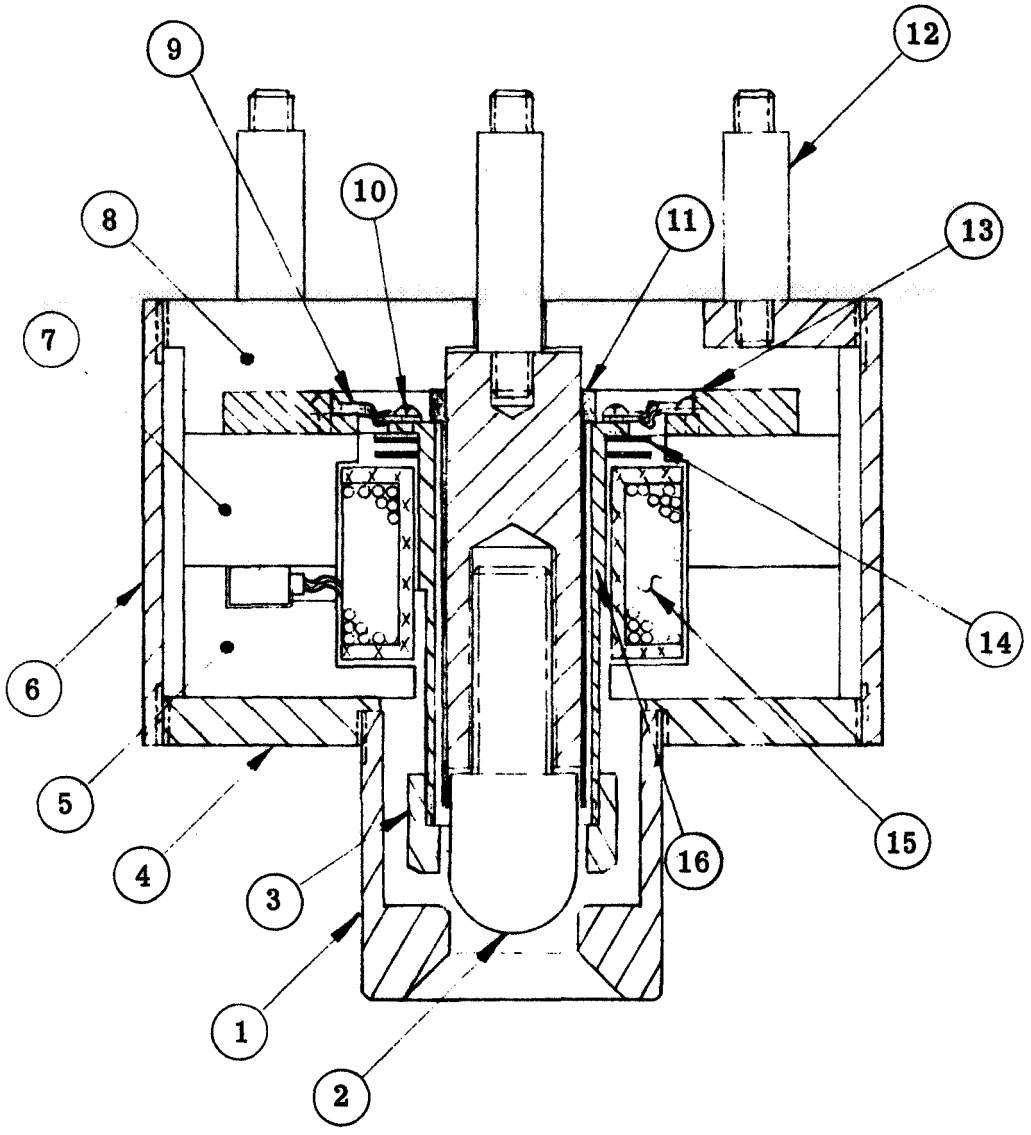

1. Anode Carbon Tip
2. Cathode Carbon Tip
3. Trigger Carbon Tip
4. Anode Front Plate
5. Insulator
6. Outside Anode Connection
7. Insulator
8. Insulator
9. Trigger Connection
10. Trigger Terminal
11. Insulator
12. Anode Terminal
13. Trigger Fix. Terminal
14. Trigger Spring
15. Coil
16. Magnetic Armature

Figure 32. Plasma Head No. 2

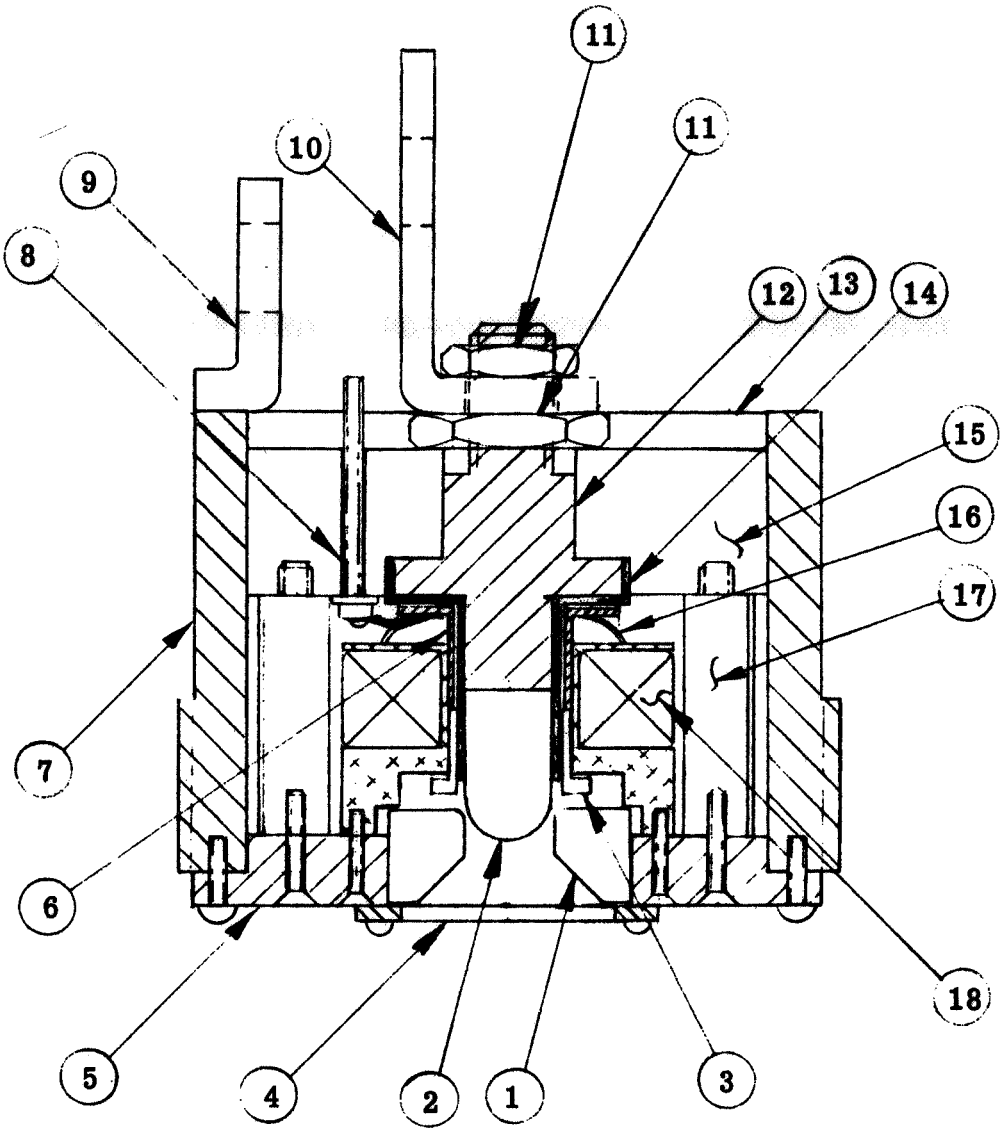

1. Anode Carbon Tip
2. Cathode Carbon Tip
3. Trigger Carbon Tip
4. Anode Tip Holder
5. Front Anode Connection
6. Magnetic Armature
7. Outside Anode Connection
8. Coil Connection
9. Anode Terminal
10. Cathode Terminal
11. Cathode Nuts
12. Cathode Copper Holder
13. Insulating Plate
14. Cathode Insulator
15. Insulator Block
16. Trigger Spring
17. Coil Holder
18. Coil Windings

Figure 33. Plasma Head No. 1

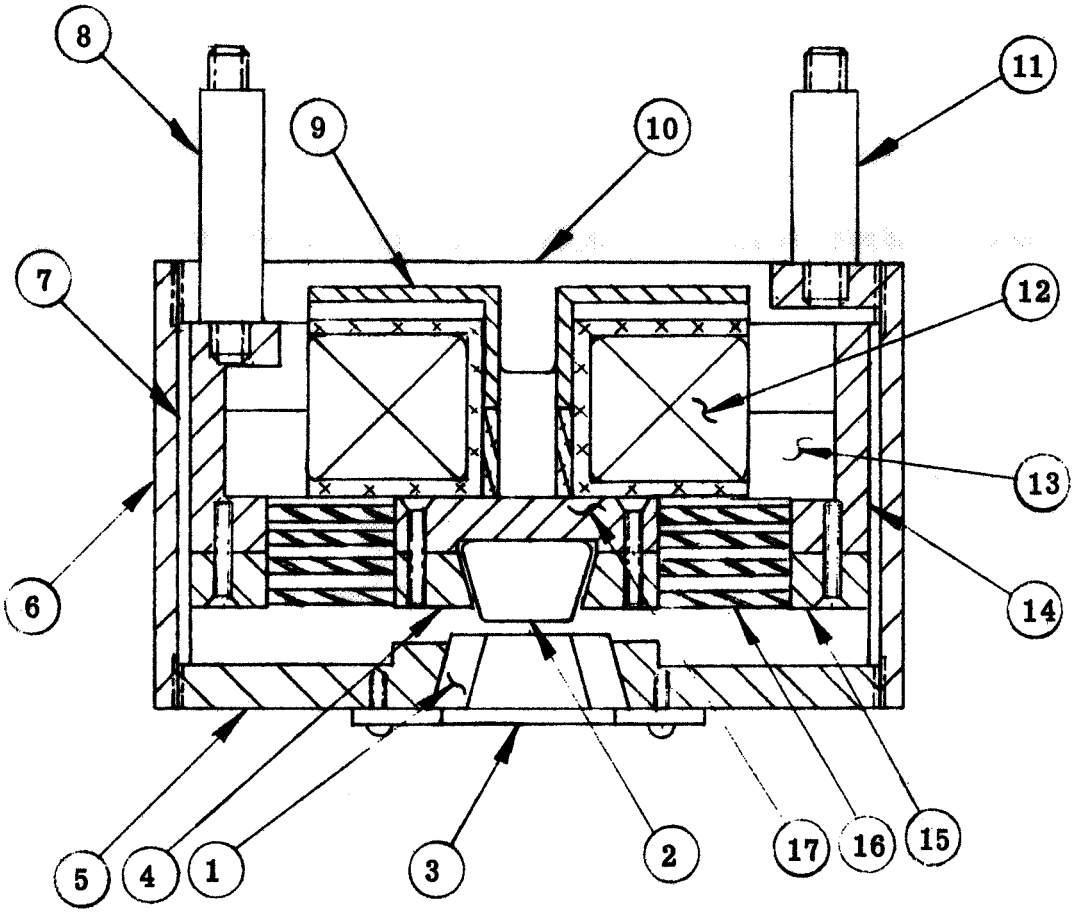

1. Anode Carbon Tip
2. Cathode Carbon Tip
3. Anode Holder
4. Cathode Holder
5. Anode Front Plate
6. Anode Outside Connection
7. Insulator
8. Cathode Terminal
9. Cathode Support
10. Insulator
11. Anode Terminal
12. Coil
13. Insulation
14. Cathode Outside Connection
15. Flexible Connection Holder
16. Flexible Copper Connection
17. Cathode Holder

Figure 34. Plasma Head No. 3

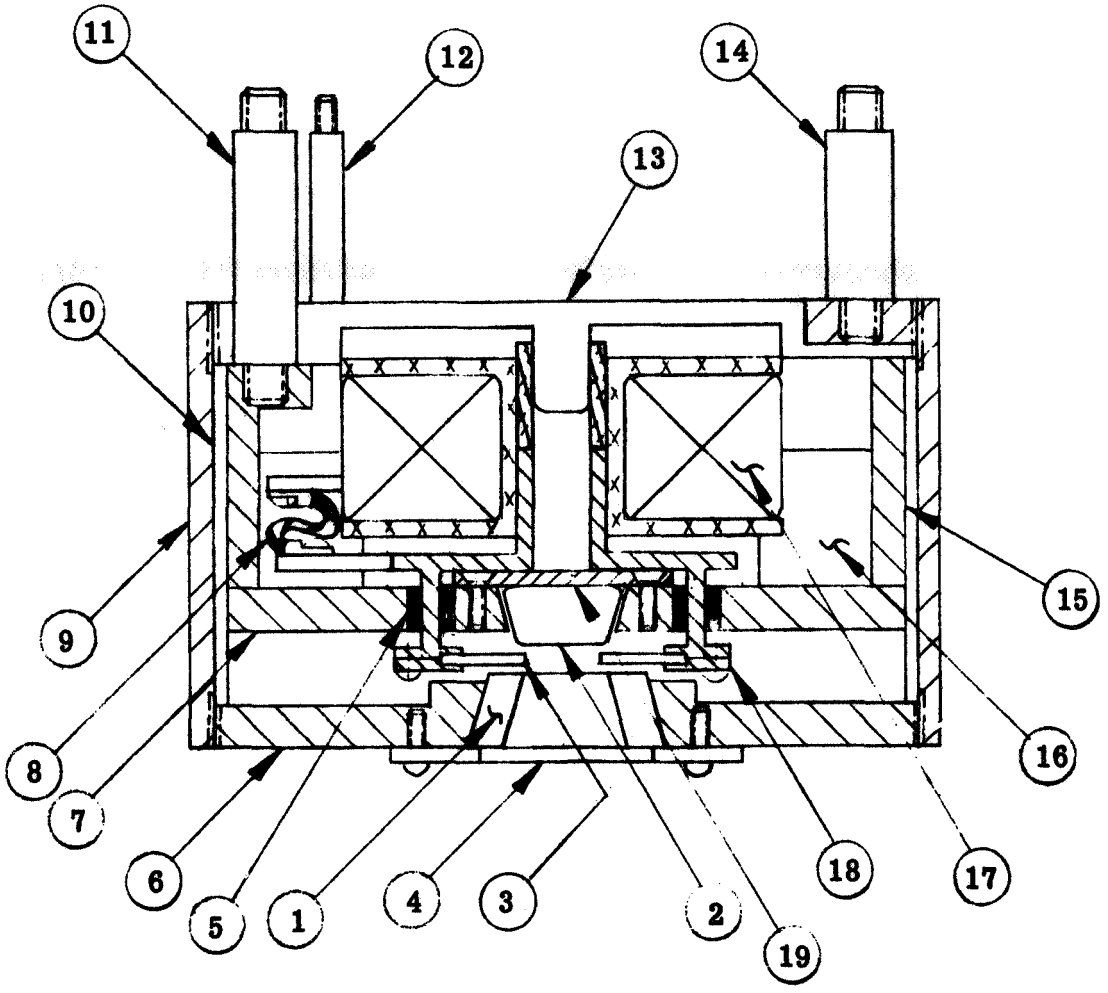

1. Anode Carbon Tip
2. Cathode Carbon Tip
3. Trigger Carbon Tip
4. Anode Holder
5. Insulator
6. Anode Front Plate
7. Cathode Front Plate
8. Trigger Connection
9. Anode Outside Connection
10. Insulator
11. Cathode Connection
12. Coil Connection
13. Insulator
14. Anode Connection
15. Cathode Outside Connection
16. Insulator
17. Coil
18. Insulating Support
19. Cathode Holder

Figure 35. Plasma Head No. 4

pulses, and the interelectrode distance needed to obtain discharges at an acceptable voltage level with this condition is of the order of a few hundred microns. Even with this relatively small distance the peak voltage required for triggering is from 10 to 30 kilovolts. This high voltage requirement leads to two types of difficulties; the high voltage discharge may occur at other locations in the circuit, or the discharge will introduce serious interference effects with instrumentation leads.

When the torsional ballistic pendulum was put in use, the high frequency power supply for triggering was housed in the gas tight capacitor enclosure which was designed for a pressure of 2 psia. The major purpose of the gas tight enclosure is to prevent rapid evaporation of the electrolyte in the condensers. In addition, the higher pressure inhibits arcing and makes it easier to construct circuitry that will operate trouble free. However, difficulty was experienced with arcing between the triggering circuit leads and it was found necessary to strengthen the enclosure to permit a gas pressure of one atmosphere (see Section 5).

Arcing can also occur within the thruster at other locations than across the electrode tips. After repeated use, electrode erosion may increase the gap between the triggering electrode and the anode and cathode. At the same time, vapor from the electrodes may deposit on the insulating material making it easier for the discharge to follow a path along the insulator surfaces. Alternately, since the triggering gap is so small, small particles of material from the electrodes could lodge across the gap shorting out the path for the triggering discharge.

Radio frequency interference effects became evident as soon as routine measurements were started with instrumentation leads extending into the torsional ballistic pendulum. The effect was initially severe enough to spoil most of the recordings obtained. Carefully constructed shielding of the circuits involved failed to eliminate the trouble and it became evident that the noise source would have to be reduced if accurate traces were to be obtained. A series of experimental triggering circuits followed, the most successful of which are described below.

The initial triggering system (Figure 36) was based upon a chain of successive triggering circuits which energize a tesla coil primary. The high frequency, high voltage induced in the tesla secondary was capable of crossing the vacuum gap of the trigger electrode with or without the use of an auxiliary storage capacitor to increase the intensity of the final triggering discharge. With the proper configuration, this system gave very reliable and reproducible operation over the complete range of vacuum levels and main capacitor bank charging voltages required. Unfortunately, the system produced intense radio interference effects and also seemed particularly subject to secondary failures due to the inadequacy of the high voltage insulation under the intense high frequency field created.

At this point it was decided to eliminate the high frequency feature, and the circuit

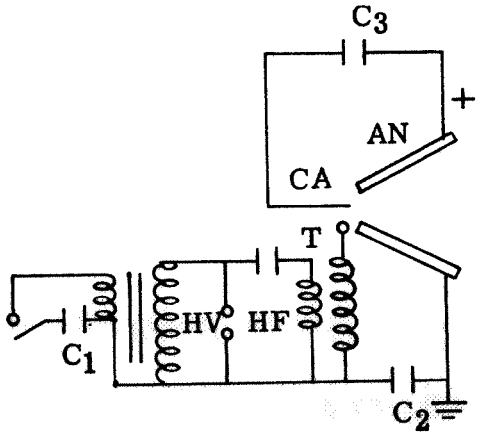

Figure 36. High Voltage High Frequency Trigger

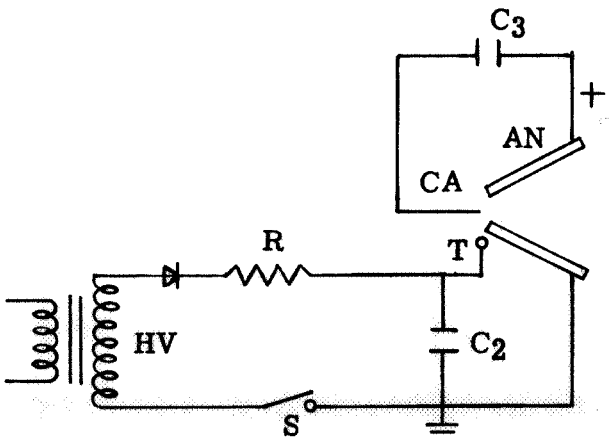

Figure 37. High Voltage DC Trigger

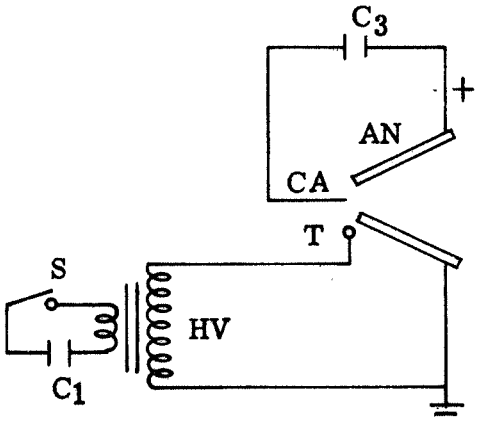

Figure 38. High Voltage Pulsed Trigger

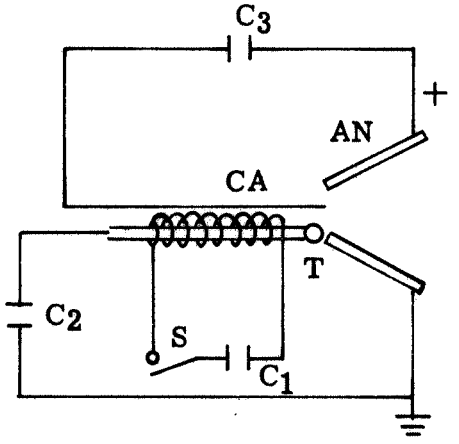

Figure 39. Low Voltage Electromechanical Trigger

illustrated in Figure 37 was developed and tested with encouraging results. A rectified d. c. high voltage supply was used to charge the auxiliary capacitor, C_1, which was connected to the trigger electrode, T. As soon as the d. c. sparking voltage was reached, the discharge of C_1 initiated the discharge of the main capacitor, C_3. This system was used successfully but was finally abandoned because the relatively high d. c. voltage required introduced too many secondary difficulties.

Next, the circuit shown in Figure 38 was tried for applying a relatively powerful high voltage pulse to the triggering electrode while minimizing the portion of the circuit exposed to the high voltage. The reliability of the system proved to be excellent. The only feature still causing concern was the high voltage insulation required for the triggering electrode. A special head designed for high voltage operation was tested extensively with good results.

The difficulties experienced with the high voltage triggering circuits that have been tried stimulated the development of the new triggering system illustrated in Figure 39. With this system the triggering electrode, T, is moved until it is brought in electrical contact with the anode. The low voltage capacitor, C_2, connected to the triggering electrode discharges producing an intense spark capable of triggering the discharge of the main capacitor, C_3. Capacitor C_1 is used to create the mechanical pull needed to move the triggering electrode with sufficient rapidity. This system has been tested extensively with completely reliable results. The difficulties associated with a high voltage triggering circuit have been eliminated, the problem of closely maintaining a small electrode gap has been avoided, and the repetition rate has been found adequate for quasi-steady testing. No interference of any kind has been detected with this design to date. The reproducibility of the main discharge pulse patterns has been verified with superimposed oscillographs. Figures 40 and 41 show respectively the initial high voltage and low voltage experimental heads which were used for the tests described.

A simpler variation of the low voltage electromechanical trigger is also being tried. In this configuration the center electrode is movable and provides the triggering action (see Figure 42). The separate triggering electrode and the separate capacitor to provide the triggering discharge are both eliminated with this arrangement. Several variations of this scheme may be obtained by reversing the polarity and by moving either the anode or cathode to provide a triggering action.

The triggering action can be initiated either manually or automatically. The switch can be closed manually using a pushbutton on the operating panel, or a timing device can be activated that closes a parallel switch repetitively at an interval selected to allow complete recharging of the main capacitors. The arrangement of the timing circuit is shown in Figure 43 for the case with a low voltage electromechanical trigger. The capacitor C_1 is charged at a controlled rate through a resistor. The switch is closed when the voltage across the capacitor reaches a predetermined value. This could be done with a silicon controlled rectifier, but at present a relay energized by the voltage across the capacitor is being used. The contacts are normally held open by a spring that resists the solenoid force until the selected voltage is applied.

All the plasma heads used in our tests have standard electrodes easily interchangeable and especially designed to carry relatively high currents. Figure 44 illustrates four geometries of back electrodes used. The design has been gradually improved from Model 1 to Model 4 which is the one most frequently used during recent tests. For each "model" various "types" are listed in the associated tables and column. Column "M" refers to the grade of material used and the other columns refer to the dimensions. Model 1 is unsatisfactory when carbon is used because of frequent breakage in the threaded part; Model 2 has a metal thread and is used exclusively for carbon; Model 3 has a wide conical part that assures a very good contact between the carbon insert and the metal holder; and

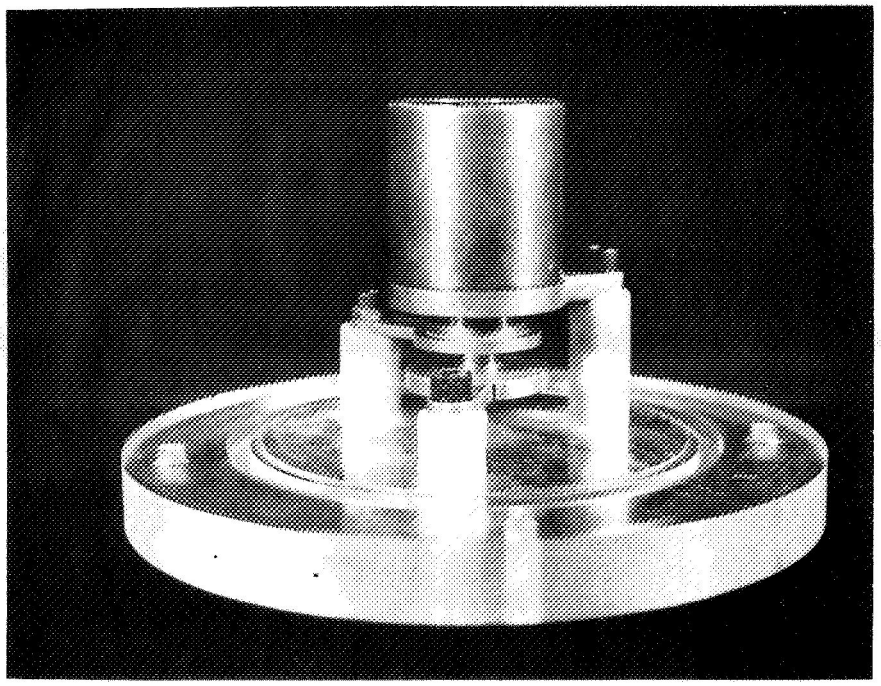

Figure 40. High Voltage Triggered Head

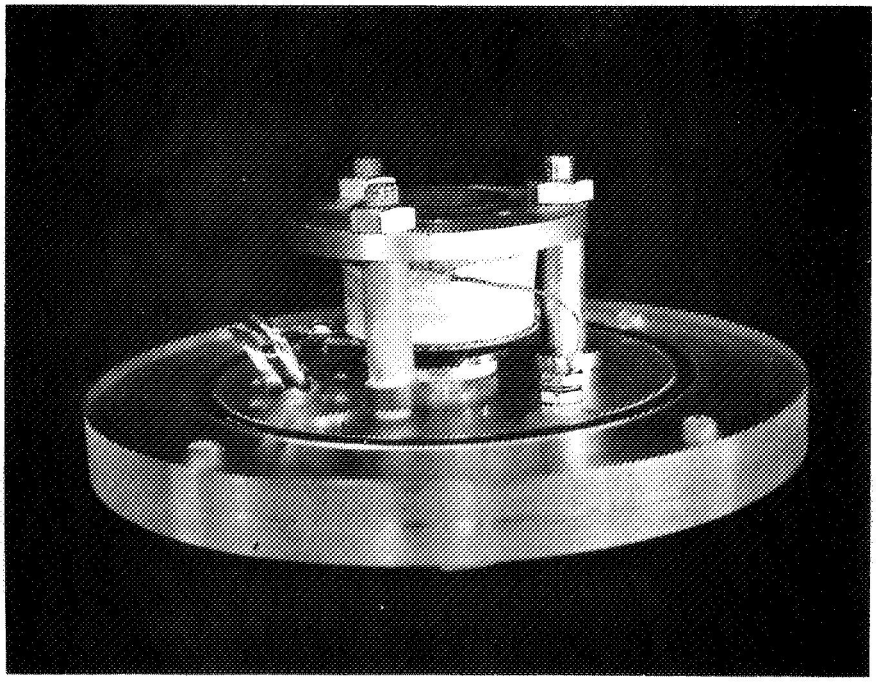

Figure 41. Low Voltage Triggered Head

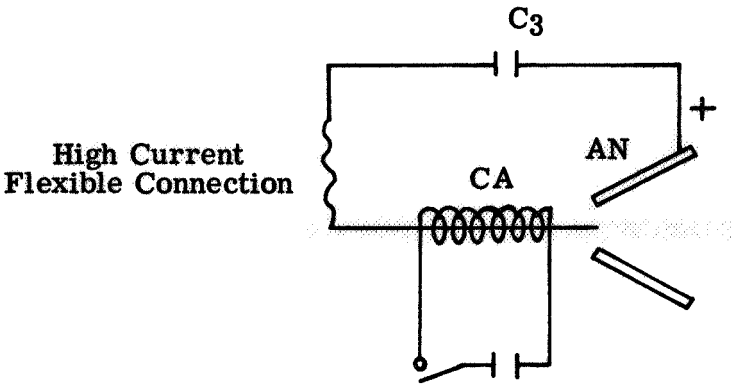

Figure 42. Triggerless Electrode Contactor

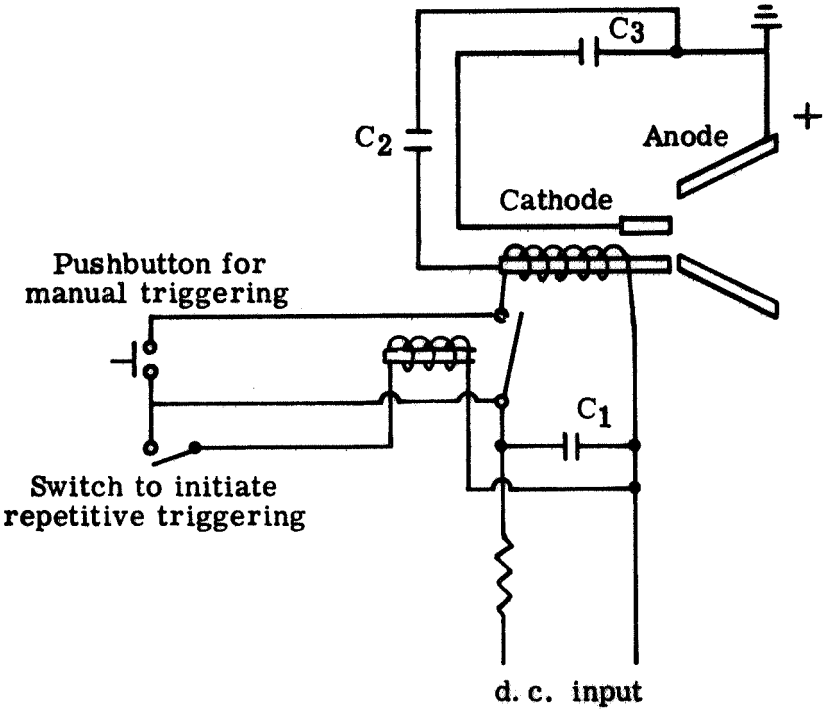

Figure 43. Circuit for Initiating the Triggering Action
(Electromechanical Trigger)

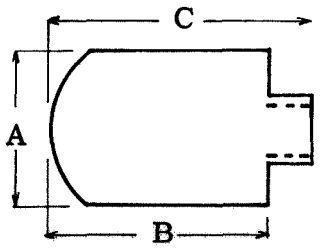

Model 1

Type	M	A	B	C	D	E
1	C5	19.0	25	60		
2	C5	12.7	27	40		

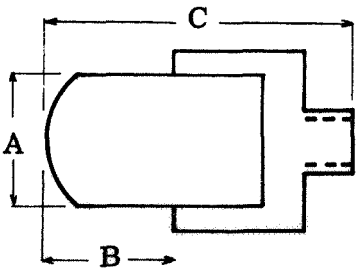

Model 2

Type	M	A	B	C	D	E
1	C5	19.0	25	90		
2	C5	12.7	25	90		

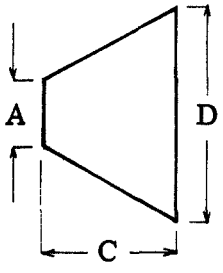

Model 3

Type	M	A	B	C	D	E
1	C5	15		12.7	19	

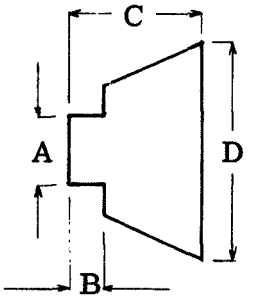

Model 4

Type	M	A	B	C	D	E
1	C5	19.0	4	12.7	22	
2	C5	12.7	4	12.7	22	
3	C5	6.3	2	12.7	22	

Figure 44. Back Electrode, Dimensions in Millimeters

Model 4 is practically the same except that it is used to test high power density small area electrodes while still assuring a satisfactory contact with the metal holder. Data on the evaporation rate of a number of electrodes are presented in Section 4.5 with the electrodes identified by model, type and polarity.

Figure 45 illustrates four geometries of front electrodes. These have also been gradually improved during the test, primarily to reduce the contact resistance. The last geometry (Model 8) has a conical form that assures a very good contact between the carbon insert and the metal holder. This model has been used most frequently for the front electrode in recent tests.

Figure 46 illustrates four geometries of triggering electrodes used in the head shown in Figure 41 to give low voltage triggering obtained through the action of an electromagnetic actuator. Due to the relatively low current discharge used to obtain the triggering effect, these electrodes demonstrate a long life with satisfactory operation.

Table II gives some information on the types of carbon used in the tests and to be used in future investigations. Types C5 and C6 have been used more frequently than the others. Types C2 and C9 will be used in the future. A photograph of some of the electrodes is shown in Figure 47.

TABLE II

PHYSICAL PROPERTIES OF CARBON AND GRAPHITE
USED FOR ELECTRODES

Type	Density g/cm^3	Impurity ppm	Resistivity $\Omega/cm \times 10^{-3}$	Porosity %	Thermal Expansion $10^{-6}/°C$
C1	1.61	6	0.63	25	2.6
C2	1.90	6	1.17	16	3.4
C3	1.45	6	5.08	31	8.4
C4	1.60	6	0.63	25	2.7
C5	1.79	200	1.77	23	2.5
C6	1.84	250	1.77	23	2.5
C7	1.79	250	1.77	23	2.5
C8	1.88	500	1.62	17	2.7
C9	1.88	5	1.77	17	2.7

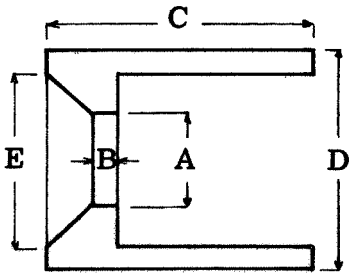

Model 5

Type	M	A	B	C	D	E
1	C5	22.0	5	40	42	36
2	C5	12.5	5	40	42	32

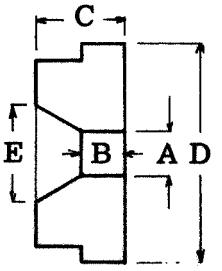

Model 6

Type	M	A	B	C	D	E
1	C5	12.7	5	13	35	26

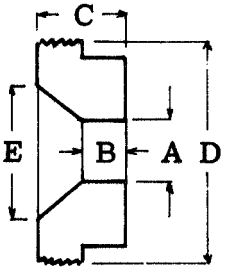

Model 7

Type	M	A	B	C	D	E
1	C5	12.7	3	12.7	43	30
2	C5	19.0	4	12.7	43	30

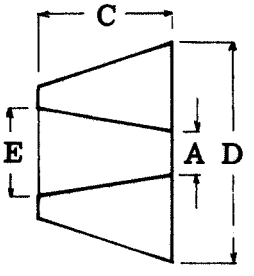

Model 8

Type	M	A	B	C	D	E
1	C5	12.7		12.7	29	17
2	C5	19.0				

Figure 45. Front Electrode, Dimensions in Millimeters

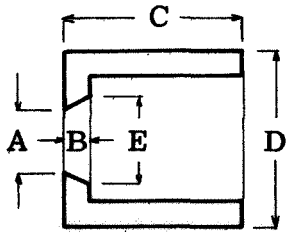

Model 9

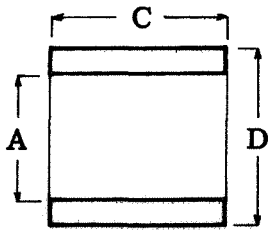

Model 10

Type	M	A	B	C	D	E
1	C5	18.0	4.0	16	30	25
2	C5	12.7	3.1	16	22	16

Type	M	A	B	C	D	E
1	C5	25		26	31	
2	C5	16		26	22	

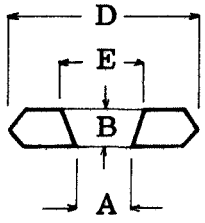

Model 11

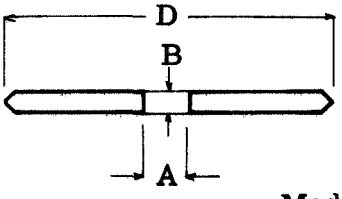

Model 12

Type	M	A	B	C	D	E
1	C5	12.7	3.2	4	40	16

Type	M	A	B	C	D	E
1	C5	12.7	3	5	40	

Figure 46. Triggering Electrode, Dimensions in Millimeters

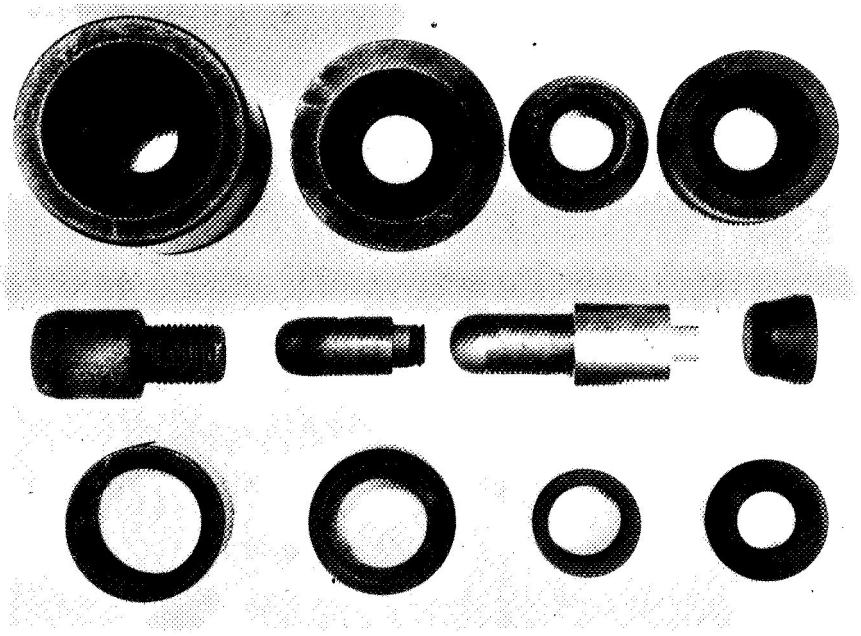

Figure 47. Models and Types of Carbon Electrodes Used in Tests

4.5 Calibration and Measurements

The purpose of this part of the work is to study the ablation patterns and evaporation rates of a number of electrode geometries using different grades of graphite at various energy levels. Each test consists of a series of pulses of identified shape, duration, and amplitude (as recorded during the series). Measurements were made of the difference in weight before and after the tests for all the electrodes in the plasma head. These weight measurements were then used to determine the evaporation rate of the electrodes.

For identification purposes all the electrodes are marked with a code with two groups of digits preceeded by a polarity sign. The first digit or group of digits indicate the model of the electrode (as, for example, is indicated in Figure 44), the second digit or group of digits indicate the sub-model or type of the electrode (which generally identify the particular material used and the dimensions). For example, the electrode code "-2/2" is a cathode of type 2 of Model 2 shown in Figure 44, which is made of carbon C5 and has a maximum diameter of 12.7 millimeters, and a total length of 90.0 millimeters.

The precision and reproducibility of the weight loss measurement is very important to reduce the number of pulses required for each series. Considering that the evaporation of material for each pulse varies from a small fraction of a milligram to one or two milligrams, the scale must be sensitive to changes of a fraction of a milligram to obtain a useful measurement without having to fire thousands of pulses during each series. For this

reason a high precision direct reading analytical scale has been used with a sensitivity of 0.03 milligram which permits standard number of pulses in a series to be reduced to 100 or even 50.

In making these precise measurements it was found that all graphites are hygroscopic and absorb water vapor from the atmosphere, producing an apparent variation of the weight. To avoid this it is necessary to desiccate the samples and immediately transfer them on the analytical scale in a dry atmosphere, both before and after the tests. With this precaution, reproducible results have been obtained with good regularity.

Although a great variety of samples, geometries and qualities of materials have been tested, much of the data were taken before techniques for maintaining the desired accuracy were fully developed. The results selected for reporting are believed to be of fair accuracy, but must still be considered preliminary.

Table III shows the results obtained with some of the most commonly used electrodes. Most of them use the front electrode as the anode. Configurations with and without separate triggering system were tested. It is interesting to note that the evaporation of the cathode when used as the back electrode varies from 1/10 to 1/4 of the anode evaporation when the anode is used as the front electrode. However, if the polarity is reversed, the evaporation from the cathode and anode is found to be about the same and the total evaporation is four times higher than the total evaporation with normal polarity. The consumption of the triggering electrode is very small and probably can be considerably decreased by improvements in design. It is also interesting to note that a substantial increase in evaporation (or at least of erosion) was obtained when the arc was triggered by direct contact of the main electrodes. This effect must be seriously studied, especially in conjunction with the thrust measurements which should give an indication of how effectively the additional electrode material is utilized as a propellant (see Section 4.2). This triggering system appears to be giving satisfactory performance, but two questionable aspects must be investigated. There is some indication that spitting is heavier when contact is made between the main electrodes. It will be necessary to examine the contact areas of the electrode surfaces to see if unusual erosion patterns appear after a long series of pulses. The other question concerns the plume pattern at the time that the arc is initiated. Carbon deposits in the interior of the thruster suggest that initially part of the plume extends downstream from the contact point. It may be necessary to modify the electrode geometry to minimize this small reverse plume effect. It is not known whether or not the same effect occurs when other types of arc triggering systems are used.

4.6 Test Results on the Plasma Head

The measurements reported in the preceding section (4.5) cover a wide range of geometries and show some interesting trends that will require further study and testing.

TABLE III

Table of Measured Electrode and Insulator Consumption Rates for a Variety of Electrode Geometries

Test Series No.	Tank Pressure torr	Pulses Total No.	Electrical Energy Storage Data					Average Propellant Consumed in Milligrams Per Pulse								
			Capacitor		Quasi-Steady Regime			Front Electrode		Back Electrode		Trigger Electrode		Insulation		Total
			volt	joule	msec	volt	kamp	type	mg	type	mg	type	mg	type	mg	mg
1	9×10^{-7}	50	400	4300	0.8	105	22	+5.1	1.10	-1.1	0.25	10-1	0.005	TB	0.010	1.30
2	9×10^{-7}	110	400	4300	0.8	95	23	+5.1	0.90	-1.1	0.20	10-1	0.005	TB	0.009	1.00
3	5×10^{-7}	103	400	4300	0.8	100	22	+5.2	0.70	-1.2	0.27	10-1	0.004	TB	0.007	0.90
4	6×10^{-7}	52	400	4300	0.8	105	22	+5.2	0.60	-1.2	0.20	10-1	0.004	TB	0.008	0.80
5	4×10^{-7}	60	400	4300	0.8	95	23	+6.1	0.50	-1.2	0.08	10-2	0.008	TB	0.010	0.58
6	8×10^{-7}	102	400	4300	0.8	90	24	+6.1	0.45	-1.2	0.07	10-2	0.007	TB	0.009	0.52
7	7×10^{-7}	51	400	4300	0.8	85	25	+6.1	0.55	-1.2	0.09	10-2	0.005	TB	0.010	0.65
8	7×10^{-7}	50	400	4300	0.8	90	24	+6.1	0.50	-1.2	0.10	10-2	0.006	TB	0.009	0.60
9	5×10^{-7}	110	400	4300	0.8	95	23	+6.1	0.60	-1.2	0.10	10-2	0.007	TB	0.012	0.70
10	4×10^{-7}	65	400	4300	0.8	85	25	+7.1	0.70	-2.2	0.10	10-2	0.005	TB	0.005	0.50
11	4×10^{-7}	50	400	4300	0.8	85	25	+7.1	0.50	-2.2	0.10	10-2	0.005	TB	0.005	0.60
12	6×10^{-7}	53	400	4300	0.8	90	24	+7.1	0.50	-2.2	0.15	10-2	0.005	TB	0.005	0.55
13	7×10^{-7}	105	400	4300	0.8	85	25	+7.1	0.60	-2.2	0.15	10-2	0.008	TB	0.005	0.75
14	4×10^{-7}	108	400	4300	0.8	95	23	+5.2	0.80	-2.1	0.28	1-1	0.010	TB	0.008	1.08
15	4×10^{-7}	101	400	4300	0.8	100	22	+5.2	0.75	-2.1	0.25	1-1	0.009	TB	0.007	1.00
16	4×10^{-7}	53	400	4300	0.8	100	22	+5.2	0.82	-2.1	0.22	1-1	0.008	TB	0.006	1.04
17	3×10^{-7}	51	400	4300	0.8	80	26	+7.2	0.90	-2.1	0.10	1-1	0.009	TB	0.005	1.00
18	4×10^{-7}	54	400	4300	0.8	80	26	+7.2	0.95	-2.1	0.10	1-1	0.008	TB	0.006	1.05
19	5×10^{-7}	103	400	4300	0.8	90	24	+7.2	0.85	-2.1	0.10	1-1	0.010	TB	0.007	0.96
20	4×10^{-7}	105	400	4300	0.8	90	24	+7.1	0.60	-2.2	0.12	10-2	0.009	TB	0.005	0.73
21	5×10^{-7}	128	400	4300	0.8	85	25	+7.1	0.55	-2.2	0.15	10-2	0.006	TB	0.005	0.71
22	4×10^{-7}	52	400	4300	0.8	85	25	+5.2	0.60	-1.2	0.20	9-1	0.008	TB	0.009	0.80
23	5×10^{-7}	55	400	4300	0.8	100	22	+5.2	0.50	-1.2	0.20	9-1	0.006	TB	0.010	0.70
24	6×10^{-7}	100	400	4300	0.9	95	23	+5.2	0.40	-1.2	0.20	9-1	0.005	TB	0.012	0.65
25	6×10^{-7}	101	400	4300	0.9	60	30	+8.1	1.00	-3.1	0.12	----	-----	TB	0.005	1.10
26	5×10^{-7}	105	400	4300	0.9	65	29	+8.1	0.90	-3.1	0.09	----	-----	TB	0.006	1.00
27	6×10^{-7}	60	400	4300	0.9	60	30	+8.1	0.90	-4.1	0.10	----	-----	TB	0.007	1.00
28	4×10^{-7}	103	400	4300	0.9	65	29	+8.1	0.70	-4.1	0.10	----	-----	TB	0.006	0.80
29	3×10^{-7}	102	400	4300	0.9	65	29	-8.1	1.50	+4.1	1.40	----	-----	TB	0.006	2.90
30	5×10^{-7}	100	400	4300	0.9	60	30	-8.1	1.60	+4.1	1.50	----	-----	TB	0.005	3.10
31	5×10^{-7}	52	400	4300	0.9	70	28	-8.1	1.40	+4.1	1.20	----	-----	TB	0.005	2.60

Unfortunately, some of the measurements did not take into consideration the absorption of moisture that was found to have an affect on the accuracy of the results. The scatter in the data between test runs made on the same configuration is evidence of this. It is natural that with the experience obtained during this series of measurements and with the precautions dictated by this experience, future data will be much more reliable and precise. The conical geometry used for some of the electrodes (see Figures 44 and 45) assures a better contact with the metal holder. The electrodes that operate by direct contact without intermediate triggering give reliable results and can be taken as a reproducible standard, but the evaporation per pulse for a power of about two megawatts is higher (about 0.9 milligram for the anode and 0.1 milligram for the cathode). It will be of interest to make additional tests using this stable thruster design with a variety of electrode geometries and graphite grades.

The relative rates of evaporation of the different types of electrodes have been discussed in the preceding section, but it is of interest to assess the energy cost to vaporize this material. The energy delivered to the electrodes ranges from 2000 to 2500 joules. The heat of vaporization for carbon is about 50 joules per milligram. Since the amount of material vaporized per pulse is between 0.5 and 3.0 milligrams, we find that the vaporization energy is only a few percent of the total pulse energy. The electrode fall region loss is usually much greater than this which suggests that the cooling of the electrodes between pulses is effective in reducing the rate of evaporation. The ability to operate with small quantities of vapor is desirable because it permits operation at high specific impulses. However, if the low vaporization rate is caused by a low electrode surface temperature at the beginning of the pulse, it may result in an uneven rate of vaporization during the pulse which would be detrimental to the efficiency. More refined instrumentation might be used to evaluate this effect. Optical techniques for examining the plume appear to be most promising since fast response instruments in the thruster would be subject to serious interference effects from the arc discharge.

It has been noted earlier that arc voltage is measured back some distance from the tips of the electrodes. Actually, connections are made to the metal electrode holder rather than to the graphite. The difference introduced in the readings is by no means trivial, especially for the earlier electrode designs. For example, back electrode Model 1.2 is one-half inch in diameter and nearly one inch in length. When the electrocal resistance of this current path is estimated, we reach the disturbing conclusion that a large fraction of the voltage drop can be accounted for in terms of resistive loss in the electrodes! The electrodes used initially were simply too small to carry the high currents required without excessive loss. This condition was remedied in the later designs with the conical contact surface that provides a much better current flow path between the metal conductor and the arc attachment point. This design change shows up in the performance figures for electrode Models 8.1 and 4.1 which show a marked reduction in voltage and increase in current. The arc appears to have an impedance of around 2.0 milliohms rather than 5.0 milliohms

as was indicated by the earlier measurements. This effect may explain the lower vaporization rates observed with the earlier electrode designs. If a large fraction of the energy is dissipated as I^2R loss more or less uniformly within the graphite, there is less energy available for concentrated heating at the arc attachment point. To obtain a better measurement of the arc impedance, it is planned to attempt the attachment of the voltage leads at a point very close to the tips of the electrodes as in the case of the conical electrodes of pages 64 and 66. Results would provide a better measurement of the true arc impedance and perhaps give a better indication of how much variation in the arc impedance can occur with changes in thruster design (and especially with changes in specific impulse). If the correct value of arc impedance is known, electrodes with an acceptable resistive loss can be designed.

5.0 THE THRUST MEASURING SYSTEM

5.1 Thrust Measure on High Current Pulses

As pointed out in Reference 1, page 27, a number of difficulties are associated with the measurement of thrust when very high currents (in our case from 20 to over 50 kiloamps) are supplied to the thruster during a short pulse. The principal difficulty is the connection to the pulse generating network which must have a low electrical resistance and therefore requires bus bars of large cross section area. This massive connection introduces stiffness which prevents free movement of the thruster, and also intense electrodynamic effects between adjacent conductors which can alter the thrust readings. Furthermore, if sensors are used in the immediate proximity of the thruster, it is difficult to shield the transducer circuit adequately from the strong signals generated by the pulsed arc discharge.

For this reason a decision was made at the beginning of the program to assemble the thruster and its complete power supply in a compact, rigid package, to be suspended inside the vacuum tank with the aid of a long steel ribbon. The unit is designed so that the thruster exerts force in a tangential direction which imparts an angular movement to the suspended platform, which can be calibrated in terms of total impulse. The action is that of a torsional ballistic pendulum. Theoretical analysis of its behavior can be found on page 28 of Reference 1, and in Section 5.4 below.

Early studies with the prototype ballistic pendulum when operated outside of the vacuum chamber presented no serious difficulties. This promising experience may have led us to underestimate the difficulties involved in making a similar instrument operational inside of the vacuum chamber. The obstacles that have now been encountered have resulted in a considerable delay in the test schedule. The principal difficulties are discussed below.

First of all, the torsional pendulum must operate in an environment with pressures as low as 10^{-7} torr. The operation must be controlled from outside so that variations can be made in such parameters as pulse power and repetition rate. Furthermore, the thruster electrodes must be removed frequently for weighing and for exchanging them with modified designs. It is well known that with a large vacuum tank (especially a vacuum tank made of insulating material) a period of days may be required for outgassing each time the chamber is opened if operation at extremely low pressures is required. This is seen to be completely unacceptable when we consider that the chamber would perhaps have to be opened thousands of times before completion of the program. This obstacle to the rapid performance of the tests has been of concern for some time. The solution that has been adopted is the relatively simple and practical setup illustrated on page 38 of Reference 1.

With the aid of a special cylindrical tool having a diameter slightly greater than that of the plasma head, it is possible to penetrate the 10^{-7} torr vacuum, disconnect the plasma head and carry it outside the tank, without altering the vacuum level. The system

performed satisfactorily during the early part of the program when the need to change the thruster did not occur as frequently as has been the case more recently. The increased frequency of change and the need to provide access for newly developed heads of different dimensions, led us to redesign and improve the primitive system. Also, modifications were made to permit a more rapid change. The delay required by these improvements will be more than compensated for by more rapid performance of future tests.

The advantages of the system for withdrawing the plasma head from the vacuum tank without losing the vacuum level have been conclusively demonstrated. However, the biggest gains from the use of the system are expected to be realized when the program begins to concentrate on the rapid testing of a large number of thruster configurations. In the early part of the program much of the effort was expended on the development of a satisfactory pulse generating network, triggering system, instrumentation and calibration systems. Work on any of this equipment which is housed in the vacuum chamber requires opening of the chamber for modifications to be made. This has caused progress to be slow for this part of the development. Delays are particularly serious in the case of equipment housed in the canister. To gain access to this equipment it is necessary to open the vacuum tank and withdraw the complete canister which successively must be opened, modified, resealed, re-entered in the vacuum tank, resuspended on the torsion member, and retested. The vacuum chamber must then be closed and evacuated. This activity represents a loss of many days and of an exceedingly high number of man hours. An operation of this type is particularly difficult in our case because of the small diameter (20 inches) of the only manport available to enter the tank. The improvement of this access is badly needed (especially if the 20-kilojoule bank is to be suspended in the vacuum tank). However, an ideal solution which is being seriously considered would be to design a method for withdrawing the canister which would be similar to the one already developed for extracting the plasma head. The diameter and length would, of course, have to be considerably larger to handle the entire canister without opening the vacuum tank; but the exposed surface area that would require outgassing after each use would still be small compared to that involved when the full chamber is pumped down. This solution appears to be practical and its cost appears to be relatively modest. With this arrangement, either system could be used, depending on the circumstances, to obtain the best utilization of the labor and time for conducting the necessary tests.

As reported in the preceding section, equipment has been put in service for separating certain routine tests from tests that require the measurement of thrust. Such parameters as pulse shape and evaporation rates can be rapidly determined without disturbing the torsional pendulum. These auxiliary measurements are conducted on plasma heads identical to the ones assembled on the torsional ballistic pendulum, but the leads are rigidly mounted on special gliding tubes that can penetrate the vacuum chamber without influencing the vacuum level. The operation of penetration or withdrawal can be accomplished in a

fraction of the time required when the unit is mounted on the pendulum and the system is more reliable and easier to use.

5.2 The Torsional Ballistic Pendulum

The torsional ballistic pendulum consists of a pressurized gas tight canister suspended by a thin strip of metal that acts as a torsional spring (Figure 48). The canister houses the pulse generating network with associated circuitry and prevents excessive evaporation of the electrolyte in the capacitors. Total impulse is related to the angular deflection of the canister following a pulse or series of pulses. The basic arrangement is essentially the same as described in Section 3.7 of Reference 1. Modifications that have been made since then include strengthening of the canister to withstand higher internal pressures, the addition of a number of electrical leads connecting to the canister, and the introduction of a new calibration system that is more suitable for use with the test chamber evacuated.

Leads to the canister are required to provide the following functions: d. c. power for charging the capacitors, main discharge oscillograph triggering signal, triggering discharge oscillograph triggering signal, arc current and voltage measurement, manual triggering of the discharge, and thermocouple connections for internal temperature measurement. These leads leave the canister through sealed bulkhead fittings and attach at equal spaces about the circumference of a ring located at the bottom of the canister on the pivot axis (Figure 49). Each lead hangs in a long loop and reattaches to a second larger ring that is concentric with the first but supported from the bottom of the vacuum chamber. Figure 50 shows the front plate of the canister with three massive terminals for the high current pulse output and for triggering (center). The small terminals at the left are to energize the triggering electrode magnet. Any kind of plasma head can be connected to the main three terminals when the vacuum tank is opened. Also, provision has been made for an alternate receptacle that can be connected to the same three terminals. This receptacle is for use with the penetrating tool which permits the installation and removal of plasma heads without loss of vacuum. Plasma heads with mating fittings must be used in this case. Figure 51 shows the back plate of the canister with most of the operating terminals. Figure 52 shows how the pendulum can be twisted without interference with the ring connections. Figure 53 is the blocking and freeing mechanism acting as the back part of the canister. Figure 54 is a schematic of the electrical circuit of the ballistic pendulum setup. L is the distributed and mutual inductance connecting the storage capacitors C (about 60,000 microfarads). Two separate wires (C and N) carry the charging current which varies with the rate of charge from a fraction of an amp to over 10 amps. The capacitor C_1 (1000 microfarads) supplies the triggering discharge and is charged through a separate connection (K). Two toroidal coils (L_1 and L_2) supply separate triggering signals, slightly separated in time, to the oscillograph - one (L - M) from the main discharge which is useful when two terminal heads are used, and one from the triggering discharge (F - G) which occurs slightly sooner. A coaxial shunt (S) supplies a voltage proportional to the current (1 volt

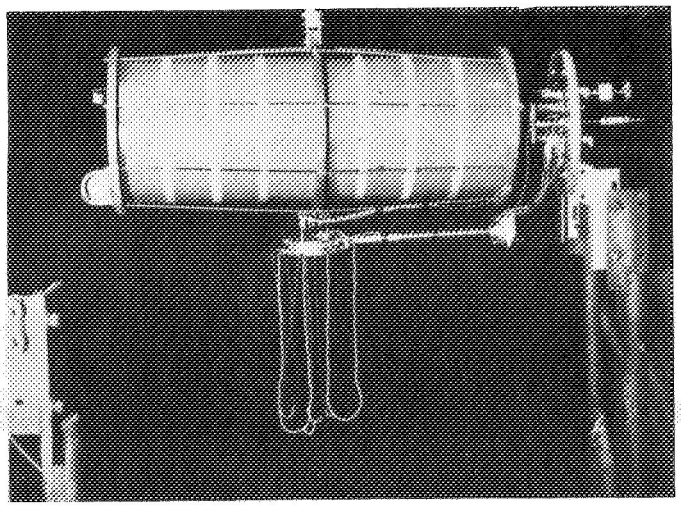

Figure 48. Demonstration of Free Deflection Using Figure 50 Connection System

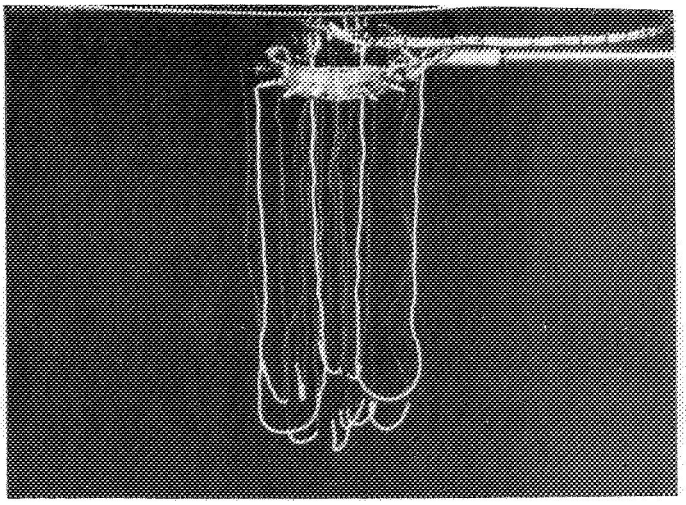

Figure 49. Double Ring to Permit Low Friction Connections

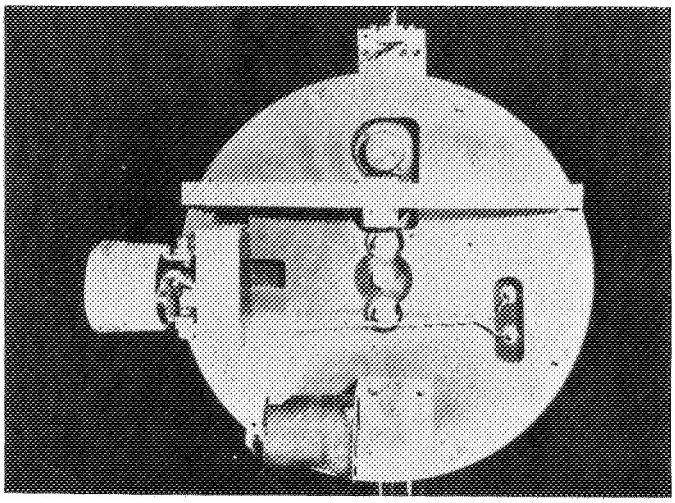

Figure 50. Front Panel to Receive Different Plasma Heads

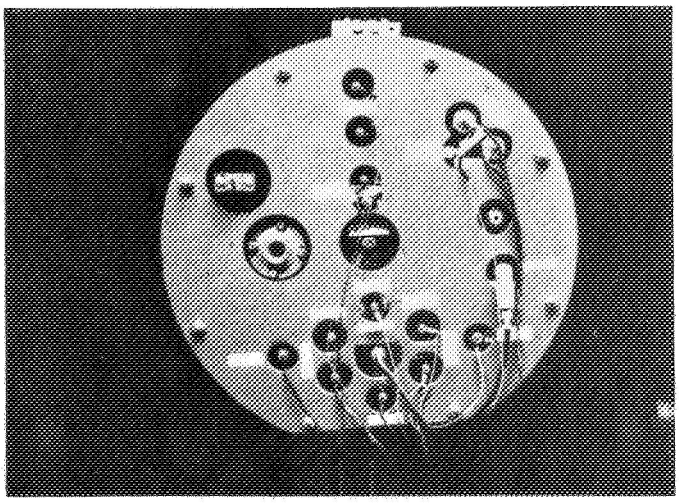

Figure 51. Back Plate With All the Connections

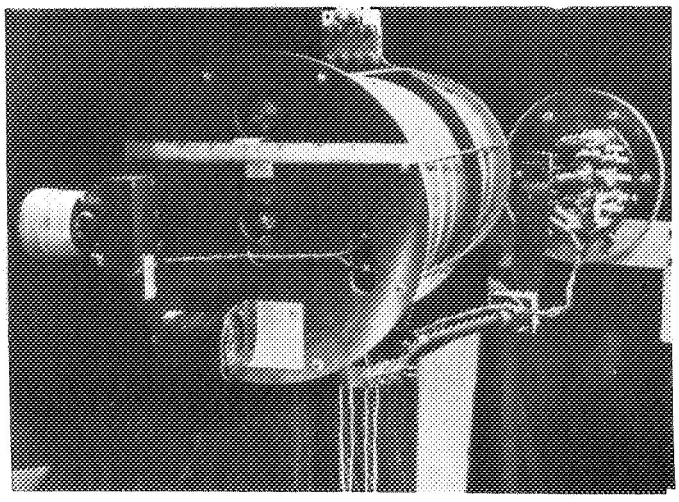

Figure 52. Suspended Ballistic Pendulum With Its Accessories

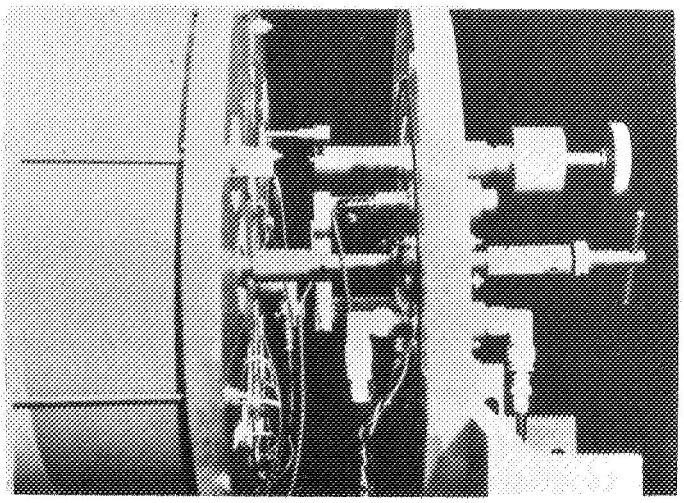

Figure 53. Mechanism for Blocking and Freeing the Pendulum

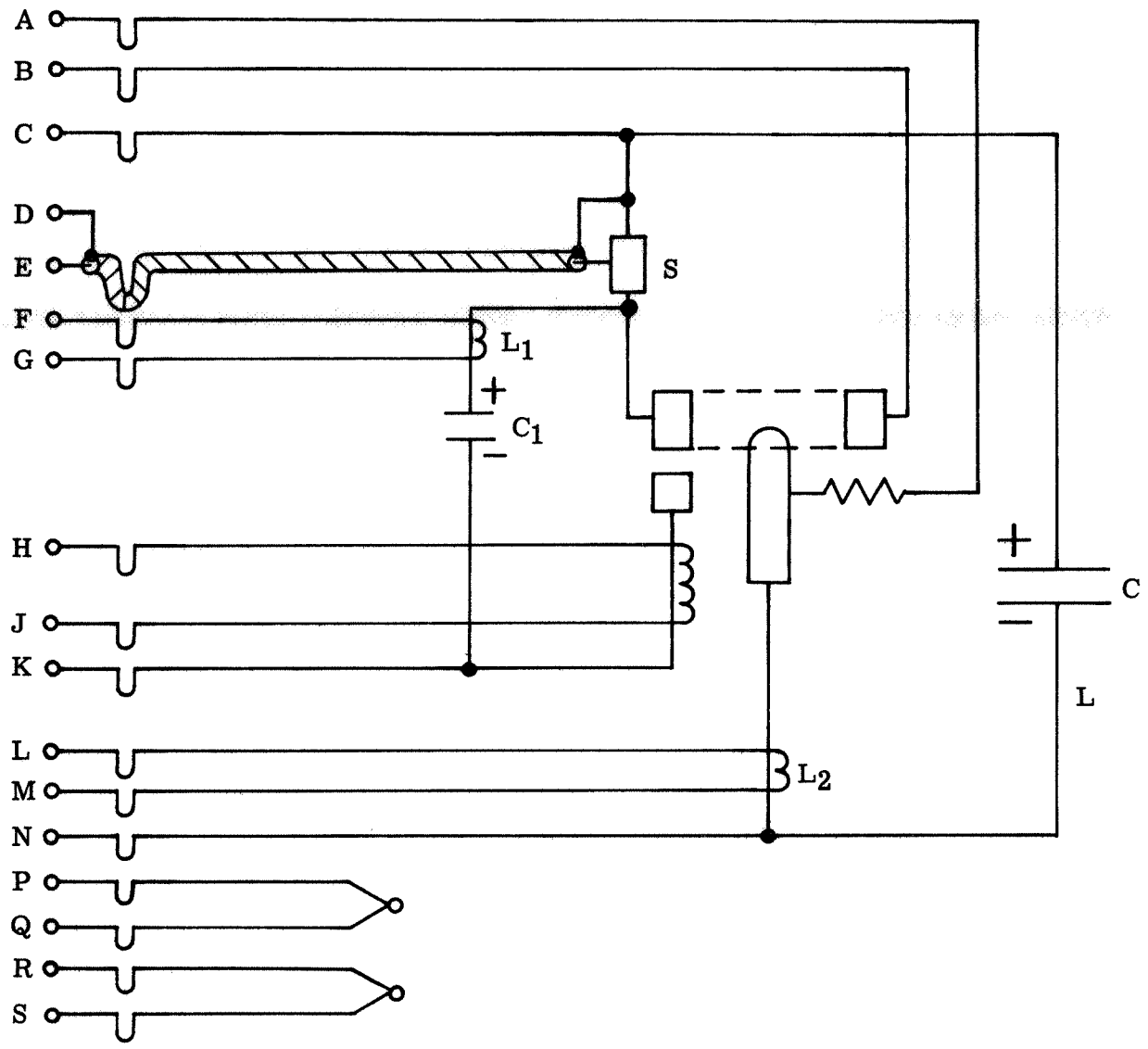

A B	Voltage from electrode tips
C	+ charging current
D E	Current read out from coaxial shunt
F G	Triggering signal for oscillograph
H J	Coil for triggering electrode
K	Triggering electrode
L M	Triggering signal for oscillograph
N	- charging current
P Q	Internal temperature thermocouple
R S	Internal temperature thermocouple

Figure 54. Schematic of Connections to Ballistic Pendulum

per 5000 amps) (D - E) and two separate connections (A - B) are used to measure the voltage as near as possible to the discharging electrodes. Leads H and J are connections to the pulsed triggering solenoid located in the plasma head. Terminals P - Q and R - S are connected to thermocouples located inside the canister to monitor the internal temperature. The connections between the fixed and movable ring are indicated with ⌐⌐ lines.

The loops do not touch each other and are made of the finest gage consistent with the current carried. Notice that the two coaxial pairs are for measurement purposes which permits exceptionally small coaxial wire to be used. As a result, good flexibility and good repeatability is maintained for rotation of the pendulum about its axis. The heaviest leads used are for charging the capacitors. To recharge a 54,000-microfarad capacitor bank to 400 volts at 2-second intervals requires an average current of 10.8 amps. This current is supplied through a pair of No. 24 AWG stranded copper leads. The leads are insulated with ceramic beads to permit high temperature operation and they reach a dull red temperature during continuous operation in a vacuum. Initial tests with the ballistic pendulum have been limited to sequences of a few pulses which keeps the wire temperature at a more moderate level. (Longer series are run on the separate thruster mounts without thrust measurement.) The flexible lead arrangement is shown in Figure 49. The deflection of the torsional ballistic pendulum is measured in degrees of arc on a scale fixed to the canister. A total of 20 degrees at each side of a zero line is visible and the distance between each degree is 10 millimeters. The reading is determined by the projected image of a straight filament on the scale which is movable to permit easy adjustment of the zero line.

The internal pressure of the canister is one atmosphere absolute and is measured by a precision altimeter type barometer which is used to indicate possible leaks at stabilized temperature or excessive heating of the internal circuitry.

To check the calibration of the torsional pendulum from time to time without releasing the vacuum in the chamber, a modified calibration method has been introduced. It consists of a pulley and weight with arrangements for lowering and lifting the weight with a remotely controlled device so that a thread with the known weight attached can be made to pull on the thrust platform for a timed interval. The calibration starts with the pendulum latch engaged and the weight supported on the platform. After the latch is released, the platform is lowered to a stop and the weight begins to pull on the pendulum. As the pendulum rotates, the weight is lowered and the simulated pulse ends when the weight is resting on the platform again. Measurements are made of the time period during which the known weight is applied and the maximum angular deflection of the pendulum. This approach is intended to provide a quick and accurate calibration while the chamber is evacuated. The tendency is to use a very small weight so that the interval during which it is applied can be long enough to time accurately. For this reason a pulley with extremely low bearing friction is required. This problem will be discussed further in Section 5.4.

A change has been introduced in the manner in which the ballistic pendulum is used. It was originally considered desirable to introduce all of the pulses of the series during one swing of the pendulum to minimize the effect of damping action. However, when the pendulum was installed in the vacuum chamber, the torsional damping at low amplitudes was found to be extremely small - even with the instrumentation leads connected. It has been found advantageous therefore to apply one pulse for each swing of the pendulum. With this procedure, which we will call "resonant pulsing," each pulse can be applied precisely when the pendulum swings through the zero point, and no correction is required for delayed application of impulse. Furthermore, it is not necessary to stop the pendulum before starting a new test series. A maximum amplitude reading (plus and minus) is taken before the series is started and again after enough pulses have been applied that the amplitude difference (which may be either positive or negative) can be read with satisfactory accuracy. The technique is somewhat analogous to that used with an analytical balance or an ultra sensitive mirror galvanometer. The procedure eliminates uncertainties as to whether the pendulum was brought precisely to rest before initiating a new series. The instrument sensitivity and the calibration method are not affected by this change in procedure and the measurement precision is increased.

The suspension of the ballistic pendulum in the vacuum tank is designed to permit easy observation of the plume for photography and spectroscopy. Pictures from the sides at right angles to the jet, from the top, from the front and from the back can be taken. To do this special windows with transparent material that can be cleaned without losing the tank vacuum are used. One window is used exclusively for a single shot movie camera which is operated automatically by the triggering signal so that it photographs the plume during each pulse. The standard sequence of about 100 shots produces 100 frames which can be projected one by one or continuously in a movie-like succession. In the latter case, slight differences between pulses can be easily detected.

5.3 New Design for 20 Kilojoules

In the early planning for this program, a ten-fold increase in the size of the old pulse generating network (2000 joules) was contemplated. This would increase the stored energy from the original value to 20 kilojoules. However, because of physical limitations, it has since been decided to limit the maximum energy available in the torsional pendulum to about 5 kilojoules. Capacitors are available for a larger pulse network, and consideration is being given to future tests of plasma heads with a 15 to 20 kilojoule power package operated either with or without the measurement of thrust. Some of the problems and possibilities are described below.

As was discussed in Section 3.2, one of the major problems which arises when the energy of the pulse is increased is that a reduction in the internal resistance of the connecting power leads is required. An effective way of accomplishing this would be to reduce the

distance of the connection between one capacitor and the next, but this would require the construction of completely different capacitors and for this reason cannot be adopted. With existing capacitors, the distance between connections is already close to a minimum with existing designs. The increased energy can be used in different ways (increased voltage, current and/or pulse duration) depending on how the capacitors are connected and what changes are made in the thruster design. Generally, the cross section of the conductors must be increased to prevent a reduction in circuit efficiency, and this results in an increased specific weight for the power package. With reasonable design compromises it is believed that the resistive losses (including losses in the capacitors) can be limited to around 50 percent of the nominal power so that up to 10 kilojoules can be made available in the arc discharge.

Considering a nominal capacity of 1000 microfarads each, the energy available at 400 volts is about 80 joules per capacitor so 250 capacitors are needed to reach 20 kilojoules. The area occupied by a single row of capacitors occupying 9 inches^2 each is 250 x 9 = 2250 inch^2 or 14,500 cm^2. If the bank is divided into two sections of 125 capacitors each and the terminals are placed one against the other, it is possible to make two rows with the best use of the mutual inductance. The rated charge of the electrolytic capacitors which we have been using is 450 volts. However, the capacitor bank is housed in the torsional pendulum canister where accessibility for repair is a problem; so, until now, the operating voltage has been limited to about 400 volts to assure maximum reliability. Since no capacitor failures have been experienced throughout a rather lengthy test program, it is now considered feasible to utilize the full rating of 450 volts. This would increase the energy stored about 20 percent, or to about 100 joules per capacitor. In this case the number of capacitors required to reach 20 kilojoules is reduced to 200.

Considering that the best orientation for the electrolytic capacitors is vertical and that the existing access opening to the test chamber is only 20 inches in diameter, the arrangement of the capacitor bank from an end view must be very nearly the same as that presently in use. To increase the stored energy by a large factor it is necessary to either cluster a group of canisters of the present size or increase the diameter of the access opening. The latter is clearly a more desirable solution since a single large canister could be completely assembled and checked out before installation. As an example of the canister size required, one of the best configurations considered in a preliminary study uses 222 capacitors arranged in 6 layers of 37 capacitors each. It is estimated that a capacitor bank of this size would fit into a cylindrical canister 22 inches in diameter and 50 inches in height. Improved arrangements of conductors connecting the capacitors would be used to reduce resistive losses while increasing the inductance obtainable per length of conductor by making use of mutual inductance effects. The canister would be suspended from a torsion member in a manner similar to the one presently used with the 5000-joule unit. The operating voltages would be 112, 225, 330 and 450 volts to store about 1250, 5000, 10,000 and 20,000

joules respectively. It is anticipated that the pendulum period can be maintained at about the same value presently used and the plasma head designs will be nearly unchanged. An order of magnitude increase in the rate of evaporation is expected, however.

5.4 Analysis of Torsional Pendulum Response

The dynamic behavior of this type of torsional pendulum has been analyzed in some detail in Reference 1, and in the Appendix of Reference 13. For our purposes here, we insert the following summary:

Define

θ = angular displacement from null position

F_θ = applied torque

k = torsional spring constant = F_θ/θ_e

θ_e = equilibrium displacement under static torque = F_θ/k

K = moment of inertia

T = natural period = $2\pi\sqrt{K/k}$

α = mean angular velocity = $\frac{2\pi}{T} = \sqrt{k/K}$

I_θ = $F_\theta t_p$ = applied impulse

The general equation of motion

$$K\ddot{\theta} = F_\theta - k\theta \tag{1}$$

has solutions for the displacement,

$$\theta = \hat{\theta}\sin(\alpha t + \Phi) + \theta_e \tag{2}$$

and for the angular velocity,

$$\dot{\theta} = \alpha\hat{\theta}\cos(\alpha t + \Phi) \tag{3}$$

where the phase, Φ, and amplitude, $\hat{\theta}$, are given by

$$\tan\Phi = \frac{\alpha(\theta_t - \theta_e)\cos\alpha t_o - \dot{\theta}_t \sin\alpha t_o}{\alpha(\theta_t - \theta_e)\sin\alpha t_o - \dot{\theta}_t\cos\alpha t_o} = -\frac{\alpha(\theta_o - \theta_e)}{\dot{\theta}_o} \tag{4}$$

$$\hat{\theta} = \left[(\theta_t - \theta_e)^2 + \left(\frac{\dot{\theta}_t}{\alpha} \right)^2 \right]^{1/2} \tag{5}$$

where θ_t and $\dot{\theta}_t$ are the position and angular velocity at any time, t_o, and θ_o and $\dot{\theta}_o$ are their values at $t = 0$.

Certain special cases are applicable to the techniques of measurement and calibration actually employed:

a) Free-swinging pendulum ($\theta_e = 0$)

$$\theta = \hat{\theta}_o \sin (\alpha t + \Phi) \tag{6}$$

$$\dot{\theta} = \alpha \hat{\theta}_o \cos (\alpha t + \Phi) \tag{7}$$

$$\tan \Phi = \frac{\alpha \theta_t \cos \alpha t_o - \dot{\theta}_t \sin \alpha t_o}{\alpha \theta_t \sin \alpha t_o + \dot{\theta}_t \cos \alpha t_o} = \frac{\alpha \theta_o}{\dot{\theta}_o} \tag{8}$$

$$\hat{\theta} = \left[\theta_t^2 + \left(\frac{\dot{\theta}_t}{\alpha} \right)^2 \right]^{1/2} \tag{9}$$

b) Constant torque applied to pendulum initially at rest ($\theta_o = \dot{\theta}_o = 0$)

$$\theta = \theta_e (1 - \cos \alpha t) \tag{10}$$

$$\dot{\theta} = \alpha \theta_e \sin \alpha t \tag{11}$$

which are simply sinusoidal oscillations of amplitude θ_e about a displaced equilibrium position, $\theta = \theta_e$.

c) Impulsive torque, $I_\theta = F_\theta t_p$, $t_p << T$

From momentum arguments, the impulse changes the angular velocity of the pendulum abruptly from $\dot{\theta}_o$ to $\dot{\theta}_o + \Delta \dot{\theta}$, where

$$K \Delta \dot{\theta} = I_\theta \tag{12}$$

If the pendulum is initially at rest at $\theta = 0$, the subsequent motion is simply

$$\theta = \hat{\theta}_1 \sin \alpha t \tag{13}$$

$$\dot{\theta} = \alpha \hat{\theta}_1 \cos \alpha t \tag{14}$$

$$\hat{\theta}_1 = \frac{\Delta \dot{\theta}}{\alpha} = \frac{I_\theta}{\alpha K} = \frac{I_\theta}{\sqrt{kK}} = \frac{\alpha I_\theta}{k} \tag{15}$$

If the impulse is applied as the pendulum passes through $\theta = 0$ with velocity $\dot{\theta}_o$, the amplitude is increased to

$$\hat{\theta} = \frac{\dot{\theta}_o + I_\theta/K}{\alpha} = \frac{\dot{\theta}_o}{\alpha} + \frac{\alpha I_\theta}{k} \tag{16}$$

which differs from (15) by exactly the free swinging amplitude (9):

$$\hat{\theta} - \hat{\theta}_o = \frac{\dot{\theta}_o}{\alpha} \tag{17}$$

In other words, the incremental change in amplitude resulting from the impulse is independent of $\dot{\theta}_o$:

$$\Delta \hat{\theta} = \frac{\alpha I_\theta}{k} \tag{18}$$

Thus, a succession of equal impulse increments, each applied to the pendulum as it swings through $\theta = 0$, (hereafter termed "resonant pulsing"), will drive it to a cumulative amplitude which depends linearly on the number of pulses. This is a useful property for the precise determination of very small impulse bits, as discussed in the following section. It also follows that application of the impulses as the pendulum passes through $\theta = 0$ in the negative direction, i. e. on its back swing, will reduce the amplitude in the same linear proportion.

d. Protracted impulse: $F_\theta = \text{const}, \quad 0 < t < t_p; \quad F_\theta = 0, \quad t > t_p$

If the impulse is applied with the pendulum at rest at $\theta = 0$, relations (10), (11) apply, which when evaluated at $t = t_p$ provide the initial conditions for the free-swinging phase:

$$\theta_p = \theta_e (1 - \cos \alpha t_p) \tag{19}$$

$$\dot{\theta}_p = \alpha \theta_e \sin \alpha t_p \tag{20}$$

Using (8), the phase angle of the free swing becomes

$$\tan \Phi = - \frac{1 - \cos \alpha t_p}{\sin \alpha t_p} \tag{21}$$

and the amplitude, from (9), becomes

$$\hat{\theta} = \theta_e \left[2(1 - \cos \alpha t_p)\right]^{1/2} = \theta_e \left(2 \sin \frac{\alpha t_p}{2}\right)$$

$$= \theta_e \alpha t_p \left[1 - \frac{(\alpha t_p)^2}{24} + \frac{(\alpha t_p)^4}{1920} - \ldots\right] \tag{22}$$

Note that $\hat{\theta}$ increases from 0 to $2\theta_e$ as t_p extends from 0 to T/2, for given F_θ. If protracted beyond T/2, the applied torque opposes the pendulum motion, and the subsequent free swing amplitude is reduced. (In the very special case of $t_p = T$, the pendulum would execute just one cycle of the forced motion (10), and be returned to its original starting position with zero velocity, hence would oscillate no further.) Note also that in the limit $t_p \rightarrow 0$, the expression for $\hat{\theta}$ is identical to that derived for the impulsive torque case (15), when I_θ is replaced by $F_\theta t_p$. The ratio of (22) to (15) can be regarded as a correction factor to relate protracted impulses to the ideal cases:

$$\frac{\hat{\theta}}{\hat{\theta}_I} = \frac{\left[2(1 - \cos \alpha t_p)\right]^{1/2}}{\alpha t_p} = \frac{2 \sin \frac{\alpha t_p}{2}}{\alpha t_p} = 1 - \frac{(\alpha t_p)^2}{24} + \frac{(\alpha t_p)^4}{1920} - \ldots \tag{23}$$

The correction exceeds one percent for $\alpha t_p > 0.49$, i.e. for $t_p > 0.078\ T$.

5.5 Calibration and Measurements

The torsional ballistic pendulum can be calibrated while it is installed in the vacuum chamber using the pulley and weight arrangement shown schematically in Figure 55. Since the instrument is very sensitive, it is affected by slight air currents and an accurate calibration is difficult to obtain outside of the chamber. Furthermore, changes in thruster weight, the weight of equipment mounted in the canister, or the arrangement of leads connecting to the canister may change the calibration. It is desirable to be able to obtain a new calibration with the instrument in place and recheck the calibration from time to time before or after the regular measurement of thrust without releasing vacuum in the chamber.

The particular combination of applied weight and duration of its application are determined by trade-offs among the various accuracies of measurement, and the characteristics of the pendulum behavior as developed in the preceding section. Ideally, one would like to keep the duration of application of the calibrating force well below 5 percent of the

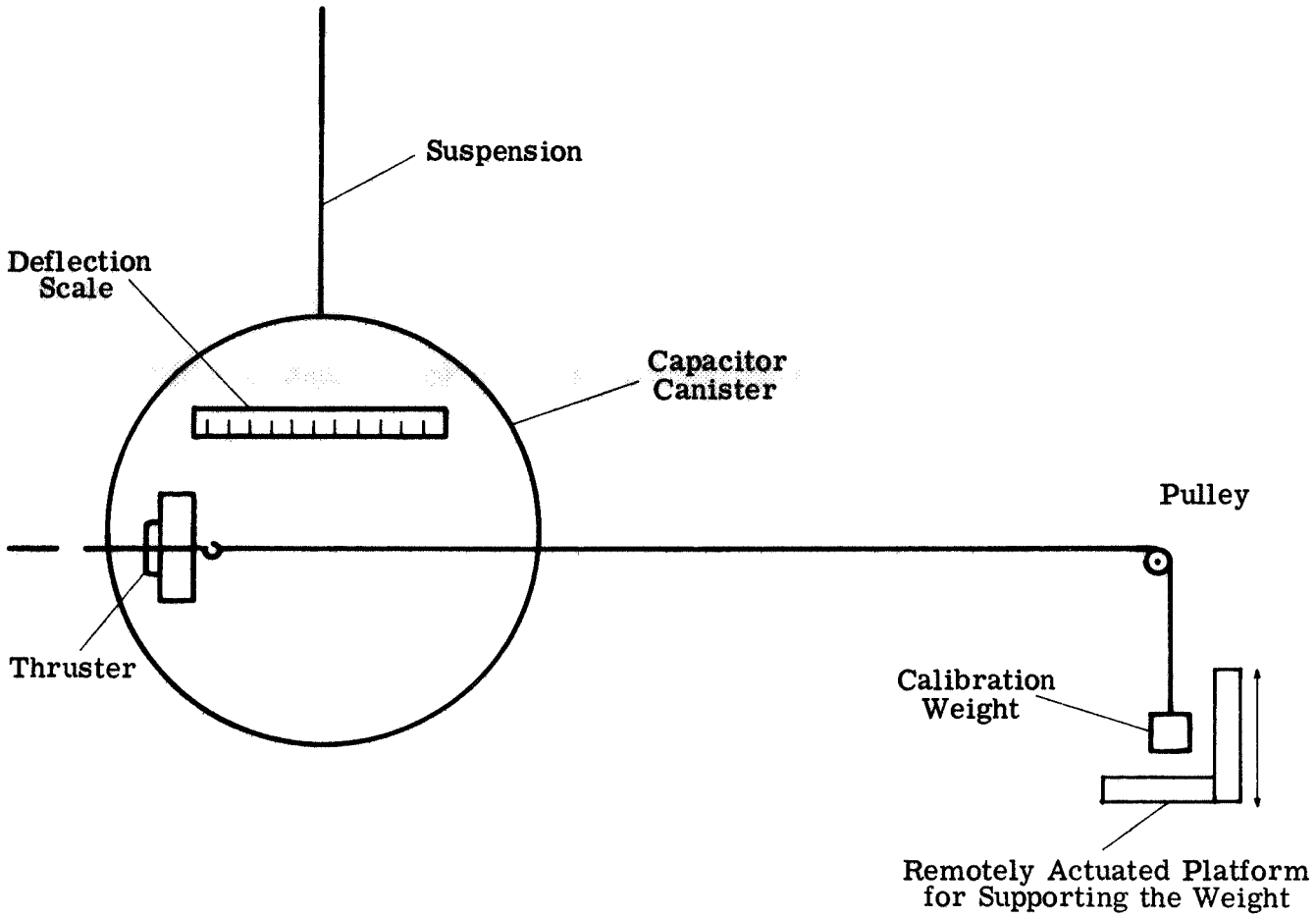

Figure 55. Schematic of Calibration of Torsional Thrust Stand

pendulum period to avoid the need for protracted impulse correction. For the 145-second period of this pendulum, this translates into a duration of only a few seconds, which for this primitive apparatus would entail relatively large errors in timing associated with release and capture of the weight.

As a compromise, we have initially employed a one gram weight applied for 10 seconds, during which the pendulum moves about 60 minutes of arc from its zero position, which is about 20 percent of its ultimate excursion to an amplitude of 285 minutes. In addition to requiring a small protracted impulse correction, this displacement is large enough to involve noticeable damping (Figure 56). In particular, the amplitude decay per cycle is significant in comparison to those produced by the thruster impulses. In addition, note that the damping coefficient of this pendulum is not a constant. Rather, it reduces substantially below one degree, thus providing further incentive to operate with very small deflection.

From the preceding findings it is evident that the ballistic pendulum can be operated with best results if its maximum excursion does not exceed 100 to 120 minutes, or still

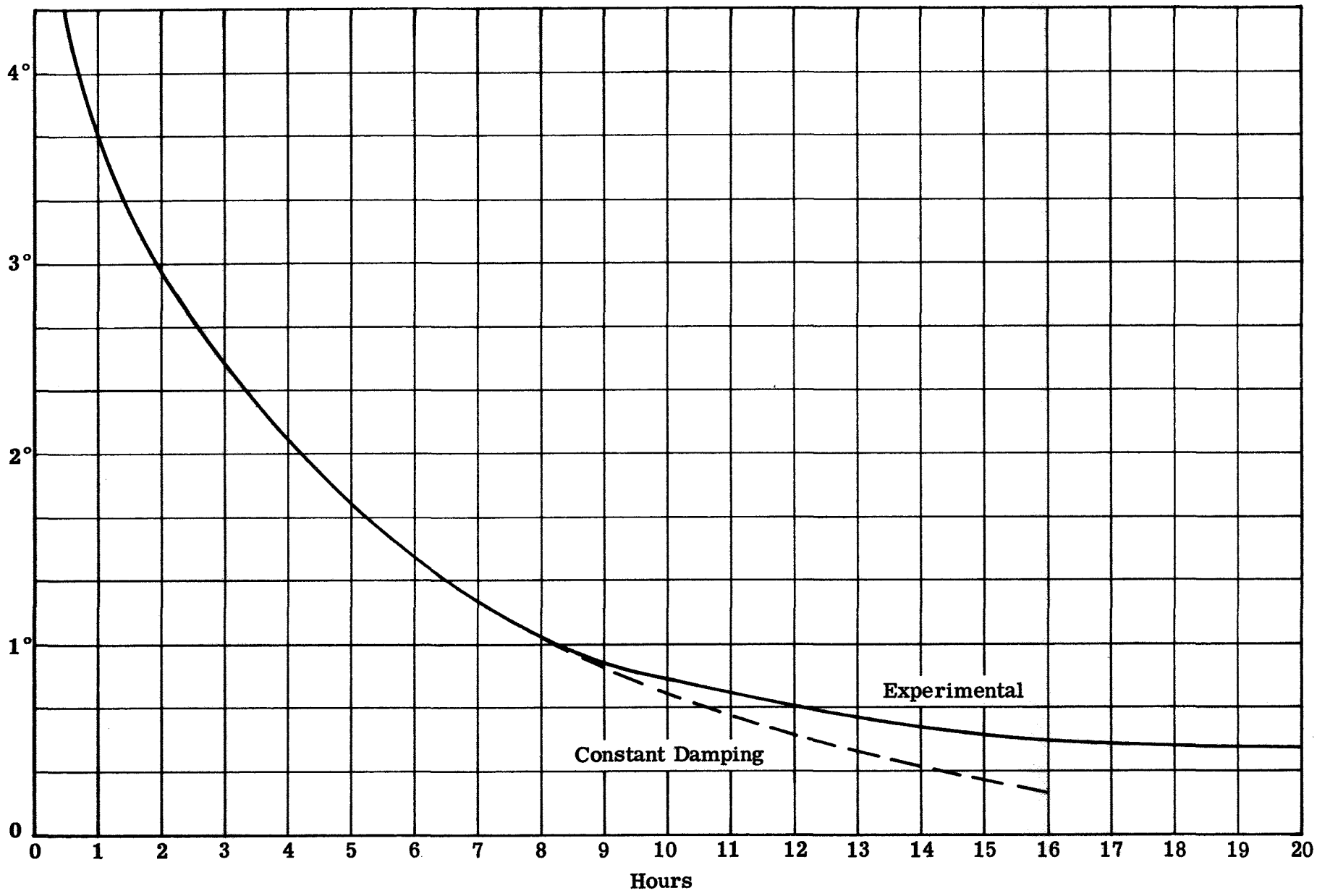

Figure 56. Damping of the Torsional Ballistic Pendulum During 20 Hours Starting at ± 4 Degrees 45 Minutes

better, if it does not exceed 60 minutes or one degree of arc. It is apparently preferable to sum the effect of a small number of pulses to keep the damping error small. The scale for a one degree deflection can easily be split into 100 parts with good reading precision. By keeping the amplitude small during all of the measurements, it is possible to retain the desired reading accuracy, to eliminate the need for a complicated correction factor and to keep the operation in the low damping regime so that resonant pulsing or repetitive application of a calibration weight can be effectively used. The pendulum has proven to be stable enough that a simple optical magnification of the scale reading is expected to give reliable results. Modification of the existing read-out system is already in progress.

It was originally intended that calibration and thrust application be done starting at the "proven" zero reading of the pendulum. It is evident observing Figure 56 that the pendulum oscillations stop by themselves only after a very long time, and auxiliary devices for stopping the pendulum have been found to be troublesome. The best method found to date for stopping the pendulum is the application of precisely controlled negative thrusting forces until complete immobilization is achieved. This can be done relatively easily with a few measured pulses when the thrusting forces are well known. Measurement from an absolutely zero position has merits and can be achieved when adequate time is available for the operation, but in most routine tests the resonance pulsing method (which does not require complete zeroing of the pendulum) has been found to be preferable.

Figure 57 illustrates how thrusting forces of extremely low values can be easily measured and compared by using a large number of successive pulses. For example, to reach the same impulse obtained with a single pulse at 400 volts, it is necessary to apply about 20 pulses at 100 volts. By applying the same impulses during negative swings, the amplitude of the pendulum can be reduced until a perfect stop is obtained.

For calibration of the instrument, pendulum deflections are taken following application of a one gram weight for 5, 10, and 20 seconds. The measured increase in amplitude of 285 minutes following the application of one gram for 10 seconds is used for this test series. When pulley friction is allowed for, the corresponding sensitivity is 31.7 minutes per gram second. In performing the calibration, the weight is applied in the thrust direction starting when the pendulum is at the zero position and continuing for the selected time interval. A method is needed for applying the weight at precisely the desired point in the swing of the pendulum. When methods have been developed for accurate timing of the weight application, it will probably be desirable to make use of the "resonant pulsing" techniques for calibration as well as for testing of the thrusters.

Many thruster tests have been conducted using the "resonant pulsing" technique. Identical pulses are applied repetitively once per swing exactly when the pendulum crosses its zero line in the positive or negative direction. The pulse adds to or subtracts from the amplitude depending on the direction of swing. It has been found that the amplitude changes in equal repeatable steps which gives a check of the reliability of the method of measurement.

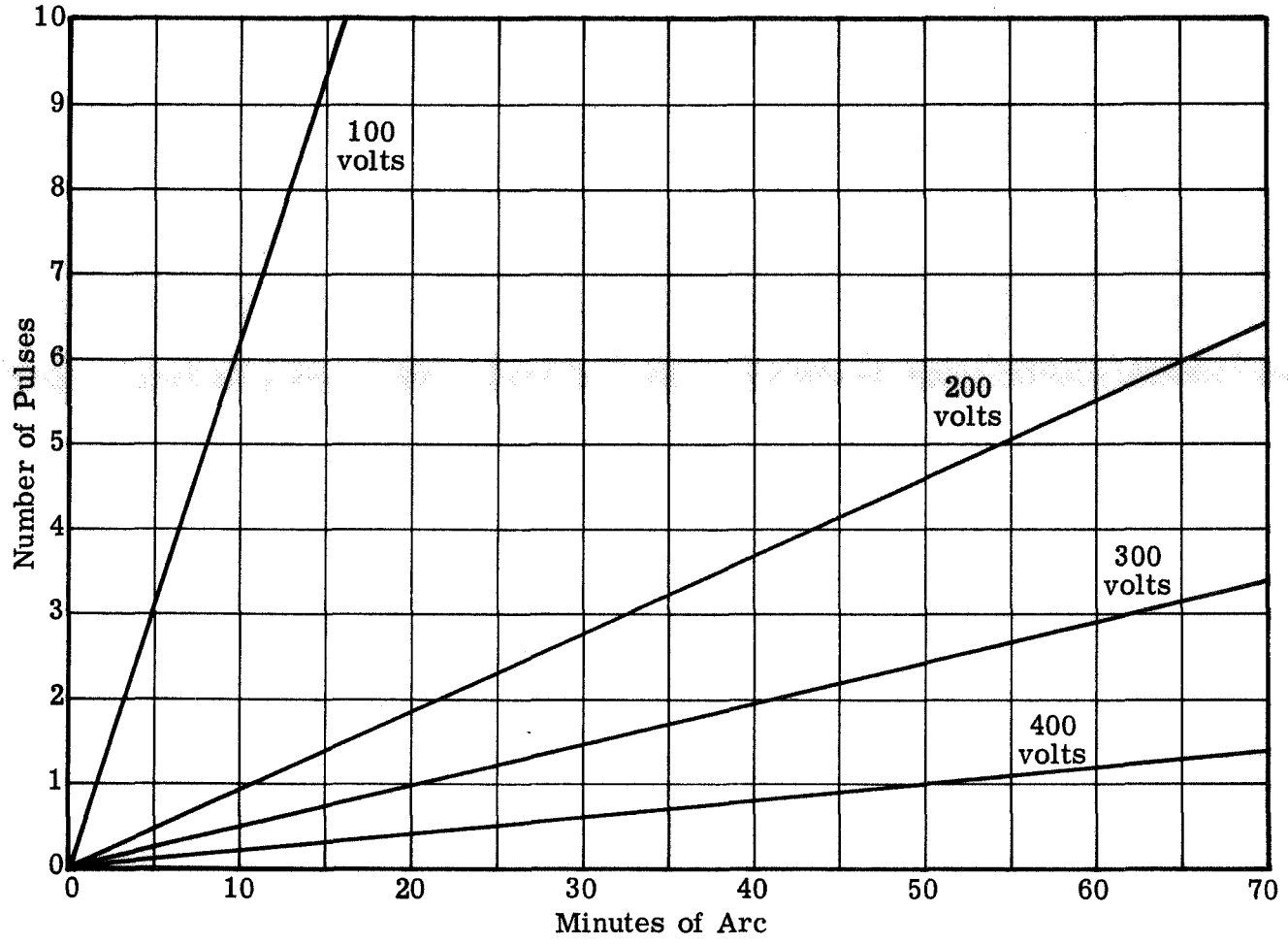

Figure 57. Pendulum Amplitude in Minutes of Arc vs Voltages and Number of Pulses

Some improvements are clearly required in the present calibration system. A major problem has been that the pulley presently in use introduces a friction force which is measured to be about 100 milligrams. This introduces an uncertainty in the measurements of impulse as well as the calibration because after the weight is removed, the amount of slack in the nylon thread between the pulley and the pendulum depends on the history of motion of the pendulum. The effect is illustrated in Figure 55. If the pulley friction were negligible, this problem could be avoided by leaving a small weight hanging from the thread continuously. Since it is considered desirable to be able to perform a calibration with a weight as small as 500 milligrams or even 100 milligrams, a friction force limited to a few milligrams is needed. A pivot of quality similar to that used in an analytical balance would be desirable for the pulley bearing. Although the task is not a simple one, the use of pulley bearing types that have low friction becomes more feasible if the pendulum amplitude is limited to a small value. An increase in the pulley diameter would also be helpful.

An alternate approach would be to use a relatively long thread attached to the pendulum at one end and a fixed point at the other, and having a weight at its mid point. No

pulley would be used, so the problems of pulley friction and pulley unbalance would be eliminated. Experiments with an arrangement of this type show that repeatable results can be obtained with very small weights. The main drawback is that the variation in the horizontal component of force acting on the pendulum must be calculated and allowed for in the calibration.

Yet another possibility, and perhaps the most viable one, involves the inclusion of a sensitive calibrated linear spring at the juncture of the horizontal thread with the rear of the thruster (Figure 58). In this way, all effects from pulley friction would be factored out, and one could read the true applied force directly at the thruster, while the calibration was in progress. An improvement to the timing problem could be accomplished using coils to apply an electromagnetic force to the pendulum. The action could be initiated either manually or by a photocell to provide application at a highly repeatable position, and the pulse duration could be timed electrically. A system of this type used in combination with a carefully regulated d. c. power supply would provide a total impulse for calibration that could be very accurately determined. Since the strength of the pulse could be accurately controlled, the system should also be useful for regulating or stopping oscillations of the pendulum. It is planned to conduct experiments with this type of calibration system during the next contractual period.

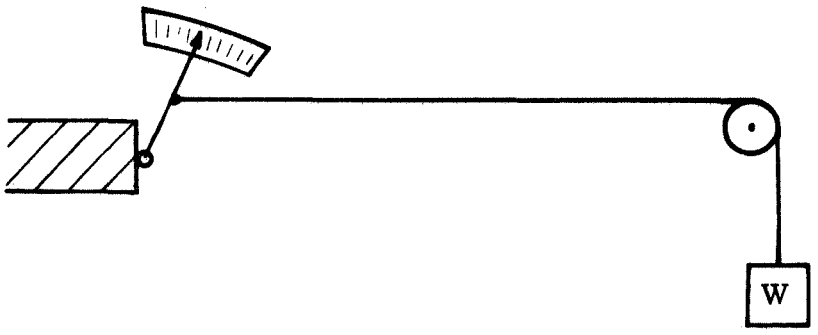

Figure 58. Interior Spring Method for Precise Calibration of Pendulum

5.6 Results Obtained with the Thrust Stand

The test program with the complete instrumentation needed to determine overall performance has been initiated and some preliminary performance data are available. Most of the effort to date has been expended in reaching the point of having an operational propulsion system and thrust stand suitable for determining the performance of electrode vapor fed quasi-steady MPD thrusters. The results that can be presented at this time are still tentative, and are intended primarily to demonstrate the viability of the facility, the propulsion system and testing techniques.

The ballistic pendulum appears to be performing very nicely in the high vacuum. Since the instrument was enclosed in the chamber, the zero reading has shown no tendency to drift and impulse measurements obtained from identical thrust pulses repeat very precisely. It has been found that the most precise results can be obtained with the smallest amplitudes compatible with the need to measure the deflection accurately. Even with 17 flexible leads connecting to the canister, the damping effect is extremely small if the amplitude is kept small. Because of damping effects, it appears that deflections over ± 2 degrees of arc should be avoided, and the instrument should be designed to permit good readout accuracy with these small deflections. (As work continues, it is planned to reduce the reading error from its present value of 5 minutes of arc to less than one minute of arc simply by viewing a finely divided reticule with high magnification. The sensitivity of the pendulum is about 32 minutes per gram second, so with the improved readout it should be possible to measure impulses of around 25 to 30 milligram seconds (less than one-tenth of a millipound second). The "resonant pulsing" method of measurement would permit the detection of pulses of the order of 10 micropound seconds or less using a series of 50 to 100 pulses fired successively.)

Even though the instrument has demonstrated good sensitivity and repeatability, all of the desired performance checks have not yet been made and the measurements of impulse now being obtained must be considered preliminary. A great deal of care has been taken to minimize electromagnetic interactions during a pulse discharge. The induction coils are arranged about a vertical centerline and the test chamber is made of insulating material. Even so, the discharge current is high enough that tests should be made to assure that the remaining interactions can be neglected. It is planned to do this by operating a plasma head with a "thrust killer" type of baffle at the exit. An appreciable response of the instrument would require further modifications to minimize electromagnetic effects. A second performance check that is needed is concerned with the effect of eddy currents of gas in the chamber on the pendulum. These are believed to be small because of the low ambient pressure and the tendency for the carbon gas to condense rapidly on the chamber walls. However, the canister has a large exposed surface area that could be influenced by small eddy effects. A check should be made by operating a thruster which is located in the approximate position that it would be in if mounted on the pendulum. However, it would be attached to a separate mounting rather than to the pendulum. It would be preferable to make this check with the metal parts that are normally installed in the canister removed to avoid a false response due to electromagnetic interactions. An appreciable response of the pendulum would indicate the presence of aerodynamic interaction effects and require the installation of baffles to shield the canister. When these checks have been completed and the accuracy of the calibration system and the readout system has been improved, the measurements obtained with the torsional pendulum can be considered precise. It is believed that this type of instrument can give very satisfactory results and that it can be adopted for use with other types of thrusters with a wide range of pulse durations including "continuously

operating" thrusters with limited and known operating times, and even fully steady thrusters of modest thrust.

In planning the tests for determining the rate of electrode consumption, it was decided to operate the thruster for enough pulses to provide a total mass ablation of about 50 milligrams at the full power operating condition. The parts are weighed on a Mettler H15 balance which has an accuracy for differential readings of ± 0.05 milligrams, so the balance error is a fraction of one percent when the mass difference for two or three parts is determined. A typical front electrode has a weight of about 10 grams and would have an atmospheric buoyancy of about 7 milligrams. It was concluded that the small changes in buoyancy due to atmospheric variations could be neglected. However, the change in moisture content with humidity is another matter. The hygroscopic properties of graphite vary with the grade, but in some cases the increase of mass due to moisture may be quite rapid and amount to a large fraction of one percent on a humid day. This could introduce errors of the order of 50 milligrams in extreme cases. The original intent was to weigh the parts quickly after high temperature operation in the vacuum chamber. However, experience indicated that a variable amount of moisture was being picked up in the time required to disassemble the equipment and weigh all of the parts involved. In any event, the early measurements did not repeat well. More recently a technique has been developed for baking the electrodes to dry them thoroughly before weighing. The parts are weighed while still warm to avoid letting them pick up moisture again. The electrodes are suspended from a fine wire to avoid heating the balance parts, but this still represents a compromise because the warm parts can set up thermal currents in the balance enclosure. A small error of this type is acceptable if a procedure can be developed that consistently introduces the same error each time the part is weighed, since we are interested in an accurate measure of weight difference. A desiccator in which the parts could be placed while cooling would probably be very helpful. At present, each measurement is performed many times and results are accepted only if good agreement is obtained. With care, it seems to be possible to obtain measurements that repeat within ± 1 milligram. However, we have not yet had enough experience with the method to know how accurate the weight differences already taken are, so for the time being the results must be considered preliminary. It may be found necessary in the future to move the balance and the oven into a room with a controlled low humidity or to greatly increase the number of pulses made before reweighing. An effort will be made to avoid the latter solution as it would greatly reduce the number of geometries that can be tested during the program and also introduce questions regarding the effect of increased electrode consumption on performance.

Another effect that became evident in the early tests is that the rate of electrode consumption is strongly dependent on electrode geometry, the grade of graphite used and the polarity of the electrodes (as well as on the energy expended per pulse). The effect is evident in Table III (p. 70) which shows as much as six to one variation in propellant consumed

per pulse (if change of polarity is included) although all of the tests were made with the same capacitor bank and the same initial charge level. In general, it is encouraging to find that the designer does have this much control over the electrode consumption rate because this probably allows him to choose the specific impulse at which the thruster will operate within fairly broad limits. It does, however, become necessary to take a certain amount of care in conducting a test to replace electrodes before erosion changes the geometry appreciably and to construct replacement parts accurately so that the geometry remains the same. A great number of tests are needed to choose the most efficient combination of electrodes and to begin to understand the evaporating process.

The effect of polarity on the performance of MPD arc jets with coaxial electrodes has been the topic of much discussion, but little quantitative information is available. The situation is further complicated when the electrodes have the additional function of supplying the working fluid. It was found during the tests that the total evaporation is more than doubled if the center electrode is used as the anode rather than the cathode. Tests are not complete on this configuration and we do not know yet what impulse changes accompany this change in propellant mass. The completion of this test series is one of the first tests planned when the program is resumed. If good performance can be obtained with reverse polarity, this might be a very attractive configuration for a thruster using consumable electrodes. It is logical to expect that most of the evaporation would occur on the center electrode which would be the anode and therefore have the greatest fall region heat loss, while at the same time the arc attachment point would be more concentrated. If most of the evaporation could be made to occur from the center electrode, this would simplify the electrode feeding problem since a center rod can be readily advanced to make up for erosion. The results in Table III confirm that the center (or back) electrode has a relatively slow evaporation rate while it is used as the cathode, and that the rate increases markedly when the polarity is switched. A surprising result is that the consumption of the front electrode (which becomes the cathode) increases also - although a smaller amount. This effect is not understood at present and will require further investigation.

During some of the tests when a series of pulses were made, oscilloscope recordings were taken of the signal given by one of the ionization gages that measure test chamber pressure (see Figure 59). Note that the signature of the pressure gage, although somewhat distorted in comparison to the current waveform, has an almost identical length to its positive response phase, suggesting that it is indeed responding to the injection of mass into the vacuum tank. It is possible, therefore, that this device can be adapted to yield systematic information about the mass consumption of the thruster on a shot-to-shot basis, and possibly on the process of carbon condensation on the vacuum chamber walls. A knowledge of this condensation is of particular interest since it strongly affects the degree to which space conditions are simulated. It seems likely that a more careful measurement of the pressure pulse signal (perhaps at several positions in the test chamber) and a better

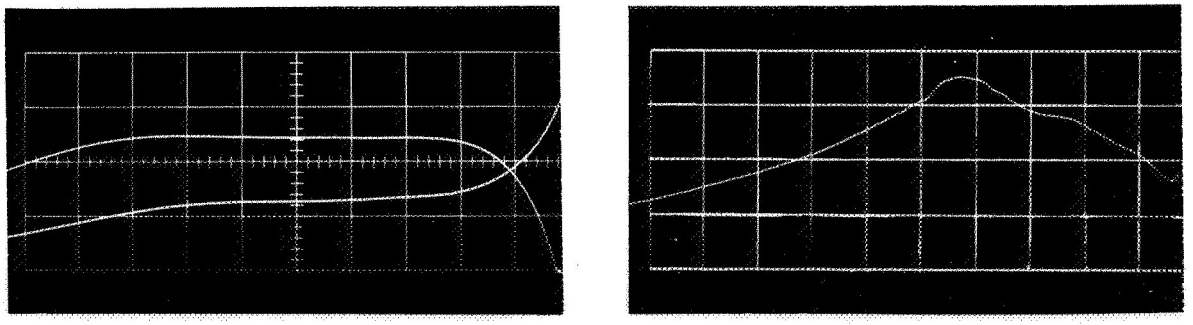

100 μsec/cm Current and Voltage Variation

100 μsec/cm Pressure Variation

Figure 59. Arc Current, Voltage, and Vacuum Tank Pressure During One Pulse

understanding of the significance of the signal could provide additional information on the time history of propellant evaporation and on the structure of the plume during a pulse.

No evidence of arc instability was noticed during these tests even though the thrusters were operated at high values of current and low values of mass flow. This suggests that the introduction of propellant directly into the arc by vaporization of material at the arc attachment point may have a beneficial affect on arc stability which permits smooth operation at high values of specific impulse even when storable propellants of relatively high molecular weight are used.

The first series of measurements of propellant consumption and thruster impulse are presented in Table IV. For the various reasons discussed earlier, the data in this table must be regarded as preliminary and subject to later revision. Nevertheless, certain patterns are apparent here which may merit a few remarks. In particular, there are some striking uniformities in various properties over a rather large range of pulse energies:

1. The efficiency of energy transfer from the capacitor line to the electrodes (Column 11) is 67 ± 3 percent, over the entire range tested. This is an unusually high value for quasi-steady experiments and indicates that the impedance is well matched, and there are minimal losses within the line.

2. With the exception of the 100-volt case, the impedance of the discharge chamber (Column 8) is a constant at 0.0055 ± 0.0004 ohm. (The 100-volt case probably involves marginal operation of the discharge, in view of the fact that the voltage developed across the electrodes is less than twice the extinction value for this current, and indeed is less than the full extinction voltage for most of the other cases.) The 0.005 Ω impedance is typical of MPD arcs in this current range, but it is very important to note here that this particular arc head is susceptible to large internal resistance in the electrodes themselves. In view of the

TABLE IV

PRELIMINARY PERFORMANCE MEASUREMENTS

1	2	3	4	5	6	7	8	9	10	11	12	13	14	15	16	17	18	19	20	21
V_o (volts)	V_R (volts)	V (volts)	J (KA)	Δm (mgm)	θ (min.)	I (mgm-sec)	Z (ohm)	VJ (10^6 watt)	VJΔt (joule)	η_d (%)	$I^2/2\Delta m$ (joule)	η_I (%)	η_c (%)	$I/\Delta m$ (sec)	I/J^2 $(\frac{\text{mgm-sec}}{KA^2})$	$\Delta m/J^2$ $(10^{-4}\frac{\text{mgm}}{(KA)^2})$	$\dot{m}$ (gm/sec)	$J^2/\dot{m}$ (KA^2/gm/sec)	8.4 J^2 (mgm-sec)	$I/8.4\ J^2$
100	24	45	4.2	0.02	2.38	75	0.0107	0.189	208	69	14	6.7	4.7	3750	4.25	11.33	0.018	969	148	0.51
200	38	65	11.0	0.11	10.86	342	0.0059	0.715	786	65	53	6.7	4.4	3110	2.82	9.10	0.100	1210	1016	0.34
300	48	90	17.5	0.26	26.0	819	0.0051	1.575	1734	64	129	7.4	4.8	3150	2.67	8.49	0.236	1297	2572	0.32
345	50	110	20.5	0.37	36.0	1134	0.0054	2.255	2480	70	174	7.0	4.9	3060	2.70	8.81	0.336	1251	3529	0.32
400	50	125	24.5	0.60	53.0	1669	0.0051	3.063	3340	70	232	7.0	4.8	2780	2.78	10.00	0.545	1101	5040	0.33

Key:

Column

1 V_o = initial voltage on 60 000 μfd capacitor line

2 V_R = residual voltage left on line after discharge

3 V = voltage measured across electrodes during quasi-steady phase

4 J = current through discharge during quasi-steady phase

5 Δm = mass consumption from electrodes, per pulse

6 θ = deflection amplitude of pendulum for single pulse

7 I = impulse computed from pendulum calibration of 31.5 mgm-sec/min

8 Z = discharge impedance during quasi-steady phase = V/J

9 VJ = power delivered to electrodes during quasi-steady phase

10 VJΔt = energy delivered to electrodes during pulse (Δt = 0.0011 sec)

11 η_d = $VJ\Delta t/\frac{1}{2} CV_o^2$ = fraction of capacitor line energy delivered to electrodes

12 $I^2/2\Delta m$ = energy delivered as impulse

Column

13 η_I = $(I^2/2\Delta m)/VJ\Delta t$ = fraction of energy delivered to electrodes which appears as impulse

14 η_c = $(I^2/2\Delta m)/\frac{1}{2} CV_o^2$ = fraction of capacitor line energy which appears as impulse

15 $I/\Delta m$ = specific impulse

16 I/J^2 = exploration of scaling of impulse with square of discharge current

17 $\Delta m/J^2$ = exploration of scaling of mass consumption with square of discharge current

18 $\dot{m}$ = mass consumption rate = $\Delta m/\Delta t$

19 $J^2/\dot{m}$ = critical mass flow index

20 8.4 J^2 = ideal electromagnetic impulse (see text)

21 $I/8.4\ J^2$ = ratio of measured impulse to ideal electromagnetic impulse

relatively poor conductivity of carbon and the long current paths through the electrodes, it is estimated that at least one-half of the indicated impedance is contributed by the solid elements of the thruster, and only the remainder by the arc itself. This suspicion is supported by previous Table III which shows arc impedances (including the electrode resistive loss) that fall between 3.5 and 4.5 milliohms for most of the electrode geometries. The last seven rows of data are for an improved design with reduced current path in the graphite and conical seats to form the contact between the graphite and the metal conductor. These tests show an average overall impedance of about 2.2 milliohms which tends to verify that a large fraction of the voltage drop is in the electrodes and can be reduced by improved design. The actual arc impedance is no doubt less than 2 milliohms for these tests, which means that a great deal of care must be taken in the design of the conducting path in order to keep the energy actually expended in the arc high.

This power loss in the electrode resistance clearly must detract from the efficiency of conversion of input power into thrust, and may account in some portion for the low values of Columns 13 and 14.

3. The mass consumption (Column 5) is quite low by conventional quasi-steady MPD standards,[15] which results in a surprisingly high specific impulse (Column 15). The ratio of consumed mass to the square of the arc current is nearly constant at about 10^{-6} gm/KA^2 (including the 100-volt case), which transcribes into a $J^2/\dot{m}$ parameter of about 1200. This is one order of magnitude higher than one would expect based upon the critical velocity model of Malliaris applied to gaseous carbon (see Figure 14 of Reference 15), but is in closer accord with experience on other vacuum arcs.[16, 17] Refinements in mass measurement techniques may eventually modify these numbers somewhat, but their order of magnitude, and the scaling with J^2 are not likely to change.

4. The low efficiencies of this first thruster (Columns 13 and 14) have two obvious sources, and probably others. We have already mentioned the resistive losses in the carbon electrodes which consume at least half of the input power meant for the discharge. This loss is readily reduced by redesign of the arc head. In addition, it is clear that the thruster is developing only a small fraction of the impulse potentially available to it via the electromagnetic reaction from the given current. Starting from the familiar relation (Equation 8-109, Reference 18):

$$F \; 2 \; \frac{\mu J^2}{4\pi} \left(\ln \frac{r_a}{r_c} + \frac{3}{4} \right)$$

and recognizing that in this thruster $r_a = r_c = 1/4''$, we might expect a thrust of

$$F\ (\text{newt}) = 0.075\ J^2\ (KA)^2$$

or

$$F\ (\text{gm}) = 7.6\ J^2\ (KA)^2$$

whence, for our 1.1 millisecond pulse, an impulse of

$$I\ (\text{mgm-sec}) = 8.4\ J^2\ (KA)^2$$

This calculation is tabulated in Column 20, and Column 21 presents the ratio of the observed impulse to this ideal value. Again, all but the 100-volt case agree on a common value: the thruster develops only about one-third of the ideal electromagnetic impulse. The cause of this is most likely connected with a discharge pattern that is even less favorable to thrust production than that assumed in the model. Whether this implies an azimuthal nonuniformity (spoke), attachment of the current on the upstream shoulder of the cathode or some other configuration is not evident but clearly indicated is an experimental survey of electrode geometries to optimize thrust for a given discharge current.

6.0 CONCLUSIONS AND RECOMMENDATIONS

The major results of the work described in this report are listed below.

1. It has been found feasible to operate quasi-steady MPD thrusters in a vacuum chamber that is maintained at a pressure below 10^{-6} torr by using consumable graphite electrodes to supply the propellant and manipulating tools to avoid releasing the vacuum in the test chamber when the thruster must be changed. The carbon gas propellant condenses readily on the test chamber walls and the facility remains thoroughly outgassed. The pressure obtained is low enough so that the gas surrounding the plume is initially in the free molecular flow regime (which was the desired goal). It has not yet been determined whether pressure waves reflect from the chamber walls as the plume expands or whether most of the carbon atoms condense on the walls at the first collision. The answer to this question has a strong bearing on how well space environmental conditions are simulated during the pulse.

2. Arc pulses which operate with nearly constant current during a one-millisecond "quasi-steady" interval can be obtained using an electrolytic capacitor bank and an innovative arrangement of the connecting leads that departs from the conventional ladder type of network. The arrangement provides the desired pulse shape in a very light compact package which allows high energy to be stored in the torsional ballistic pendulum. The efficiency of energy transfer from the capacitor system to the arc electrodes is about 70 percent.

3. Graphite has been found to be an excellent material for consumable electrodes. The electrodes ablate evenly maintaining a smooth geometry, the heat of vaporization is high which results in operation in an attractive specific impulse range, the material has good resistance to thermal shock, it condenses readily which eases the vacuum system design problem, and thrusters running with graphite electrodes operate with no evidence of instability at exceptionally high values of the $J^2/\dot{m}$ parameter. These advantages are partially offset by the relatively high electrical resistivity of graphite which results in high resistive losses unless the plasma head is carefully designed to minimize this effect.

4. Triggering of the arc discharge was found to be more difficult when ambient pressure is reduced. Much higher voltages are required and the danger of arcing at other locations in the circuit increases. A thruster design that operates satisfactorily at moderate pressures in the laboratory may be completely incapable of operation in space. However, this problem has been largely avoided by the development of a triggering system that operates at low voltage and initiates the arc by momentary contact of the electrodes. This development has also reduced electromagnetic interference problems in the instrumentation leads.

5. Concern that too much graphite would be vaporized by the arc (resulting in operation at a low specific impulse) has been dispelled by early measurements of the electrode consumption rate. The heat of vaporization of the electrode material consumed is a small fraction of the estimated electrode fall region loss. The electrode consumption rate is also readily controlled by changes in the arc chamber geometry. Apparently, enough cooling is readily provided by radiation and conduction to keep the evaporation rate in the desired range. The accurate measurement of the amount of propellant consumed requires a great deal of care because of the tendency for graphite to absorb moisture from the atmosphere when it is removed for weighing.

6. The torsional ballistic pendulum has demonstrated adequate sensitivity and excellent repeatability now that it is installed in the vacuum chamber. No drift has been detected in either the zero reading or the sensitivity. Some additional work is needed to be sure that all interaction effects have been eliminated and to improve the accuracy of the calibration and the readout. The damping coefficient has been found to be very low, particularly at low amplitudes, which makes it feasible to apply a "resonant pulsing" technique in which one pulse per cycle is applied as the pendulum swings through its zero point. This technique greatly enhances the sensitivity of the instrument by allowing a long series of minute impulses to be summed.

7. Performance measurements that have been obtained are preliminary, but appear to indicate specific impulses in an attractive range, while the efficiency appears to be quite low. A low efficiency was anticipated for the plasma head design tested because the calculated resistive loss in the graphite electrodes is more than half of the total energy in the discharge. No evidence of instability in the arc discharge was noted even though the thrusters were operated at high currents and low mass flows.

8. The arc impedance appears to be somewhat lower than had originally been assumed and the resistive losses in the circuit and in the plasma head parts are higher than had been intended. Greater care will be required in the design of the conducting components to assure that a large fraction of the discharge energy is expended in the arc.

9. On the basis of the above results and experience to date, the following improvements and studies are indicated to continue systematic evaluation of quasi-steady thrusters with consumable electrodes:

   a. The precision of the readout system for the torsional ballistic pendulum should be improved to permit accurate measurements to be made with small

amplitude oscillations, and the accuracy of the calibration system for the pendulum should be improved. Experiments should be conducted to measure electromagnetic and aerodynamic interference effects acting on the pendulum during and immediately following a pulse. If necessary, modifications should then be made to keep these effects at an acceptably low level.

b. An improved procedure is needed for weighing the electrodes before and after tests to avoid errors due to the absorption of atmospheric moisture by the graphite. This measurement is of primary importance to the entire performance assessment, and no compromise in its accuracy can be tolerated.

c. The thruster to be tested must have low resistive loss in the graphite electrodes. There are obvious changes in the design that should be made to minimize this loss. Thruster design number three is a step in this direction and tests on this unit have been initiated. It is difficult to calculate the resistive loss accurately because a complete knowledge of the current density at the arc attachment point and the temperature variation in the electrode is not available. However, it is believed that some information can be obtained experimentally by attaching voltage measuring leads at locations very close to the arc foot.

d. Now that the test facility is beginning to give usable results, attention should shift to the testing of a wide variety of thruster geometries with different grades of electrode graphite, different polarities, different operating conditions, and different methods of triggering the arc discharge. The tests already show that the electrode consumption rate is strongly affected by thruster geometry. It is important to establish which variables are most effective in changing the consumption rate so that the specific impulse can be controlled. The propulsive efficiency is also expected to be strongly affected by thruster design and an exploration of these effects will be a major part of the effort. In particular, the effect of electrode geometry on impulse for a given quasi-steady current should be explored, in an effort to optimize the electromagnetic component of the thrust.

e. Quasi-steady thrusters with consumable electrodes appear to operate with a stable arc discharge at very high values of the $J^2/\dot{m}$ parameter, but the reason for this is not understood. Experiments are needed to determine the limits of stable operation of this type of thruster and to evaluate possible explanations for differences in the stability limits.

f. When some understanding is acquired of the type of geometry needed to obtain satisfactory performance, a study can start of configurations that can be adopted for electrode feeding. A wide range of possible geometries can be visualized at present, but these are expected to narrow down as information on performance becomes available.

g. It may be worthwhile to pursue the use of fast response ionization gages as possible monitors of the electrode evaporation rate throughout a quasi-steady discharge pulse, and to learn more about the rate of condensation of expelled carbon gas on the vacuum chamber walls.

h. Finally, it seems important to assess the importance of current pulse shape on the performance of the thruster, for given initial energy storage. In particular, the relative merits of protracted quasi-steady pulses, versus short, intense pulses, needs to be established for this class of thruster.

REFERENCES

1. A. C. Ducati and R. G. Jahn, "Exploratory Electromagnetic Thruster Research, Phase III," NASA CR66923 (Feb. 1970).

2. A. C. Ducati, et al, "Recent Progress in High Specific Impulse Thermo-ionic Acceleration," AIAA Paper No. 65-06, presented at AIAA 2nd Aerospace Sciences Meeting, New York (Jan. 25-27, 1965).

3. A. C. Ducati, Giannini Scientific Corporation, presentation to Eighth AFOSR Contractors' Meeting on Ion and Plasma Propulsion Research, Los Angeles, California (April 29-30, 1965).

4. A. C. Ducati, et al, "Exploratory Electromagnetic Thruster Research, Phase II," Giannini Scientific Corporation Interim Report 2SS108-1513 (Oct. 1968).

5. G. N. Glasoe and J. V. Lebacqz, Pulse Generators, vol. 5 of the Ratiation Laboratory Series, McGraw-Hill Book Company (1948).

6. A. E. Knowlton, Standard Handbook for Electrical Engineers, Ninth Edition, McGraw-Hill Book Company (1957).

7. Stanley L. Leonard, "Basic Macroscopic Measurements," chap. 2 of Plasma Diagnostic Techniques, Edited by Richard H. Huddlestone and Stanley L. Leonard, Academic Press (1965).

8. "The Measuring of Impulse Currents" - the High Current Shunt section starting on page 357 of Plasma Diagnostic Techniques, Edited by Richard H. Huddlestone and Stanley L. Leonard, Academic Press (1965).

9. Evor E. Campbell and Edwin M. Sherwood, High Temperature Materials and Technology, John Wiley and Sons, Inc. (1967).

10. The Industrial Graphite Engineering Handbook, Union Carbide Corporation, Carbon Products Division.

11. P. J. Schneider, Temperature Response Charts, John Wiley and Sons (1963).

12. B. J. McBride, et al, "Thermodynamic Properties to 6000°K for 210 Substances Involving the First 18 Elements," NASA SP-3001 (1963).

13. Paul S. Epstein, Textbook of Thermodynamics, John Wiley and Sons (1937).

14. A. C. Ducati and R. G. Jahn, "Investigation of Pulsed Quasi-Steady MPD Arc Jets," Plasmadyne 60-day Progress Report, PR-090-10140 (Sept. 1970).

15. A. C. Malliaris, et al, "Quasi-Steady MPD Propulsion at High Power," NASA CR-111872 (Feb. 1971).

16. William J. Guman and Paul E. Peko, "Solid Propellant Pulsed Plasma Micro-Thruster Studies," AIAA Paper No. 68-85, presented to AIAA 6th Aerospace Sciences Meeting, New York (Jan. 22-24, 1968).

17. A. S. Gilmour, Jr., "Concerning the Feasibility of a Vacuum Arc Thrustor," AIAA Paper No. 66-202, presented to AIAA Fifth Electric Propulsion Conference, San Diego, California (March 7-9, 1966).

18. R. G. Jahn, Physics of Electric Propulsion, McGraw-Hill Book Company, New York (1968).

UNCLASSIFIED
Security Classification

DOCUMENT CONTROL DATA – R & D
(Security classification of title, body of abstract and indexing annotation must be entered when the overall report is classified)

1. ORIGINATING ACTIVITY (Corporate author)	2a. REPORT SECURITY CLASSIFICATION
Plasmadyne, a division of Geotel, Inc. 3839 South Main Street Santa Ana, California	UNCLASSIFIED 2b. GROUP NASA CR-111970

3. REPORT TITLE

INVESTIGATION OF PULSED QUASI-STEADY MPD ARC JETS

4. DESCRIPTIVE NOTES (Type of report and inclusive dates)
Scientific

5. AUTHOR(S) (First name, middle initial, last name)

Adriano C. Ducati Robert G. Jahn

6. REPORT DATE	7a. TOTAL NO. OF PAGES	7b. NO. OF REFS
June 1971	102	19

8a. CONTRACT OR GRANT NO.	9a. ORIGINATOR'S REPORT NUMBER(S)
NAS 1-10140 b. PROJECT NO. c. d.	FR-061-10140 9b. OTHER REPORT NO(S) (Any other numbers that may be assigned this report)

10. DISTRIBUTION STATEMENT

11. SUPPLEMENTARY NOTES	12. SPONSORING MILITARY ACTIVITY
	National Aeronautics and Space Adm. Langley Research Center Hampton, Virginia 23365

13. ABSTRACT

This report describes the work performed for continued evaluation of MPD arc thrusters operating in the quasi-steady mode and using electrode vapor as the propellant. Most of the effort has been directed toward the development of a propulsion system and a test facility that will permit efficient testing with the desired environmental conditions. Some preliminary performance data have been obtained and are reported and discussed toward the close of this report. In order to resolve questions regarding the effect of ambient gas on performance, a high priority has been placed on testing at pressures low enough that the flow surrounding the plume is in the free molecular regime. Electromagnetic interactions with the environment are minimized by the use of a vacuum chamber made of insulating material. Extensive operation of thrusters using carbon gas as the propellant shows no evidence of instabilities even though the thrusters are normally operated at high values of current and low mass flow. The preliminary data indicate that these carbon arcs have impedances of a very few milliohms, independent of the current over a range of 10 to 30 kiloamps. Their match with the capacitor line is such that some 70 percent of the initially stored energy is delivered to the electrodes. The mass consumed per pulse is quite low, and roughly proportional to the square of the current over the range tested, leading to a nearly constant specific impulse. The overall thrust efficiency is quite low, as was expected from the high internal resistance of the carbon electrodes in this first thruster design and their relatively ineffective geometry for electromagnetic thrust optimization. The steps for direct improvement of both testing technique and thruster performance are clearly defined by the studies completed to date.

DD FORM 1 NOV 65 1473

UNCLASSIFIED
Security Classification

14. KEY WORDS	LINK A		LINK B		LINK C	
	ROLE	WT	ROLE	WT	ROLE	WT
Arc Jet Environment						
Electrode Erosion and Evaporation						
Electrolytic Capacitors						
High Specific Impulse						
MPD Arc Jet						
MPD Test Environment						
Plasma Accelerator						
Plasma-Pulsed Accelerator						
Propulsion						
Pulse Networks						
Quasi-Steady						
Thrust Balance						
Vacuum Chambers						
Evaporation						
Sublimation						
Carbon and Graphite						
Carbon Vapor						
Resonant Pulsing						